THE HONG KONG
POLYTECHNIC UNIVERSITY
香港理工大學
Pao Yue-kong Library
包玉剛圖書館

Copyright Undertaking

This thesis is protected by copyright, with all rights reserved.

By reading and using the thesis, the reader understands and agrees to the following terms:

1. The reader will abide by the rules and legal ordinances governing copyright regarding the use of the thesis.
2. The reader will use the thesis for the purpose of research or private study only and not for distribution or further reproduction or any other purpose.
3. The reader agrees to indemnify and hold the University harmless from and against any loss, damage, cost, liability or expenses arising from copyright infringement or unauthorized usage.

If you have reasons to believe that any materials in this thesis are deemed not suitable to be distributed in this form, or a copyright owner having difficulty with the material being included in our database, please contact lbsys@polyu.edu.hk providing details. The Library will look into your claim and consider taking remedial action upon receipt of the written requests.

Pao Yue-kong Library, The Hong Kong Polytechnic University, Hung Hom, Kowloon, Hong Kong

http://www.lib.polyu.edu.hk

THE HONG KONG
POLYTECHNIC UNIVERSITY
香港理工大學

Department of Electrical Engineering

HYBRID NETWORK REDUCTION AND ARTIFICIAL NEURAL NETWORK BASED APPROACHES IN FAST VOLTAGE STABILITY ANALYSIS

FU YING

B. Sc., M. Sc.

Thesis submitted for the degree of
Doctor of Philosophy in Engineering

Hong Kong, November 1999

Pao Yue-Kong Library
PolyU • Hong Kong

DEDICATE TO

MY BELOVED HUSBAND

AND FAMILY

Abstract of Thesis entitled:

'HYBRID NETWORK REDUCTION AND ARTIFICIAL NEURAL NETWORK BASED APPROACHES IN FAST VOLTAGE STABILITY ANALYSIS'

submitted by

FU YING

B. Sc., M. Sc.

For the degree of

Doctor of Philosophy in Engineering

At The Hong Kong Polytechnic University in

November 1999

Abstract

The development of tools for fast on-line voltage stability analysis is a major issue in the operation of modern power system due to the recent trends in deregulation and competitive operation environment. This thesis is focused on the study of fast voltage stability analysis for both static and dynamic security assessment. Two new techniques are developed: network reduction and integrated artificial neural network approaches. An overview of current trends in voltage stability analysis, as well as the current solution techniques, is first presented. Following the introduction on external modeling, an extended Ward equivalent model is then presented. Artificial Neural Networks (ANNs) approaches have been developed to voltage stability evaluation as they are able to solve power system problems where difficulties have been experienced with conventional numerical techniques. Three types of ANN models: multi-layer neural network, Kohonen neural network, and hybrid supervised/unsupervised neural network, are developed in this work. A new methodology for static voltage stability by means of network reduction is presented. By the use of this methodology, Q-V or P-V curve can be quickly determined. The extended Ward equivalent is one of the most popular methods on external network equivalent. However, it is found that the method is not suitable for on-line use. An improved method is developed with hybrid ANN and external network equivalent. This new method combines the merits of the two techniques since it uses the extended Ward equivalent to build boundary equivalent line modeling and ANN to on-line match boundary equivalent power injection. Hence, this new approach is proposed for fast on-line assessment application. Voltage stability is also a dynamic problem, which mainly involves the loads and the means for voltage control. The dynamic characteristics of induction motor are introduced in this thesis. An improved ANN based method for voltage stability analysis is also developed. This method is based on self-organizing hierarchical neural network (SHNN), which integrates input feature self-organizing map neural network and multi-layer feed-forward neural network. Research results and analysis are presented to show the applicability and efficiency of these methods in power systems operation.

Acknowledgements

The work presented in this thesis was carried out under the supervision of Dr. T. S. Chung, Professor and Leader of Power Systems Research Group, Department of Electrical Engineering, The Hong Kong Polytechnic University. It is with great pleasure and deep gratitude that the author acknowledges his invaluable guidance and continuous encouragement, which enable the completion of this work.

The author would like to take this opportunity to thank Professor Li Xingyuan of Sichuan University, and Professor Wen Fushuan of Zhejiang University for the kind help and encouragement. The author is grateful to Dr. Wang Kewen, Dr Fang Wanliang and Dr Ge Shaoyun for many useful discussions.

The financial support provided by the Research Committee of Hong Kong Polytechnic University through the award of scholarship and funding for international conference attendance is also gratefully acknowledged.

The profitable discussions with Professor P. Kundur, are gratefully acknowledged. Last, but not least, every effort substantiated from the Department of Electrical Engineering is gratefully acknowledged.

Contents

Chapter 1 Introduction **1**

1.1 Power System Stability Classification 1

1.2 Voltage Stability 2

1.2.1 Concepts 2

1.2.2 Voltage Stability Analysis 4

1.3 Network Reduction Techniques 8

1.4 Outline of the Thesis 9

1.5 Statement of Originality 12

1.6 Publications 14

Chapter 2 Network Reduction Techniques for Voltage Stability Study **17**

2.1 Introduction 17

2.2 External Network Modelling 17

2.2.1 Network Reduction on Voltage Stability Analysis 19

2.2.2 Method of External System Modeling 19

2.3 Load-Flow Equations and Notation 21

2.4 Review of Ward Equivalent 23

2.4.1 Conventional Ward Equivalent Approach 23

2.4.2 Extended Ward Equivalent Approach 26

2.5 Partition of External Network 33

2.6 ANN Used in Network Reduction 35

2.7 Summary 36

Chapter 3 Artificial Neural Network Techniques **37**

3.1 Introduction 37

3.2 Multi-layer Feed-lorward Neural Network 38

3.2.1 Topology of the ANN 38

3.2.2 The BP Algorithm 42

3.3 Kohonen Self-organizing Feature Map 43

3.4 Hybrid Unsupervised/Supervised Concept 50

3.5 Apply ANNs on Network Reduction and Voltage Stability 52

3.6 Summary 53

Chapter 4 A Simple Network Reduction Based Voltage Stability Analysis **55**

4.1 Introduction 55

4.2 *V-Q* Curves and *P-V* Curves 56

4.3 Stability Analysis via Network Equivalent 60

4.3.1 Tow-Point Load-Flow Calculation (TPLC) Method 60

4.3.2 Modified Tow-Point Load-Flow Calculation (MTPLC) Method 63

4.4 Test Results 64

4.5 Summary 66

Chapter 5 An Innovative Hybrid ANN External Equivalent Approach **71**

5.1 Introduction 71

5.2 Methodology 74

5.2.1 Hybrid ANN External Equivalent: Method 1 75

5.2.2 Hybrid ANN External Equivalent: Method 2 77
5.3 Test Results 79
5.3.1 Test System 79
5.3.2 Configuration of ANN and Data Description 83
5.3.3 Contingency Analysis 85
5.4 Summary 94

Chapter 6 Self-organizing Hierarchical Neural Network Based Voltage Stability Estimation 95
6.1 Introduction 95
6.2 Dynamic Load Models 97
6.2.1 Philosophy of the Simulation 98
6.2.2 Fundamental Equations 99
6.2.3 Procedure of Simulation 101
6.3 Voltage Collapse Proximity Indicator 102
6.3.1 Formulation of Voltage Collapse Proximity Indicator 102
6.3.2 Discussion of Voltage Collapse Proximity Indicator 104
6.4 Neural Network Approach to Voltage Stability Analysis 105
6.4.1 Block Diagram of the Learning Model 105
6.4.2 Neural Network Approach to Voltage Stability Analysis 108
6.5 Result and Discussions 108
6.5.1 Training Sets Generation 111
6.5.2 Selection of Network Parameters 112
6.5.3 Results of the First SHNN Model 112

6.5.4 Results of the Second SHNN Model 115

6.6 Summary 118

Chapter 7 Conclusions 119

7.1 Summary 119

7.2 Main Contributions 120

7.3 Future Work 122

References 124

Appendices 144

Appendix I System Data of New-England 39-Bus Test System 144

Appendix II System Data of WSCC 9-bus Test System 147

Appendix III System Data of the 59-bus Test System 148

Appendix IV System Data of EPRI 36-bus Test System 153

List of Abbreviations

ANN: Artificial Neural Network

EMS: Energy Management System

TPLC: Two Point Load-flow Calculation

MTPLC: Modified Two Point Load-flow Calculation

BP: Back Propagation

SOM: Self-Organizing Map

SHNN: Self-organizing Hierarchical Neural Network

List of Symbols and Notations

E:	vector of complex voltage
I:	vector of complex current injection into the network
S:	vector of complex power injection into the network
Y:	bus admittance matrix
E_k:	complex voltage at bus k
I_k:	complex current injection into the network from bus k
S_k:	complex power injection into the network from bus k
P_k:	complex active power injection into the network from bus k
Q_k:	complex reactive power injection into the network from bus k
$\Delta\widetilde{Q}_k$:	extra reactive power injection into the network form bus k
o_i :	outputs of units in layer i in ANN
net_j :	the total input to a unit in layer j in ANN
f:	activation function or transfer function of the ANN
d_{pk} :	desired outputs of the ANN for pattern p
o_{pk} :	actual outputs of the ANN for pattern p
η :	learning rate constant in ANN
α :	momentum constant in ANN
E_p:	error function of the ANN for pattern p
E_{max}:	error tolerance
W_{ij}:	connection weight between input unit i and output unit j of the ANN
A_j:	continuous valued activation value for the output node j in Kohonen neural

network

$\alpha(t)$: decreasing function of time in Kohonen neural network

c: maximally responding unit in Kohonen neural network

N_c: topological neighborhood in Kohonen neural network

$\bar{B}_k$: the equivalent susceptance from bus k to the fictitious PV bus

V_i: voltage magnitude at boundary bus i in post-contingency

θ_i: phase angle at boundary bus i in post-contingency

V_i^0: voltage magnitude at boundary bus i in pre-contingency

θ_i^0: phase angle at boundary bus i in pre-contingency

P_i: equivalent active power injection at boundary bus i in post-contingency

Q_i: equivalent reactive power injection at boundary bus i in post-contingency

P_i^0: equivalent active power injection at boundary bus i in pre-contingency

Q_i^0: equivalent reactive power injection at boundary bus i in pre-contingency

ΔV_i: the change of voltage magnitude at boundary bus i

$\Delta\theta_i$: the change of phase angle at boundary bus i

ΔP_i: the change of equivalent active power injection at boundary bus i

ΔQ_i: the change of equivalent reactive power injection at boundary bus i

G_{kj}: conductance between node k and j

B_{kj}: susceptance between node k and j

e_k: real components of node voltage k

f_k: imaginary components of node voltage k

Pe_k: active powers injected to node k

Qe_k: reactive powers injected to node k

rm_k : resistance of the equivalent circuit of induction motor k

xm_k: reactance of the equivalent circuit of induction motor k

s_k : slip of induction motor k

Φ_k : moment of inertia of induction motor k

ω_0: $\omega_\theta = 2\pi f_\theta$, f_θ : frequency of the system

Chapter 1

Introduction

1.1 Power System Stability Classification

Power system stability has been and continues to be a major concern in system operation since the early days of power system operation. It may be broadly defined as that property of a power system that enables it to remain in a state of operating equilibrium under normal operating conditions and to regain an acceptable state of equilibrium after being subjected to a disturbance [83].

Table 1.1 shows a classification scheme based upon two criteria: time scale and driving force of instability [105].

Table 1.1 Power system stability classification

Time scale	Driving force of instability		
	Generator-driven		Load-driven
Short-term	Rotor angle stability		Short-term Voltage stability
	Transient	Steady-state	
Long-term	Frequency stability		Long-term voltage stability

1.2 Voltage Stability

As transmission systems become more stressed due to increased loads and large inter-utility power transfers, efficient system operation is becoming increasingly threatened due to problems of voltage instability and collapse. This is evident from the several major system collapses due to voltage instability experienced in recent years in France, Belgium, Sweden, Japan and the United States [25, 26, 53].

1.2.1 Concepts

- *Voltage stability*: the ability of a system to maintain voltage so that when load admittance is increased, load power will increase, and so that both power and voltage are controllable

- *Voltage collapse*: the process by which voltage instability leads to very low voltage profile in a significant part of the system

- *Voltage security*: the ability of a system, not only to operate stably, but also to remain stable following any reasonably credible contingency or adverse system change

A system enters a state of voltage instability when a disturbance, increase in load demand, or change in system condition causes a progressive and uncontrollable drop in voltage. The main factor causing instability is the inability of the power system to meet the demand for reactive power. The heart of the problem is usually the voltage drop that occurs

when active power and reactive power flow through inductive reactances associated with the transmission network.

In complex practical power systems many factors contribute to the process of system collapse because of voltage instability: strength of transmission system, power-transfer levels, load characteristics, generator reactive power capability limits, and characteristics of reactive power compensating devices. In some cases, the problem is compounded by uncoordinated action of various controls and protective systems.

Voltage instability or collapse is a dynamic process. The work "stability" implies a dynamic system. A power system is a dynamic system. We will see that, in contrast to rotor angle (synchronous) stability, the dynamic process mainly involves the loads and the means for voltage control. Voltage stability has been called load stability [16].

For the purpose of analysis, it is useful to classify voltage stability into the following two subclasses [83]:

- *Large-disturbance voltage stability* is concerned with a system's ability to control voltages following large disturbances such as system faults, loss of generation, or circuit contingencies. This ability is determined by the system-load characteristics and the interactions of both continuous and discrete controls and protections.

A criterion for large-disturbance voltage stability is that, following a given disturbance and following system-control actions, voltages at all buses reach acceptable steady-state levels.

- *Small-disturbance voltage stability* is concerned with a system's ability to control voltages following small perturbations such as incremental changes in system load. This form of stability is determined by the characteristics of load, continuous controls, and discrete controls at a given instant of time.

A criterion for small-disturbance voltage stability is that, at a given operating condition for every bus in the system, the bus voltage magnitude increases as the reactive power injection at the same bus is increased. A system is voltage-unstable if, for at least one bus in the system, the bus voltage magnitude (V) decreases as the reactive power injection (Q) at the same bus is increased.

The basic processes contributing to small-disturbance voltage instability are essentially of a steady-state nature. Therefore, static analysis can be effectively used to determine stability margins, identify factors influencing stability, and examine a wide range of system conditions and a large number of post-contingency scenarios [53].

1.2.2 Voltage Stability Analysis

Experts worldwide have labeled voltage security as the hidden threat to transmission networks. Thus the development of tools for fast voltage stability analysis has emerged as an important issue in the operation and planning of modern power system and has attracted

ever increasing attention. There are two important aspects in voltage stability studies: 1) voltage stability assessment, *i.e.*, accurately quantifying voltage stability margin; 2) voltage instability mechanisms analysis, including identifying area and buses most susceptible to voltage collapse [13].

Two general types of tools have been developed for voltage stability analysis: dynamic and static. Dynamic analysis uses time-domain simulations to solve nonlinear system differential / algebraic equations. Static analysis is based on the solution of conventional or modified power flow equations.

System dynamics influencing voltage stability are usually slow. Therefore, many aspects of the problem can be effectively analyzed by using static methods, which examine the viability of the equilibrium point represented by a specified operating condition of the power system. The static analysis techniques allow examination of a wide range of system conditions and, if appropriately used, can provide much insight into the nature of the problem and identify the key contributing factors. Dynamic analysis, on the other hand, is useful for detailed study of specific voltage collapse situations, coordination of protection and controls, and testing of remedial measures.

Static Analysis

In recent years, a number of special techniques have been proposed in the literature for voltage stability analysis using the static approach [54, 118]. These methods include: power flow-based methods [82, 108, 123], sensitivity analysis [22, 76], singular value decomposition [80, 120], modal (eigenvalue) analysis [13, 48], optimization-based

approached [7, 79, 105, 124], Lyapunov's direct method, Singular value decomposition, MVAR margin using optimization, and other methods based on Q-V characteristics [53]. At the same time, a large number of papers have addressed the issue of quantifying the distance of a specific operating stage to voltage collapse. In [11], the degeneracy of the load flow Jacobian matrix, its minimum singular value, and its condition number were used as indices of power system small-disturbance voltage stability. The concept of multiple load flow solutions was proposed to deal with voltage stability problems in [123]. Different voltage instability indictors were used to quantify the proximity of a particular operating state to the point of voltage collapse. Continuation methods were also applied to compute the exact collapse point and the voltage security margins in MW [20, 108]. The energy method had been used for voltage security assessment [21, 100-101].

Static analysis involves only the solution of algebraic equations and therefore is computationally much more efficient than dynamic analysis. Static analysis is ideal for the bulk of studies in which voltage stability limits for many pre-contingency and post-contingency cases must be determined. In modern power system operation, information such as load-ability and voltage instability mechanisms is becoming vitally important to operators in control centers. In this context, much attention is being paid to further develop these algorithmic-based approaches for on-line voltage stability analysis.

Dynamic Analysis

Voltage collapse is also a complex dynamic phenomenon, and the reason of voltage collapse is discussed in [39, 102].

Dynamic analysis provides the most accurate replication of the time responses of the power system [40, 55, 83, 114, 123]. Time-domain simulations, in which appropriate modelling is included, capture the events and their chronology leading to instability. However, time-domain simulations are time consuming in terms of CPU and engineering requirements for analysis of results. In addition, dynamic analysis does not readily provide information regarding the sensitivity or degree of instability. These limitations generally make dynamic analysis impractical for examination of a wide range of system conditions or for determining stability limits.

Artificial Neural Networks (ANNs) Used in Voltage Stability Analysis

More recently there is a growing interest in the use of ANNs to solve power system problems where difficulties have been experienced with conventional technique [110]. Work reported in [2, 14-15, 29, 31-32, 34, 36, 68, 85, 95, 97-98, 104, 115-116] apply ANN to solve diverse areas of power system problems. In this context, ANNs have also been applied to voltage stability analysis [1, 8-9, 35, 49, 52, 62, 65, 69, 117].

Most of the published work in the area of voltage stability has employed multi-layer perceptron networks trained by back-propagation. As an attractive alternative to the multi-layer perceptron, Kohonen neural networks offer some advantages, particularly in the applications of clustering type problems. Results of applications to power system static security assessment are very encouraging [35]. As an attractive alternative, a hybrid neural network which consists of supervised and unsupervised neural networks is reported in [49, 70]. For security assessment, unsupervised networks often act as a data pre-processor for either a contingency analysis tool or another ANN. The unsupervised layer is used for data

reduction, the supervised layer for data retrieval, which usually includes the security class of the operating state.

1.3 Network Reduction Techniques

Voltage instability in power network is a phenomenon of highly nonlinear nature posing operational as well as prediction problems in power systems control. To obtain a solution to the problem, both static and dynamic modeling methods have been applied. All the methods are subject to relatively extensive and time consuming calculation procedures.

Voltage collapse is a local phenomenon since it is well known that reactive power cannot be transferred over long distances due to heavy reactive losses in the distribution system. So the complete power system model may be decomposed into several local network models when dealing with the voltage / reactive problems [107]. Local concept is also used in [77]. Therein, the suitable approach is by equivalencing the areas which are external to the system for which security monitoring and security analysis are to be performed.

There are many methods developed to address this problem [10, 12, 24, 27-28, 43, 45-46, 50, 56-58, 60, 66-67, 72, 75, 86, 92, 99, 107, 109, 111-113, 119]. The traditional solution methods of steady-state external equivalents include linearization methods, Ward-type external equivalent, Dimo's REI-type external equivalent and on-line identification of equivalents [81, 91, 125]. Meanwhile, some approaches such as modal approach, decomposition and coherent approach have been developed to obtain equivalents of the dynamic component [4-5, 37, 38, 90].

1.4 Outline of the Thesis

Varieties of factors (financial, regulatory, and environmental to mention a few) are forcing electric utilities to operate their systems in ways which make maximum use of transmission capability. Consequently, voltage stability has become the limiting constraint for an increasing number of systems, superseding rotor angle stability as the primary concern. Therefore, fast voltage stability analysis is one of the main concerns. The main objectives of this project are:

1) To develop suitable external network model for steady state analysis of power system.

2) To develop ANN based voltage stability analysis methods.

The main text of this thesis is summarized as follows:

Development of Network Reduction Method

Modern power system transmission networks are increasingly highly interconnected neighboring utilities. Studies of power system characteristics usually involve the solution of large numbers of equations, both algebraic and differential. Each utility energy management system (EMS) is responsible for only a small part of the complete interconnected network, and this is usually known as the internal system; the remainder of the network, not monitored by EMS, is the external system. To effectively monitor the internal system and to assess its static security, a suitable model for representing the external system is necessary. An overview of current trends in utility external network model is first presented in Chapter

2. Ward-type equivalents are suggested and have been used for steady-state security analysis. An overview of Ward equivalent is presented in the chapter.

The slower forms of voltage instability are often analyzed as steady-state problems; power flow simulation is the primary study method. The voltage collapse phenomenon is often explained by means of static techniques, and analyzed by means of Q-V and P-V curves, which are based on series of conventional power-flow calculation. These two methods determine steady-state loadability limits which are related to voltage stability. As Q-V and P-V curves are presently the basic tools used to analyze voltage stability in many utilities, it is worthwhile to develop a method which can quickly obtain them. In this context, a new network reduction method, called Modified Two-Point Load-flow Calculation (MTPLC) method, is then developed in Chapter 4. This new voltage stability analysis approach with network equivalence has been shown to provide a fast method to plot Q-V and P-V curves at the given node where voltage stability is to be studied. The slope of Q-V and P-V curves of each node is obtained and can be used to study the voltage stability quickly.

ANNs Based Network Reduction

Artificial neural networks (ANNs) have been applied to voltage stability evaluation as they have been successfully applied to some power system problems. The potential of the application of ANNs as an alternative approach for solving certain difficult power system problems, where the conventional techniques have not achieved the desired speed, accuracy, or efficiency, is quite promising. The concepts and theories of multi-layer supervised neural

network and Kohonen unsupervised neural network are presented in Chapter 3. In addition, hybrid supervised and unsupervised neural network concept is also introduced in Chapter 3.

Conventionally, the network configuration changes are according to schedule, while the load level is continuously changing throughout the day, so the boundary power injections would need to be updated from time to time. The extended Ward equivalent cannot simulate significant events in the external system and their impact on the internal system. It may cause some errors in on-line application. Therefore, much research work in recent years is on fast boundary matching and improving existing equivalent method for on-line applications. The boundary power injection matching can be considered as a pattern recognition problem which is suitable for application of ANN. To reflect the topology changes of the internal system, when the information concerning external system is incomplete in on-line application, multi-layer neural networks is a good candidate for on-line identification of external system equivalent. The detailed study of this work is given in Chapter 5.

ANN Based Voltage Stability Analysis

Most of the published work in the area of voltage stability has employed multi-layer perceptron networks trained by back-propagation for quantifying stability margins. However, in respect of voltage stability assessment of practical systems, a major difficulty of this type of neural networks is that it depends highly on the number of training data because the network itself does not take into account the properties of input data. Thus, a large number of inputs are needed, including contingency and system topology. This obviously poses problems in practical applications.

As an attractive alternative to the multi-layer perceptron, Kohonen neural networks offer some advantages, particularly in the applications of clustering type problems. A Kohonen self-organizing neural network is an unsupervised neural network which maps m-dimensional input vectors to two-dimensional outputs. Input patterns with similar features, which contain sufficient information about the voltage stability of power systems, are clustered together in the output map. However, Kohonen neural networks cannot give information about voltage weakness of power systems quantitatively, i.e. in MW or MVar. This is a drawback of Kohonen neural network when used in voltage stability analysis.

A hybrid neural network which consists of a self-organizing map network and a multi-layer feed-forward network, called Self-organizing Hierarchical Neural Network (SHNN), is developed and described in Chapter 6.

1.5 Statement of Originality

An important task in power system operation is to decide whether the system is currently operating safely, critically or unsafely. Hence, fast voltage stability analysis is very important to monitor voltage stability limit and to present control strategy which can ensure economic operation under normal condition and prevent voltage collapse during contingencies. The original contributions and important developments of this thesis are as follows:

- A new voltage stability analysis approach with network equivalence has been shown to

provide a fast method to plot *Q-V* and *P-V* curves at the study node where voltage stability is to be studied. After performing two points load flow, the slope of the *Q-V* and *P-V* curves is quickly plotted out. Results show that the Modified Two-Point Load-flow Calculation (MTPLC) method may be useful in fast voltage security assessment.

- Modern power system transmission networks are increasingly highly interconnected neighboring utilities. To effectively monitor the internal system and assess its security, a suitable model for representing the external system is necessary. ANN based external system equivalence is a promising concept for network reduction and ANN application. A novel hybrid Artificial Neural Network (ANN) and Ward-type equivalent approach for fast on-line voltage security assessment of power systems is developed. The proposed approach possesses the good properties of Ward equivalent method and can update the parameters of the equivalent model for representing real time topology change of the external system. Moreover, the boundary equivalent power injection can be matched quickly by using hybrid Artificial Neural Network.

- A self-organizing hierarchical neural network (SHNN) based voltage stability analysis is developed. The approach is a hybrid of input feature selection technique and multilayer feed-forward neural network. Two SHNNs are developed and used sequentially in this approach. The self-organizing map layer is used for feature extraction of operating conditions in terms of voltage stability, and the input of the multi-layer feed-forward layer comes from the self-organizing map layer. The SHNN is trained by the samples of off-line simulation results.

1.6 Publications

Arising from this research project, three journal papers have already been accepted for publication in leading international journals, and three journal papers are under review. In addition, five conference papers have been presented and one accepted for presentation. These papers are listed below:

Referred journal papers published:

1) T. S. Chung and Y Fu, "A fast voltage security assessment method via extended Ward equivalent and neural network approach", IEEE Power Engineering Review, October 1999, pp. 40-43

2) Y Fu and T. S. Chung, "A hybrid approach to external system equivalent for power system voltage security assessment", accepted for publication in International Journal of Electric Power Systems Research.

3) Ying Fu and T. S. Chung, "A hybrid artificial neural network (ANN) and Ward equivalent approach for on-line power system voltage security assessment", accepted for publication in Automation of Electrical Power Systems

Journal papers under review:

4) T. S. Chung and Fu Ying, "On-line voltage stability and security calculation using a new network equivalent technique", submitted to International Journal of Electrical Power & Energy System.

5) Ying Fu and T. S. Chung, "An innovative feature selection based neural network approach to dynamic voltage stability estimation", submitted to International Journal of Electric Power Systems Research.

6) Fu Ying and T. S. Chung, "A ANN based Ward equivalent approach for power system security assessment", submitted to International Journal of Electric Machines and Power Systems.

International conference papers published / accepted:

7) Y Fu, T. S. Chung and X. Y. Li, "An improved approach to voltage stability analysis via network equivalence", Fourth international conference on IEE 450 APSCOM-97, November 1997, Hong Kong, pp. 231-235

8) Y. Fu and T. S. Chung, "A new approach to external system equivalent for power system voltage security assessment, 1998 Large Engineering Systems Conference on Power Engineering (LESCOPE'98), June 1998, Halifax, Canada, pp. 255-259.

9) T. S. Chung and Fu Ying, "An ANN-based network equivalent approach for power system on-line voltage security assessment", International conference on Power System Technology (POWERCON'98), August 1998, Beijing, China.

10) Fu Ying and T. S. Chung. "Feature selection technique based neural network approach to voltage security assessment". International Conference on Electrical Engineering (ICEE'99). Aug. 1999. Hong Kong. pp. 32-35.

11) T. S. Chung and Fu Ying. "A hybrid approach in external system equivalent for voltage assessment". International Conference on (IPEC'99). May 1999. Singapore.

12) Fu Ying and T. S. Chung. "An Innovative Fast Voltage Security Assessment Based on a Hybrid ANN External Equivalent Approach." (Conference Proceedings paper accepted for publication and presentation at IEEE Power Engineering Society Winter Meeting 2000 (2000WM-298). January 2000. Singapore).

Chapter 2

Network Reduction Techniques for Voltage Stability Study

2.1 Introduction

Modern electric power systems are characterized by the growing size and complexity of the enormous number of generating units, loads, and transmission lines that are included in the system. Studies of power system characteristics usually involve the solution of large numbers of equations, both algebraic and differential.

In recent years, extensive studies have been directed towards simplifying the representation of the power system for specific applications. Many equivalent techniques have been developed, both steady state and dynamic. The most popular steady-state equivalent approaches are Ward equivalent methods and Radial Equivalent Independent (REI) method. The other methods are variations of these two basic methods. The load flow equations and notation are firstly presented in this chapter; then, Ward equivalent is reviewed. How to use ANN in external equivalent is also discussed in this chapter.

2.2 External Network Modelling

Power systems are interconnected. An energy control center for a member of the interconnection is responsible for the control of a part of interconnected system. The control

center receives telemetered data of real-time measurements. The monitored part of the power system that these measurements cover normally consists of the energy control center's own system and is called the internal system. The system is connected to neighboring systems, and this is called the external system. The effect of the external system in the internal one in steady sate is reflected by the real and reactive power flows from the external system into the boundary buses. The set of real-time measurements is processed in the control center through the state estimator to obtain the best estimate of the present state of the internal system. Once the state is obtained, other quantities of interest, for example, real and reactive power generations, line flows, bus voltages, can be calculated and their values can be checked against the specified limits.

Security is defined as the ability of a system to withstand imminent disturbances (possible next contingencies), such as line outages or generator outages. In other words, a power system is said to be secure if no contingency in next-contingency list will cause line overload, abnormal voltage, *etc*. To evaluate the consequence of each contingency, which is a postulated future case, state estimation can no longer be used because there are no measurements available. Therefore, a load flow will have to be simulated for contingency evaluation. A load-flow model of the internal system for the contingent case is available from the state estimator; thus it would be possible to run a load flow just from the internal system if the flows from the external system to the boundary buses are known. However, the response of the external system to the contingency makes the flows from the external system to the boundary buses different from their present values. Therefore, for online contingency evaluation, an external network model that for the contingency response of the external system must be used in conjunction with the model of the internal system internal

system. More common is the case in which a reduced model has to be used. A reduced mode of the external system that approximately represents the steady-state effect of the external system on the internal system for contingency evaluation is commonly called an external network equivalent or simply an external equivalent.

2.2.1 Network Reduction on Voltage Stability Analysis

Voltage instability in power network is a phenomenon of highly nonlinear nature posing operational as well as prediction problems in power systems control. To obtain a solution to the problem, both static and dynamic modeling methods have been applied. All the methods are subject to relatively extensive and time consuming calculation procedures.

Voltage collapse is a local phenomenon since it is well known that reactive power cannot be transferred over long distances due to heavy reactive losses in the distribution system. The distant buses usually do not influence the affected bus voltage stability to a great extent if any. Therefore, a suitable approach is equivalencing the areas, which are external to the system for which security monitoring and security analysis are to be performed.

2.2.2 Method of External System Modeling

There are many methods developed to address this problem. The traditional solution methods of steady-state external equivalents include linearization methods, Ward-type external equivalent, Dimo's REI-type external equivalent and on-line identification of equivalents [10, 24, 42, 91-94, 99, 113]. Some approaches such as modal approach,

decomposition and coherent approach have been developed to obtain equivalents of the dynamic component [112]. A 1987 CIGRE report [26] recommends analysis method of voltage stability based on static models. and the steady-state external equivalent method is used in analysis.

An external model may be constructed online. offline. or a combination of both. Once it is constructed. it is attached to the load-flow model of the internal system for contingency evaluation. The external model should be a good representation of the effect of the external system on the internal system. From the state estimation. the load-flow solution of the internal system at the present time is known (This case. without contingency. is referred to as the base case). It is then required that the solution of the load-flow model. consisting of the internal system plus the external model for the base case. be the same as the one obtained from the state estimation. This is accomplished by so-called boundary matching which consists of the following steps:

1. From the state estimation. obtain the estimated flows from the boundary buses into the internal system.

2. Using the external system model together with the complex voltages of the boundary buses from the state estimation. compute the flows from the external network into the boundary buses.

3. For each boundary bus. add power injections so that the flows into and out of that bus are balanced.

After boundary matching, the adjusted external model (the original external model plus the boundary injections) is attached to the internal system as the load-flow for evaluating system response to contingencies.

2.3 Load-Flow Equations and Notation

In this thesis, vectors and matrices are printed in bold face, e.g. **EY**. E_k denotes the kth component of the vector **E**, and Y_{kj} denotes the kjth element of the matrix **Y**. E_k^* is the complex conjugate of E_k. $\Delta \mathbf{P}/\mathbf{v}$ represents a vector, the kth component of which is $\Delta P_k / v_k$. [**E**] represents a diagonal matrix, the kth diagonal of which is E_k.

Let $E_k = V_k e^{j\theta_k}$ be the complex (phasor) voltage at bus k, I_k and $S_k = P_k + jQ_k$ be, respectively, the complex (phasor) current injection and the complex power injection into the network from bus k. Thus in matrix notation

$$\mathbf{S} = [\mathbf{E}]\mathbf{I}^* \tag{2.1}$$

The complex current injection can be expressed using the network bus admittance matrix $\mathbf{Y} = \mathbf{G} + j\mathbf{B}$.

$$\mathbf{I} = \mathbf{YE} \tag{2.2}$$

Substituting equation (2.2) into equation (2.1) and separating the real and imaginary parts, the standard load flow equations are obtained in polar coordinates [17]

$$P_k = \sum_l V_k V_l \{ G_{kl} \cos(\theta_k - \theta_l) + B_{kl} \sin(\theta_k - \theta_l) \} \tag{2.3}$$

$$Q_k = \sum_l V_k V_l \{ G_{kl} \sin(\theta_k - \theta_l) - B_{kl} \cos(\theta_k - \theta_l) \} \tag{2.4}$$

Two kinds of data are required to set up the load-flow equations (2.3) and (2.4). The first is the data regarding the network configuration and the branch admittances, *i.e.* to specify the bus admittance matrix **Y**. This is called the network data, and it is based on the breaker status and line impedances, *etc.* The second kind of data is that used to determine the operating point of a given network. This is called operating-point data, and it includes real and reactive power demand at a *PQ* bus, the real power generation and the voltage magnitude at a *PV* bus. The network data changes rather infrequently, whereas the operating-point data may change from minute to minute.

The incremental form of the load-flow equations (2.3) and (2.4) can be approximated by the following decoupled load-flow equations [18]:

$$\left(\frac{\Delta \mathbf{P}}{\mathbf{V}}\right) = \mathbf{B}' \Delta \theta \tag{2.5}$$

$$\left(\frac{\Delta \mathbf{Q}}{\mathbf{V}}\right) = \mathbf{B}'' \Delta \mathbf{V} \tag{2.6}$$

where for systems consisting of only basic bus types, $\mathbf{B}'$ has the dimension of the total number of buses minus one and is obtained from $-\mathbf{B}$ (of the bus admittance matrix **Y**

$= \mathbf{G} + j\mathbf{B}$) by, first, neglecting the shunts; secondly, using the reciprocal of the branch reactance as branch susceptance and, thirdly, setting taps to nominal values. $\mathbf{B}''$ has the dimension of the total number of *PQ* buses and is obtained from $-\mathbf{B}$ by, first, deleting rows and columns corresponding to *PV* buses; secondly, doubling the shunts [93], and thirdly, ignoring phase shifters. For systems having other types of buses, some modifications may be needed.

2.4 Review of Ward Equivalent

An interconnected power system can be separated into three parts: internal, boundary and external (Fig. 2.1).

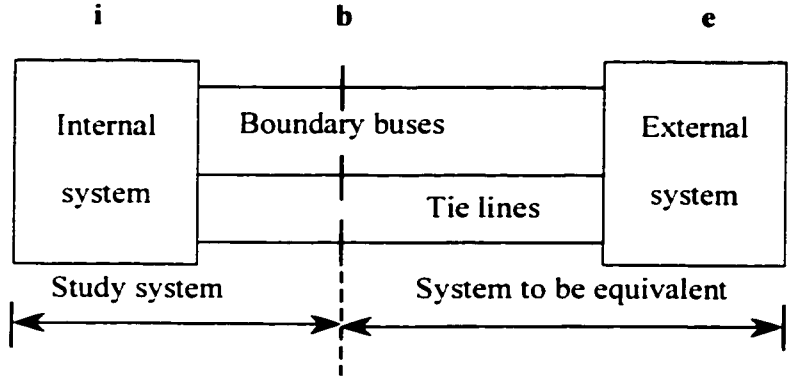

Fig. 2.1 Interconnected power system

2.4.1 Conventional Ward Equivalent Approach

In the basic version of the Ward equivalent, the whole external system is equivalenced (Fig. 2.2). Hence the set of buses can be partitioned into external (subscript *e*), boundary (subscript *b*), and internal (subscript *i*) buses. For an original unreduced system, we obtain:

$$\begin{bmatrix} \mathbf{Y}_{ee} & \mathbf{Y}_{eb} & \mathbf{0} \\ \mathbf{Y}_{be} & \mathbf{Y}_{bb}^{e} + \mathbf{Y}_{bb}^{t} & \mathbf{Y}_{bt} \\ \mathbf{0} & \mathbf{Y}_{tb} & \mathbf{Y}_{tt} \end{bmatrix} \begin{bmatrix} \mathbf{E}_e \\ \mathbf{E}_b \\ \mathbf{E}_t \end{bmatrix} = \begin{bmatrix} \mathbf{I}_e \\ \mathbf{I}_b \\ \mathbf{I}_t \end{bmatrix} \tag{2.7}$$

where **Y** is bus admittance matrix.

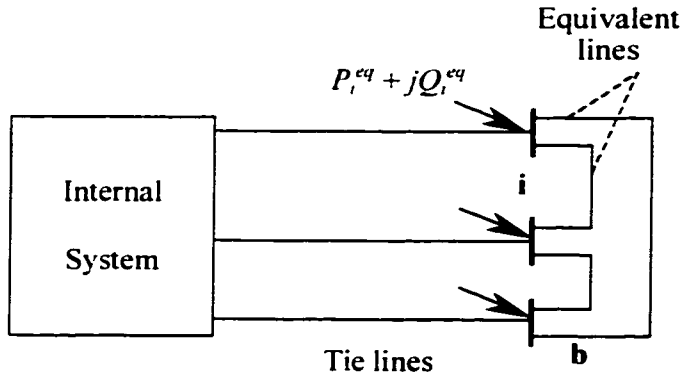

Fig. 2.2 Ward Equivalent Network

By Gaussian elimination to eliminate the variable $\mathbf{E}_e$ in Equation (2.7), one obtains

$$\begin{bmatrix} \ddots & \cdots & \cdots \\ \mathbf{0} & \mathbf{Y}_{eq} + \mathbf{Y}_{bb}^{t} & \mathbf{Y}_{bt} \\ \mathbf{0} & \mathbf{Y}_{tb} & \mathbf{Y}_{tt} \end{bmatrix} \begin{bmatrix} \mathbf{E}_e \\ \mathbf{E}_b \\ \mathbf{E}_t \end{bmatrix} = \begin{bmatrix} \cdots \\ \mathbf{I}_b + \mathbf{I}_{eq} \\ \mathbf{I}_t \end{bmatrix} \tag{2.8}$$

where the off-diagonal elements of $\mathbf{Y}_{bb}^{t}$ are the negative of the branch boundary admittances. The diagonal elements of $\mathbf{Y}_{bb}^{t}$ include admittances of branches connecting boundary-boundary buses and boundary-internal buses. $\mathbf{Y}_{bb}^{e}$ is a diagonal matrix the elements of which are the sum of admittances of branches connecting boundary to external buses. Then,

$$\mathbf{Y}_{eq} = \mathbf{Y}_{hh}^{e} - \mathbf{Y}_{he}\mathbf{Y}_{ee}^{-1}\mathbf{Y}_{eh} \tag{2.9}$$

$$\mathbf{I}_{eq} = \mathbf{Y}_{he}\mathbf{Y}_{ee}^{-1}\mathbf{I}_{e} \tag{2.10}$$

Under steady state condition the effect of the external on the internal system is reflected by the active and reactive power flow from the external system into the boundary buses. It is easy to calculate the equivalent injections at boundary buses. The resulting boundary injection power from the external injection $\mathbf{S}_e = [\mathbf{E}_e]\mathbf{I}_e^*$ can be obtained from equation (2.10):

$$\mathbf{S}_{eq} = [\mathbf{E}_h]\mathbf{Y}_{he}^{*}(\mathbf{Y}_{hh}^{*})^{-1}[\mathbf{E}_e^{*}]^{-1}\mathbf{S}_e^{*} \tag{2.11}$$

Since boundary matching is to be performed for online applications, there is no need actually to compute $\mathbf{S}_{eq}$ as in equation (2.11).

To summarize, there are four basic steps in the construction of a Ward equivalent:

1. Determination of the external network data from available information.

2. Obtaining the Ward equivalent network $\mathbf{Y}_{eq}$ by Gaussian elimination as in equation (2.9).

3. Using the values for the complex voltages at the boundary buses from the internal state-estimation to compute the flows in the Ward equivalent branches.

4. Boundary matching.

For contingency studies, it is generally observed that the Ward equivalent gives reasonably good results for active power flows. The poor results usually occur in the reactive power flows when there are external PV buses. The problem arises owing to the failure of the Ward equivalent to represent PV buses.

After eliminating all external PQ buses but retaining external PV buses, Ward-PV equivalent network is obtained. Ward-PV equivalent can provide accurate results for both active and reactive power flows. However, if the number of such buses is high, or it is inconvenient or impossible to retain external buses by eliminating all external PQ buses but retaining external PV buses, some alternative methods are required.

2.4.2 Extended Ward Equivalent Approach

Monticelli *et al.* [93-94] have derived a Ward-type equivalent, called the extended Ward equivalent, which is intended to combine the simplicity of the Ward equivalent with the response of the Ward-PV equivalent (Fig. 2.3). The extended Ward equivalent is the Ward equivalent with additional reactive support at the boundary buses such that its reactive response is close to that of the Ward-PV equivalent.

In Fig. 2.2 and equation (2.7), the external buses are further partitioned into PQ bus (subscript Q) and PV bus (subscript V). Then, the original system before reduction has the bus admittance matrix as follow:

$$\begin{array}{c} \\ Q \\ V \\ b \\ i \end{array}\begin{array}{c} \begin{array}{cccc} Q & V & b & i \end{array} \\ \begin{bmatrix} \mathbf{Y}_{QQ} & \mathbf{Y}_{QV} & \mathbf{Y}_{Qb} & \mathbf{0} \\ \mathbf{Y}_{VQ} & \mathbf{Y}_{VV} & \mathbf{Y}_{Vb} & \mathbf{0} \\ \mathbf{Y}_{bQ} & \mathbf{Y}_{bV} & \mathbf{Y}^{e}_{bb} + \mathbf{Y}^{i}_{bb} & \mathbf{Y}_{bi} \\ \mathbf{0} & \mathbf{0} & \mathbf{Y}_{ib} & \mathbf{Y}_{ii} \end{bmatrix} \end{array} \tag{2.12}$$

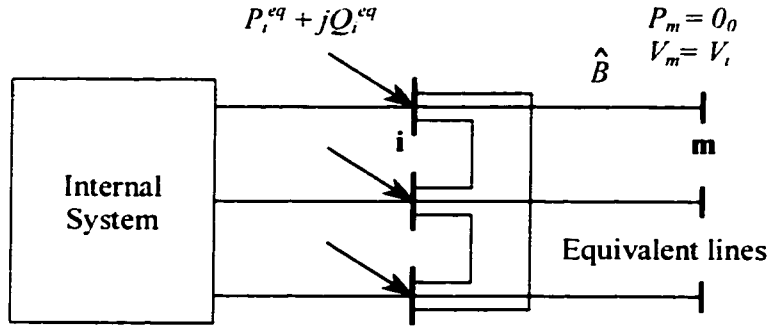

Fig. 2.3 Extended Ward Equivalent

After elimination of external PQ buses but retaining all external PV buses, the Ward-PV equivalent network is obtained, and the associated bus admittance matrix is:

$$\begin{array}{c} \\ Q \\ V \\ b \\ i \end{array}\begin{array}{c} \begin{array}{cccc} Q & V & b & i \end{array} \\ \begin{bmatrix} \ddots & \cdots & \cdots & \cdots \\ \mathbf{0} & \mathbf{Y}'_{VV} & \mathbf{Y}'_{Vb} & \mathbf{0} \\ \mathbf{0} & \mathbf{Y}'_{bV} & \mathbf{Y}'^{e}_{bb} + \mathbf{Y}'^{i}_{bb} & \mathbf{Y}_{bi} \\ \mathbf{0} & \mathbf{0} & \mathbf{Y}_{ib} & \mathbf{Y}_{ii} \end{bmatrix} \end{array} \tag{2.13}$$

Recall that the $\mathbf{B}''$ matrix in the decoupled reactive power flow equation (2.6) is derived from $-\mathbf{B}$ of $\mathbf{Y} = \mathbf{G} + j\mathbf{B}$ by deleting rows and columns corresponding to PV buses, doubling the shunts, and ignoring phase shifters. Thus after deleting the rows and columns of V, the incremental decoupled reactive power flow equation of the Ward-PV equivalent takes the form:

$$\begin{bmatrix} \mathbf{B}''_{ww} + (\mathbf{B}'_{hh})'' & \mathbf{B}''_{ht} \\ \mathbf{B}''_{th} & \mathbf{B}''_{tt} \end{bmatrix} \begin{bmatrix} \Delta\mathbf{V}_h \\ \Delta\mathbf{V}_t \end{bmatrix} = \begin{bmatrix} \Delta\mathbf{Q}_h / \mathbf{V}_h \\ \Delta\mathbf{Q}_t / \mathbf{V}_t \end{bmatrix} \tag{2.14}$$

where w represents the Ward equivalent network, and the same subscripts and superscripts are used for the corresponding $\mathbf{B}''$ and $\mathbf{Y}$, and the necessary modifications on the retained *PV* buses are not performed because they are not of direct interest here. From equation (2.14), it is seen that the reactive power response of the Ward-*PV* equivalent to the changes in boundary bus voltages $\Delta\mathbf{V}_h$ is:

$$[\Delta\mathbf{Q}_h^{ww}] = [\mathbf{V}_h]\mathbf{B}''_{ww}\Delta\mathbf{V}_h \tag{2.15}$$

For the Ward equivalent, one can proceed further to eliminate the external *PV* buses (U) corresponding bus admittance matrix to be:

$$\begin{bmatrix} \ddots & \cdots & \cdots & \cdots \\ \mathbf{0} & \ddots & \cdots & \mathbf{0} \\ \mathbf{0} & \mathbf{0} & \mathbf{Y}^w_{hh} + \mathbf{Y}'_{hh} & \mathbf{Y}_{ht} \\ \mathbf{0} & \mathbf{0} & \mathbf{Y}_{th} & \mathbf{Y}_{tt} \end{bmatrix} \tag{2.16}$$

Since there are no *PV* buses in the Ward equivalent, the incremental decoupled reactive power flow equation (2.6) of the Ward equivalent is given by:

$$\begin{bmatrix} \mathbf{B}''_{w} + (\mathbf{B}'_{hh})'' & \mathbf{B}''_{ht} \\ \mathbf{B}''_{th} & \mathbf{B}''_{tt} \end{bmatrix} \begin{bmatrix} \Delta\mathbf{V}_h \\ \Delta\mathbf{V}_t \end{bmatrix} = \begin{bmatrix} \Delta\mathbf{Q}_h / \mathbf{V}_h \\ \Delta\mathbf{Q}_t / \mathbf{V}_t \end{bmatrix} \tag{2.17}$$

From the above equation, the reactive power response of the changes in boundary voltages becomes:

$$[\Delta \mathbf{Q}_h^w] = [\mathbf{V}_h]\mathbf{B}_w''\Delta \mathbf{V}_h \tag{2.18}$$

By comparing equations (2.15) and (2.18), it is apparent that if the Ward equivalent is desired to have the same reactive response as the Ward-*PV* equivalent, reactive injections should be added at the boundary buses of the amount

$$\Delta \tilde{\mathbf{Q}}_h = [\mathbf{V}_h](\mathbf{B}_{wv}'' - \mathbf{B}_w'')\Delta \mathbf{V}_h \tag{2.19}$$

This scheme gives excellent overall accuracy [93], but it is not very convenient to use because the reactive support at the boundary buses as required by equation (2.19) cannot be directly incorporated in a load-flow program. An approximation to equation (2.19) that can be directly implemented in a load-flow program will be derived.

Let $\bar{\mathbf{B}} = (\mathbf{B}_{wv}'' - \mathbf{B}_w'')$

It is desired to construct a network the corresponding $\mathbf{B}''$ matrix of which is $\bar{\mathbf{B}}$. The kth component of equation (2.19) is:

$$\begin{aligned} \Delta \tilde{Q}_k / V_k &= \bar{B}_{kk}\Delta V_k + \sum_{m \neq k} \bar{B}_{km}\Delta V_m \\ &= \bar{B}_k \Delta V_k + \sum_{m \neq k} \bar{B}_{km}(\Delta V_m - \Delta V_k) \end{aligned} \tag{2.20}$$

where

$$\bar{B}_k = \bar{B}_{kk} + \sum_{m \neq k} \bar{B}_{km} \tag{2.21}$$

Let the *km*th element of $\mathbf{B}''_{wv}$ and $\mathbf{B}''_{w}$ be B^{wv}_{km} and B^{w}_{km}, respectively. The *k*th diagonal element of $\mathbf{B}''_{wv}$ is

$$-\sum_{\substack{m\neq k\\ m\in h}} B^{wv}_{km} - \sum_{j\in l'} B^{wv}_{kj} - B_k \text{ shunt} \tag{2.22}$$

The *k*th diagonal element of $\mathbf{B}''_{w}$ is

$$-\sum_{\substack{m\neq k\\ m\in h}} B^{w}_{km} - B_k \text{ shunt} \tag{2.23}$$

Substituting equations (2.22) and (2.23), B^{wv}_{km}, and B^{w}_{km} into equation (2.21), one obtains:

$$\tilde{B}_k = -\sum_{j\in l'} B^{wv}_{kj} \tag{2.24}$$

That is, the susceptance ($-\tilde{B}_k$) from bus *k* to the fictitious *PV* bus is equal to the sum of the susceptances from bus *k* to the external *PV* buses in the Ward-*PV* equivalent.

If equation (2.20) is considered again the following observations are made:

- The combined effect of the second term to the internal system is zero, *i.e.*

$$\sum_{k}\sum_{m\neq k} \tilde{B}_{km}(\Delta V_m - \Delta V_k) = 0 \tag{2.25}$$

- When $(\Delta V_m - \Delta V_k)$ is small, the second term is small.

- When $(\Delta V_m - \Delta V_k)$ is appreciable, it means ΔV_m and ΔV_k respond very differently. Physically, this happens when *m* and *k* are not tightly coupled, *i.e.* the impedance between them is large, or $\tilde{B}_{km}$ is small.

- When B_{km}^{wv} and B_{km}^{w} are equal, the second term becomes zero.

In view of these observations, the second term in equation (2.20) is neglected and the reactive response from the external system, equation (2.19) is approximated by

$$\Delta\tilde{Q}_k = V_k \tilde{B}_k \Delta V_k \tag{2.26}$$

When applying the extended Ward equivalent, extra injections $\Delta\tilde{Q}_k$ can be added to the non-eliminated buses to correct reactive power response of conventional Ward equivalent.

To summarize, the construction of an extended Ward equivalent has the following basic steps:

1. Obtain a Ward equivalent of the external system. (External shunts are converted to injections.)

2. Start again from the original system. Ground all external *PV* buses. Apply Gaussian elimination on the bus admittance matrix Y to eliminate all external buses to obtain the equivalent shunts at the boundary buses, which are the admittance $j\tilde{B}_k$.

In contingency analysis, the fictitious *PV* buses will respond with the supply or absorption of reactive power when the voltage magnitude of boundary buses is greater or less than in the pre-contingency operating condition. The voltage magnitudes of these fictitious PV buses can be obtained from the state estimation of the internal system. The reactive power response from the external system can then be simulated once the fictitious branches $\tilde{B}$ are determined.

The extended Ward equivalent gives reasonable accuracy for both active and reactive power flows. In on-line applications, the operating conditions of the external system vary with time. The extended Ward equivalent model can reflect the load condition changes of the external system by matching the boundary equivalent power injections, but fail to simulate significant configuration changes since it is very difficult to obtain all the on-line topology information from the external system. Furthermore, even if the information is known, it will require much computation to perform the equivalencing frequently. The extended Ward equivalent method is therefore not suitable for on-line modeling of significant configuration changes of the external system.

2.5 Partition of External Network

In order to monitor effectively the internal system and keep the external system model up to date and realistic, the fictitious branch $\bar{B}$ must be updated as the topology of the external system changes. Clearly the values of $\bar{B}$ depend on the topology and parameters of the external system and these can be stored in advance. In theory, the line status of the external system can be obtained from the external system. But since the external system is usually very large, it is impossible to know all topology information from the external system in on-line applications.

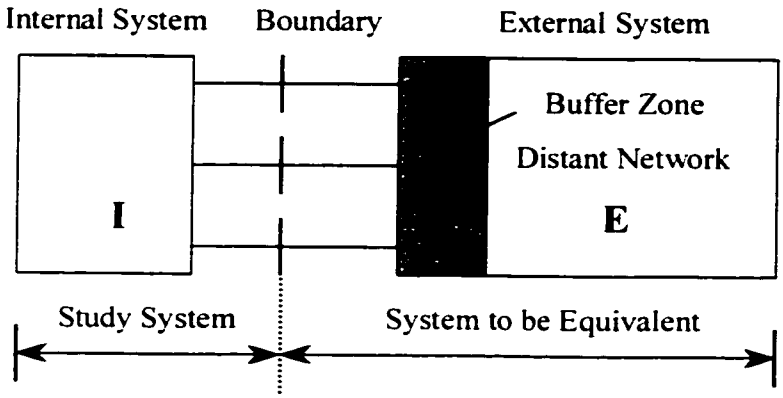

Fig. 2.4 Power system with four subsystems

Reference [59] leads us to the more sophisticated techniques which employ "external models". The idea is to have security analysis based on a network model which has generally three subnetworks as follows:

Subnetwork 1: The internal transmission network is modeled in detail due to its primary importance to the security of the internal system.

Subnetwork 2: A portion of the external network that is electrically close to the internal system and hence has significant impact on the security of the internal system. This part of the external network is modeled in detail in order to produce accurate load flow calculations and subsequent contingency analysis.

Subnetwork 3: The other portion of the external network that is electrically more distant and thus has less influence on the internal system. It is modeled by reduced equivalents.

Reference [59] pointed out that the external system could be divided into two parts, one with a detailed load flow model and one without. The part of the external network, for which the detailed load flow model is retained, is referred to as the inner external system, and the remaining part, for which a reduced model is used, as the outer external system (Fig. 2.4). The inner external system is called a buffer zone and the outer external system is called distant network.

The line outages in buffer zone would strongly affect the equivalent parameter of the external system. On the contrary, the distant network has less or no effect on the equivalent parameter of the external system and thus the information of the line status in the distant network is not required.

Since the buffer zone is electrically close to the internal system and has significant impact on the security of the internal system, its line outages would strongly affect the equivalent parameter of the external system. In this case, the fictitious branches $\hat{B}$ should be updated to correctly matching the external power injection. On the contrary, the distant network has less or no effect on the equivalent parameter of the external system and the information of the line status in the distant network is not required.

2.6 ANN Used in Network Reduction

ANNs have been successfully applied to some power system problems where difficulties have been experienced with conventional techniques. Multi-layer feed-forward neural networks have the advantages of robustness to input and system noise, handling situation of incomplete information and corrupt data, learning from example, and performing in real time. With these properties, multi-layer neural network is a good candidate for on-line identification of external system equivalent.

When the loading conditions change or in contingencies, the equivalent power injection will be updated using the real-time data. The implementation of the new approach can be expressed by the following mapping:

(operation condition)

$\Rightarrow$ (boundary equivalent power injection condition)

This mapping is carried out with a multi-layer neural network, which is a very powerful pattern classifier. The details of this method will be introduced in Chapter 5.

2.7 Summary

A review of various external network modeling methods is presented. Ward-type equivalent methods and Radial Equivalent Independent (REI) methods are most popular steady-state equivalent approaches. The load flow equations and notation are firstly presented in this chapter. Then, theories and concepts of basic Ward equivalent and extended Ward equivalent are discussed in this chapter. Moreover, the external system is divided into two parts: inner external network and outer external equivalent in order to effectively monitor the internal system and keep the external system model up to date. How to use ANN in external equivalent is also briefly discussed in this chapter.

Chapter 3

Artificial Neural Network Techniques

3.1 Introduction

Artificial neural networks (ANNs) are computational models built around massive parallel interconnected proceeding elements. ANN methodology has been applied in areas where conventional techniques have not achieved the desired speed and accuracy. Successful applications of ANN on power system have been widely reported, which include the following: voltage stability enhancement, reactive power planning, voltage security assessment, alarm processing, harmonics load identification, fault diagnosis, load forecasting, *etc*. Since ANNs are quick in response time and can be easily adapted, they become good candidates for on-line application in areas where inadequate input data are available or excessive computational burden has rendered other approaches impractical for implementation.

This chapter is organized as follows: first, the basic theory of multi-layer neural network is discussed. Secondly, the concept of Kohonen unsupervised neural network is presented. Thirdly, the concept of hybrid supervised and unsupervised neural network is presented. A guideline on how to choose input is discussed in this chapter.

3.2 Multi-layer Feed-forward Neural Network

A multi-layer feed-forward neural network with error back-propagation learning (BP) is one of the most widely utilized neural networks. It consists of three basic elements: 1) an organized topology of interconnected neurons, 2) a suitable learning algorithm, and 3) a method of recalling information.

Appropriate selection of input variables is the key to the success of ANN applications. Usually heuristic knowledge is required in choosing input variables. The computational power of the ANN is a result of the addition of hidden layers. But there are no general guidelines to determine the number of hidden layers and neurons. Many applications have proved that ANNs with one single-hidden layer possess sufficient capability of capturing complicated relations between input and output variables. Determination of the output layer is usually straightforward.

3.2.1 Topology of the ANN

A typical feed-forward neural network is illustrated in Fig. 3.1. A three-layered network is shown, but in principle there could be more than one layer of internal representation units. The architecture of the multi-layer neural networks consists of an input layer, an output layer, and several intermediate layers which contain hidden units.

Processing elements in an ANN are known as neurons. There is a connection strength or weight associated with each connection. The neuron calculates its output by finding the weighted sum of its inputs and then applying an activation function which produces an

activation level inside the neuron. The activation function is passed through an output, or transfer function, which produces the actual output for that neuron. Generally, the activation function is Sigmoid function and linear for the hidden and output layers, respectively. The network can recognize input patterns once the weights are adjusted using a suitable learning process [88, 89].

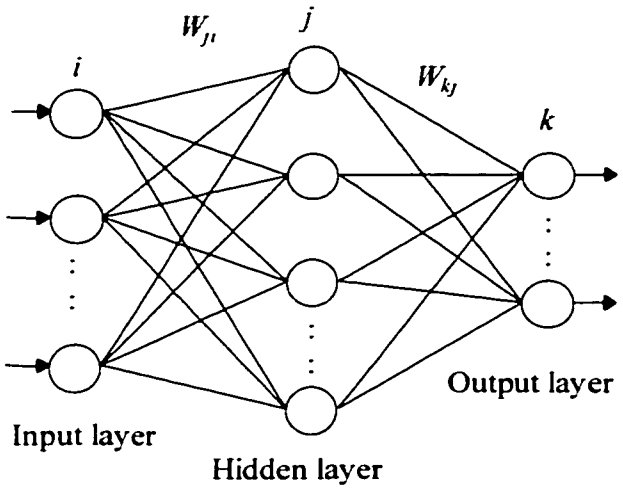

Fig. 3.1 Three layers neural network

Thus if o_i are the outputs of units in layer i, the total input to a unit in layer j is

$$net_j = \sum_i W_{ji} o_i \tag{3.1}$$

and the output of a unit in layer j is

$$o_j = f(net_j) \tag{3.2}$$

where f is the activation function or transfer function.

A convenient logistic activation function is represented by the relation

$$o_j = f(net_j) = \frac{1}{1+\exp(-(net_j - \theta_j)/\theta_0)} \tag{3.3}$$

This f function yields an output which varies continuously from 0 to 1. The quantity θ_j serves as a "threshold" and positions the transition region of the f function. The quantity θ_0 determines the abruptness of the transition. An example of such a function is shown in Fig. 3.2.

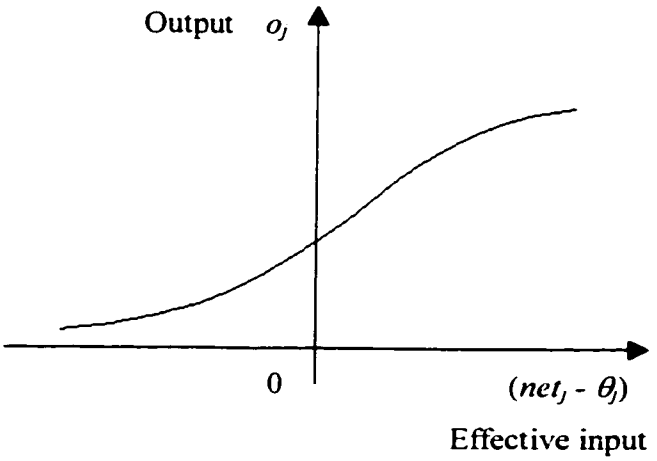

Fig. 3.2 A Sigmoidal activation function

In learning the hidden representation, that is, the weights and the threshold values, the network functions solely in a feed-forward manner as described by expressions (3.1) and (3.3).

The Input Layer

Appropriate selection of input variables is the key to the success of many ANN applications. Usually heuristic knowledge is required in choosing input variables.

A general guide for the input layer is that it should include as many neurons as needed for desired input information. However, as indicated in reference [51], the system data selected for this layer should show close correlation with the power system parameters which help to predict the system insecurity. The selection of appropriate inputs is one of the most important tasks. Different objective has different input information. One of the key issues in such applications is how to select limited variables, with salient features as the input information of the neural network, to represent the power system operating conditions in a large-scale power system.

The Hidden Layer

The computational power of the ANN is a result of the addition of hidden layers. But there are no general guidelines to determine the number of hidden layers and neurons. Using a larger number of hidden neurons per unit may result in better performance. Adding hidden neurons can improve network performance, however, only to a certain extent. Tests reported in [115] showed that too many hidden neurons cannot increase precision as expected, on the contrary, sometimes even decrease precision. Moreover, oscillation may possibly occur. Many applications have proved the ANNs with one single-hidden layer possess sufficient capability of capturing complicated relations between input and output variables.

The Output Layer

Determination of the output layer is quite straight-forward. For voltage estimation problem, one output neuron is required. The unipolar sigmoidal activation function is preferred.

3.2.2 The BP Algorithm

The back-propagation learning algorithm is one of the most frequently used methods in training multi-layer neural networks. The BP algorithm is based on the concept of gradient descent search to minimize the error through the adjustment of weights. For a three layer ANN with i inputs, one hidden layer with j neurons and k output neurons, the error function is defined as follows:

$$E_p = \frac{1}{2}\sum_{k=1}^{K}(d_{pk} - o_{pk})^2 \tag{3.4}$$

where d_{pk} and o_{pk} are the desired and actual outputs of the ANN for pattern p, respectively; $p = 1, 2, \ldots, P$ with P being the number of training patters. Individual weight adjustments are computed by:

$$\Delta W_{kj} = -\eta \frac{\partial E_p}{\partial W_{kj}} \tag{3.5}$$

where η is a learning rate constant. Through some derivations, the following recursive formulas for the adjustment of weights with the momentum term are obtained.

For the output layer:

$$W_{kj}^{l+1} \Leftarrow W_{kj}^{l} + \eta \Delta W_{kj}^{l} + \alpha \Delta W_{kj}^{l-1} \tag{3.6}$$

where $\Delta W_{kj}^{l} = \delta_{ok} y_j$; $\delta_{ok} = (d_k - o_k) o_k (1 - o_k)$; y_j is the output of the jth hidden neuron; α is a momentum constant between 0.1 and 0.8; $k = 1, 2, \ldots, K$ and $j = 1, 2, \ldots, J$.

For the hidden layer:

$$v_{ji}^{l+1} \Leftarrow v_{ji}^{l} + \eta \Delta v_{ji}^{l} + \alpha \Delta v_{ji}^{l-1} \tag{3.7}$$

where $\Delta v_{ji}^{l} = y_j (1 - y_j) x_i \sum_{k=1}^{K} \delta_{ok} w_{kj}^{l}$; and $i = 1, 2, \ldots, I$; x_i is the value of the ith input variable.

For a given error tolerance E_{max}, learning rate η, momentum α and maximum learning cycle, the ANN with randomly initialized weights is trained through repeated presentation of the training patterns until the error goal or maximum training cycle is reached.

3.3 Kohonen Self-organizing Feature Map

The unsupervised learning concept, also called self-organization, can be effectively used to discover similarities among unlabelled patterns.

Mathematical models describing the self-organizing map (SOM) networks were developed by Tuevo Kohonen between 1979 and 1982 [103]. Kohonen self-organizing feature map belongs to a class of unsupervised neural networks which are very effective for pattern classification problems. It serves two purposes, the quantization and dimensionality reduction of data. It is shown that the inherent classification properties of the feature map make it a suitable candidate for solving the classification task in power system areas like load forecasting, fault diagnosis and security assessment.

Referring to Fig. 3.3, a Kohonen network typically consists of an input layer and a two-dimensional Kohonen layer, which maps a distribution of N-dimensional vectors into two dimensions in a nonlinear way, preserving the ordering of high-dimension input data. The input vectors are fully connected to each Kohonen neuron. Input vectors are presented sequentially in time without specifying the desired output. With the Kohonen network, input data with similar features are mapped to clusters after enough input vectors have been presented. The similarity between input vectors can be measured by the Euclidean distance between two m-dimensional vectors. The algorithm that forms the output map requires a neighborhood to be defined around each node as shown in Fig. 3.4. This neighborhood slowly decreases in size to end up with just a single neuron as the learning proceeds.

As shown in Fig. 3.3, N inputs $X_1, X_2, \ldots, X_N$, are mapped onto M output nodes $Y_1, Y_2, \ldots, Y_M$. Each input unit i is connected to an output unit j through connection weight W_{ij}. The continuous valued input pattern and connection weights will give the output node j continuous valued activation value A_j,

$$A_j = \sum_{i=1}^{N} W_{ij} X_i = W_j X \tag{3.8}$$

where $X = [X_1, X_2, \ldots, X_N]$ is the input vector and $W_j = [W_{1j}, W_{2j}, \ldots, W_{Nj}]^T$ is the connection weight vector for output node j.

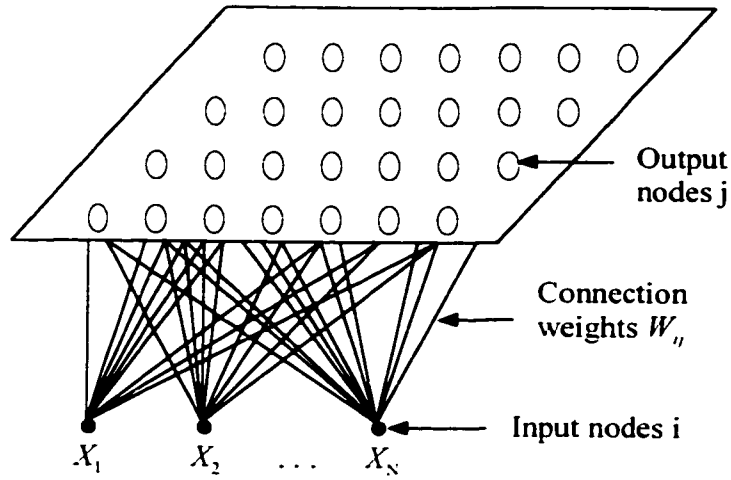

Fig. 3.3 Structure of self-organizing feature maps

A competitive learning rule is used, choosing the winner c as the output unit with weight vector closest to the current input pattern vector,

$$\|X - W_c\| = \min_j \|X - W_j\| \tag{3.9}$$

where $\|\cdots\|$ defines the Euclidean distance, or norm, between the two vectors.

It must be pointed out that, for the best match criterion stated in equation (3.9) to be applicable, the weight vectors must be normalized to unit length in weight space.

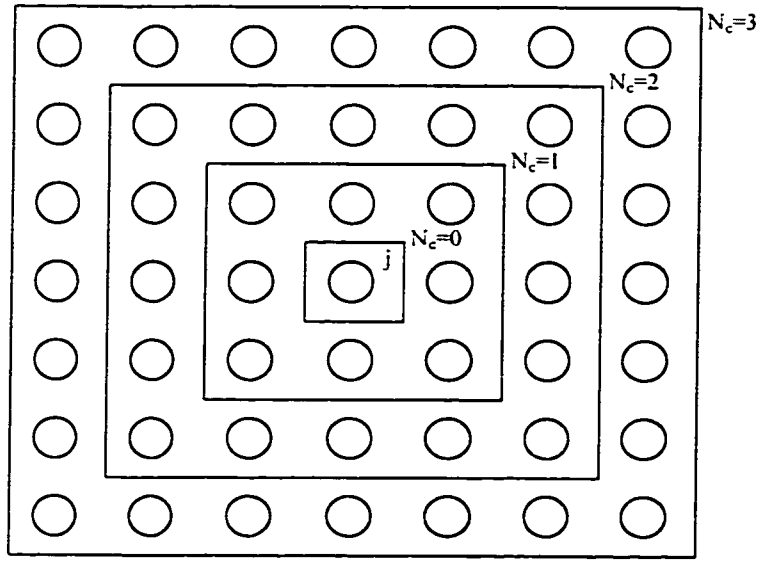

Fig. 3.4 Neighboring nodes for *j*th node

The learning rule is of the form

$$\frac{dW_{ij}}{dt} = \alpha(t)\left[A_j(t)X_i(t) - A_j(t)W_{ij}(t)\right] \tag{3.10}$$

where $\alpha(t)$ is a decreasing function of time, to guarantee convergence to a unique limit.

Around the maximally responding unit *c*, a topological neighborhood N_c is defined, such that all units which lie within a certain radius from unit *c* are included in N_c. Taking all

units which are inside N_c to be $A_j(t)=1$, and outside N_c, $A_j(t)=0$, equation (3.10) is simplified to

$$\left.\begin{aligned} \frac{dW_{ij}}{dt} &= \alpha(t)\left[X_i(t)-W_{ij}(t)\right] && \text{for } j \in N_c \\ &= 0 && \text{for } j \notin N_c \end{aligned}\right\} \qquad (3.11)$$

When an input pattern is presented to the neural network without specifying the desired output, the net computes a 'winner' node according to equation (3.9) and updates the weights of that node and its neighboring nodes as specified in equation (3.11). The input pattern is then said to be mapped to the output node.

The procedure of selection and tuning is iterated such that different regions of the two-dimensional grid network become tuned to different input pattern vectors. Thus, the self-organizing process leads to the creation of a topographic two-dimensional map of the input space on to the network, such that each unit may be identified according to which input pattern vectors from the training set it has learned will give the best response. This then allows the units to be grouped into regions or clusters, so that all units in the same cluster respond maximally to the same input pattern vectors. The interesting feature of the mapping is that input patterns that have similar features tend to cluster together, whereas dissimilar features are forced apart.

Kohonen [103] suggested that, for good self-organizing results, both the radius of the neighborhood N_c, and the gain $\alpha(t)$, should decrease as the number of presentations of

input patterns increases. The number of output nodes is defined by the size of the grid network. The radius of neighborhood N_c, is initialized to be 3 and reduce to 0 after 50 iterations, as illustrated in Fig. 3.4. Here, one iteration refers to the action whereby the P input patter vectors $X(1), X(2), \ldots, X(P)$, are presented once at the input nodes.

The time dependence for $\alpha(t)$ is chosen to be of the form $1/t$, which give satisfactory results in this study.

The following summaries the algorithm used in this thesis for training the Kohonen network:

1) *Initialize weights*: Weights between input and output are initially set to small random values and an initial neighborhood is also given.

2) *Present new input*: Present input vectors to the network.

3) *Compute distance to all neurons*: The distance of an input vector from each neuron, can be calculated by use of equation (3.9).

4) *Find the winning neuron*: The Kohonen neuron with the minimum distance is called a winner. In other words, the winner's weight vector is the closest to the input vector.

5) *Update weight vectors of a winning neuron and its neighborhood*: During

training, the winner adjusts its weights to be closer to the values of input data and the neighbors of the winner also adjust their weights to be closer to the same input data vector according to the following relation:

$$W_i = W_i + \alpha(X - W_i)$$
$$i \in \{ Kohonen\ layer \} \tag{3.12}$$

where neuron i belongs to the neighborhood. The term α is a gain term that decreases in time. It may start at a value such as 0.4 and decrease over time to 0.1 or lower [78].

The adjustment of neighboring neurons is instrumental in preserving the order of the input data. Thus the winning neuron is, in a measurable way, the closest to the input values and, thus, represents the input vectors.

6) *Iterate the procedure from step 2*: After training, the weight vectors are self-organized and represent prototypes of classes of input vectors. Input vectors belonging to the same class share same similarities. Applying equation (3.12), the network will map a vector with unknown features to the cluster which its closest training vector has been mapped to.

The output of the SOM can be used as input to a supervised classification neural network such as a back propagation network. The essential advantage of this network is the clustering produced by the SOM which reduces the input space into representative features

using a self-organizing process. Hence the underlying structure of the input space is kept, while the dimensionality of the space is reduced. SOM is one way to achieve this low dimensional representation.

3.4 Hybrid Unsupervised/Supervised Concept

Most of the published work in the area of voltage stability analysis is based on multi-layer feed-forward networks trained by back propagation (BP) for quantifying stability margins. However, a major difficulty of this type of neural networks is that it depends much on the number of training data because the network itself does not take into account the properties of input data. Thus there are voluminous input data related to the output. It would be very time-consuming to train a neural network with all the input data, and the number of connection weights and neurons would be extremely large. It is, thus, essential to reduce the number of inputs to a neural network and to select optimum number of mutually independent inputs which are able to clearly define the input-output mapping. A new ANN based procedure (SOM + ANN) has been implemented in this thesis in order to enhance the accuracy. In this study, we call this procedure as Self-organizing Hierarchy Neural Network (SHNN), which will be used in the later chapter.

The applications of multi-layer neural network and Kohonen network in voltage stability analysis have been reviewed. As it can be seen, these two types of neural network were applied to the different aspects of voltage stability analysis.

Various approaches using this technique share the basic concept that the unsupervised stage tries to map many not very dissimilar patterns to the same output, thus reducing the

burden assigned to the supervised stage. In fact, the supervised stage can perform its learning procedure on the clustered data rather than that on the entire data set. Thus, the information provided to the supervised stage is alternatively composed.

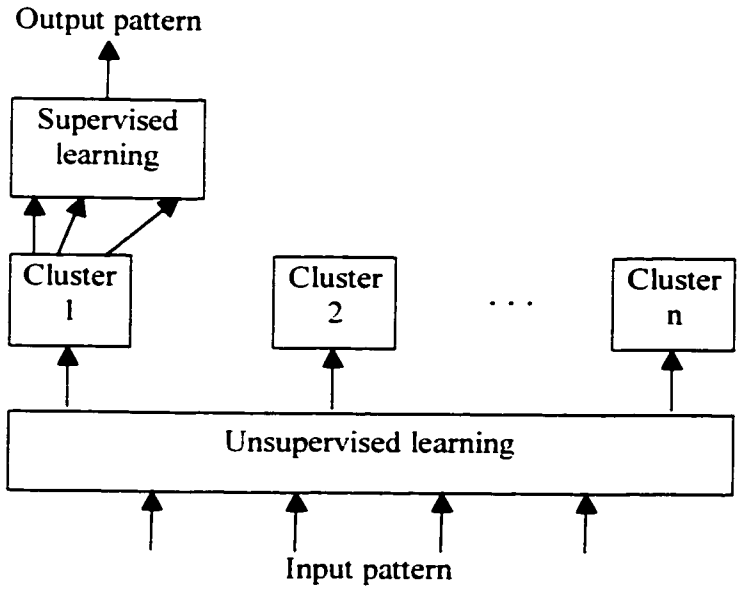

Fig. 3.5 Unsupervised/supervised concept - type 1

The relearning task brings up the issue of information and memory management. A supervised learning system and a hierarchical system are shown in Fig. 3.5 and Fig. 3.6. In Fig. 3.5 we illustrate a situation where in almost every cluster there are a few local regions and separate supervised learning procedures are necessary. In Fig. 3.6 large numbers of training set patterns become represented by prototypes or cluster centers. These cluster centers are then sent forward to a supervised training phase. In fact, an unsupervised learning process performs the role of front-end data compression. Relearning requires localized information when hierarchical structure is used.

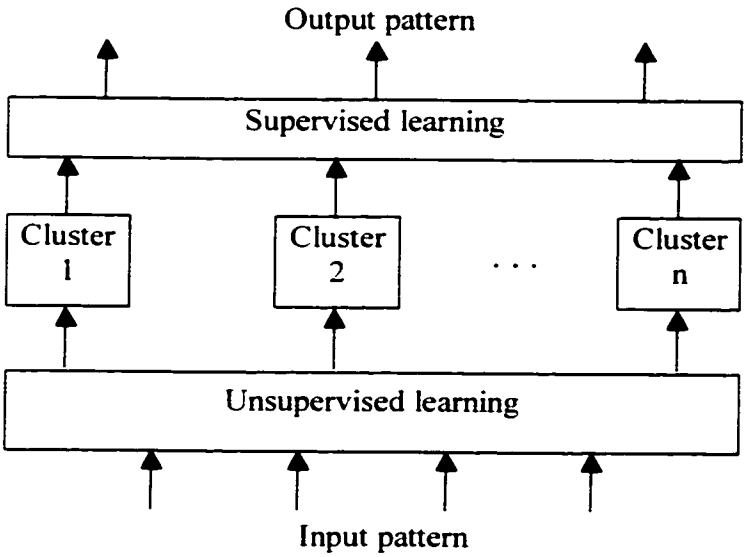

Fig. 3.6 Unsupervised/supervised concept - type 2

The unsupervised/supervised learning concept relieves the net of the burden of trying to associate many dissimilar patterns with the same output. If two groups, which are not alike, happen to end up in the same cluster, the message is that either pattern description is not adequate or the vigilance factor is not adequately stringent. Using this concept, the supervised learning process is carried out on the cluster-wise data structure rather than on the entire data set.

3.5 Apply ANNs on Network Reduction and Voltage Stability

ANNs only depend on input/output samples to form its necessary parameters in pattern recognition, so it is suitable for model identification with rapid response and robustness after being properly trained.

The key issues of voltage security assessment are: (i) the fast identification of insecure contingencies: and (ii) the severity of their impact on power system operation. The solution of these problems involves prediction, pattern recognition, classification and fast solution, and these tasks are well suited for the ANN technology. In this thesis, multi-layer neural networks are used for voltage stability analysis.

The idea of external network equivalent is to build an external network model which accounts for the effect of the external system on the internal system in case of contingencies. The boundary equivalent power injections matching problem may be considered as a pattern recognition problem by recognizing boundary parameters under various power systems operating conditions from trained ANN which stored some similar pattern. In this thesis, ANN is used for on-line boundary injection matching.

The major difficulty of multi-layer neural network is that it depends highly on the number of training data. Thus a large number of inputs are needed. A hybrid neural network which consists of Kohonen network and a multi-layer network is proposed in this thesis for voltage stability analysis.

3.6 Summary

The basic theories and applications of two typical ANNs: multi-layer supervised neural network, and Kohonen unsupervised neural network, are analyzed in this chapter. The idea of hybrid supervised unsupervised neural network is also presented in this chapter.

The multi-layer neural network and a hybrid supervised unsupervised neural network will be applied in later chapter of this thesis.

Chapter 4

A Simple Network Reduction Based Voltage Stability Analysis

4.1 Introduction

Voltage instability in power system is a phenomenon of highly nonlinear nature posing operational as well as prediction problems in power systems control. To obtain a solution to the problem, both static and dynamic modeling methods have been applied. However, most of them are not suitable for real-time application subject to relatively extensive time consuming calculation procedures.

The slower forms of voltage instability are often analyzed as steady-state problem; power flow simulation is the primary study method. The voltage collapse phenomenon is often explained by means of static techniques, and analyzed by means of Q-V and P-V curves at selected load buses [80]. The buses selected for Q-V and P-V analysis must be chosen carefully, and a large number of such curves may be required to obtain complete information [83]. As Q-V and P-V curves are presently the basic tools used to analyze voltage stability in many utilities, it is useful to develop a method which can quickly obtain them.

Modern power systems are large-scale systems in view of topology or system structure. Each power system is one part of the interconnected system. To effectively monitor the internal system and assess its static security, a suitable model for representing the external system is necessary. If a complex system is equivalent to an equivalent one-machine system, the problem becomes much simpler.

In this chapter, a simple network reduction approach is developed for voltage stability analysis. This novel approach is called Modified Two-Point Load-flow Calculation (MTPLC) method. By using this method, Q-V and P-V curves at a study node can be plotted quickly.

This Chapter highlights the way to fast evaluate Q-V and P-V curves. The load flow calculation is based on power calculation, so the constant power load is usually adopted in load flow calculation. The load adopted in this chapter is constant power load. More discussion about the load will be in Chapter 6.

4.2 Q-V Curves and P-V Curves

P-V curves are useful for conceptual analysis of voltage stability and for study of radial systems. The method is also used for large meshed network where P is the total load in an area and V is the voltage at a critical or representative bus. P can also be the power transfer across a transmission interface or interconnection. Voltage at several busses can be plotted. A disadvantage is that the power flow simulation will diverge near the nose or maximum power point on the curve. Another disadvantage is that generation must be realistically rescheduled as the area load is increased.

A Q-V curve expresses the relationship between the reactive support Q at a given bus and the voltage at that bus.

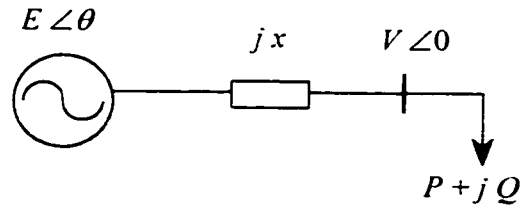

Fig. 4.1 Simple radial system

A complex power system may be approximately represented from the node as a simple equivalent radial system – a synchronous generator ($E\angle\theta$) supplying a load ($P+jQ$) through a reactance x (omit resistance) as shown in Fig. 4.1. The load flow equations become:

$$P = \frac{EV}{x}\sin\theta \tag{4.1}$$

$$Q = \frac{EV}{x}\cos\theta - \frac{V^2}{x} \tag{4.2}$$

Combining (4.1) and (4.2), the relationship between bus voltage magnitude (V) and load (P and Q) can be obtained in the form of:

$$E^2 = \frac{(Px)^2 + (Qx + V^2)^2}{V^2} \tag{4.3}$$

Keep P, x and E constant, a series of Q-V curves is obtained. Similarly, P-V curves can be obtained. Load flows are not convergent at the critical point, which shows instability of the system.

Fig. 4.2 is sketch of Q-V curves. Each Q-V curve represents the relationship between V and Q for a fixed value of P. The system is stable in the region where the derivation dQ/dV is positive. The voltage stability limit (critical operating point) is reached when the derivative is zero. Thus the parts of the Q-V curves to the right of the minima represent stable operation, and the parts to the left represent unstable operation.

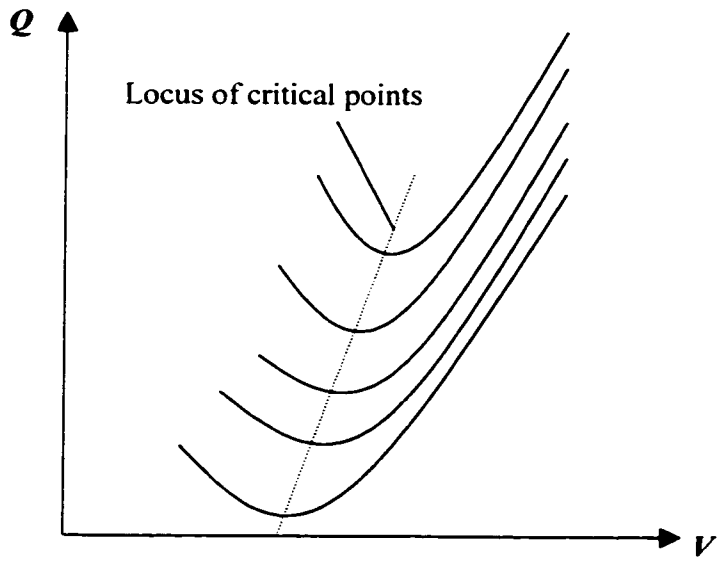

Fig. 4.2 Q-V curves

It must be noted at this point that the Q-V curve is a characteristic of both the network and the load. As the curve aims at characterizing the steady-state operation of the system, the load must be accordingly represented through its steady-state characteristic.

For large systems, the curves are obtained by a series of power flow simulations. *Q-V* curves plot voltage at a test or critical bus versus reactive power on the same bus.

Voltage security is closely related to reactive power, and a *Q-V* curve gives reactive power margin at the test bus. The reactive power margin is the MVAr distance from the operating point to either the bottom of the curve, or to a point where the voltage squared characteristic of an applied capacitor is tangent to the *Q-V* curve (Fig. 4.3). The test bus could be representative of all busses in a "voltage control area" (an area where voltage magnitude changes are coherent).

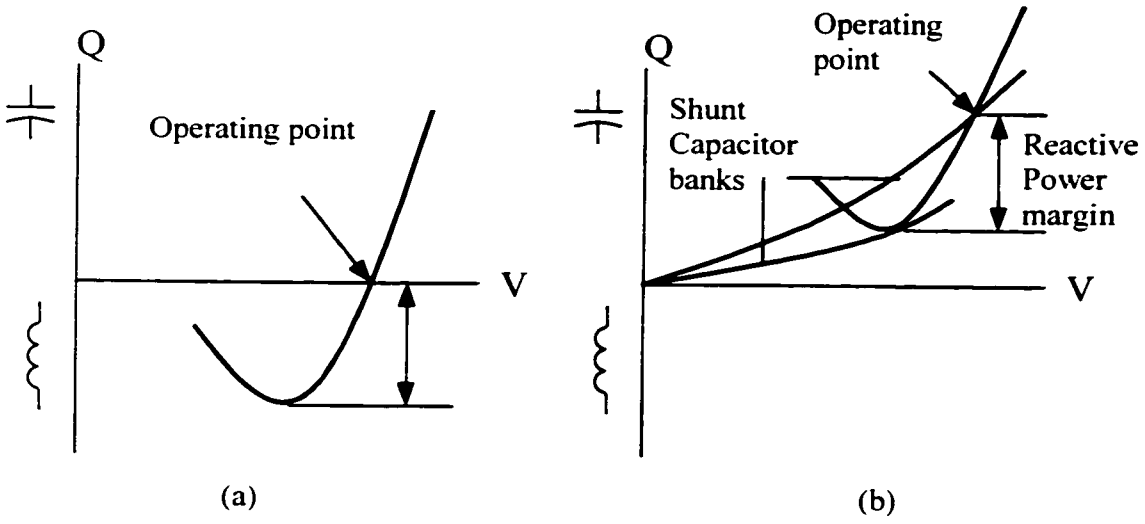

Fig. 4.3 Reactive power margins

The slope of the *Q-V* curve indicates the stiffness of the test bus (the ΔV for a ΔQ). For more insight, the reactive power of generators can be plotted on the same graph. When nearby generators reach their VAr limits. The slope of the *Q-V* curve becomes less steep and the bottom of the curve is approached.

With these advantages, Q-V curves are presently the workhorse method of voltage stability analysis at many utilities.

4.3 Stability Analysis via Network Equivalent

In order to study the voltage stability at a given node, the complex power system may be approximately represented from the node as a simple equivalent radial system as shown in Fig. 4.1. If E and x in equation (4.3) are known, the Q-V curve and P-V curve are plotted.

The constraints of equivalence are to maintain boundary node's voltage, power and current intact. A new equivalence approach may be obtained according to this idea. The main point is to calculate boundary conditions using the original system, and then determining equivalent parameters with these boundary conditions.

4.3.1 Two-Point Load-Flow Calculation (TPLC) Method

The step-by-step procedure carried out in the determination of equivalent parameters E and x at a node are as follows:

1) For a given node and the initial load P_1 and Q_1, calculate voltage V_1 by using a load flow program, *e.g.* by using software Power System Analysis Software Package (PSASP) [84].

2) Let $P_2 = P_1 + \Delta P$, $Q_2 = Q_1 + \Delta Q$, calculate V_2 (note: Δ means a small increment, *e.g.* 0.1 p.u.).

3) Assume that E and x are constants in these two conditions, then:

$$f(x) = [(P_1 x)^2 + (Q_1 x + V_1^2)^2]/V_1^2 - [(P_2 x)^2 + (Q_2 x + V_2^2)^2]/V_2^2 = 0 \qquad (4.4)$$

4) Solve equation (4.4), take the positive real one as the value of x.

5) Calculate E by substituting x into equation (4.3);

6) Go to step 2, record P, Q, V and corresponding E, x until the load flow is not feasible.

The method to calculate E and x is called Two-Point Load-flow Calculation (TPLC) method. If E and x are unchanged, then after the calculation of one group of E and x using TPLC, Q-V curve and P-V curve can be plotted by (4.3). Otherwise, E and x would need to be modified to obtain more accurate curve.

A lot of calculation results show that E and x can be taken as constant initially, and then approach another value near bifurcation point. So E and x must be modified. The results presented in table 4.1 and table 4.2 are for two study cases only.

Table 4.1 Calculated results of E and x (WSCC System [84], bus STNA-230, P=1.25 p.u.)

Q_1 (p.u.)	Q_2 (p.u.)	V_1 (kv)	V_2 (kv)	E	x
0.1	0.2	237.039	235.081	1.0440	0.0854

0.3	0.4	233.089	231.061	1.0440	0.0854
0.5	0.6	228.994	226.887	1.0441	0.0854
0.7	0.8	224.738	222.544	1.0440	0.0854
0.9	1.0	220.298	218.002	1.0441	0.0855
1.1	1.2	215.651	213.236	1.0440	0.0854
1.3	1.4	210.759	208.210	1.0440	0.0854
1.5	1.6	205.585	202.872	1.0440	0.0854
1.7	1.8	200.068	197.160	1.0440	0.0854
1.9	2.0	194.133	190.977	1.0442	0.0855
2.1	2.2	187.668	184.186	1.0441	0.0855
2.3	2.4	180.496	176.562	1.0441	0.0855
2.5	2.6	172.319	167.685	1.0441	0.0854
2.7	2.8	162.526	156.608	1.0441	0.0854
2.9	3.0	149.444	139.549	1.0439	0.0854

Table 4.2 Calculated results of E and x

(New-England 39-bus System [84], bus 4, P=10 p.u.)

Q_1 (p.u.)	Q_2 (p.u.)	V_1 (kv)	V_2 (kv)	E	x
2.0	2.1	340.461	340.008	1.0198	0.0124
3.0	3.1	335.871	335.404	1.0198	0.0124
4.0	4.1	331.135	330.653	1.0199	0.0124
5.0	5.1	326.241	325.742	1.0200	0.0125

Q_1 (p.u.)	Q_2 (p.u.)	V_1 (kv)	V_2 (kv)	E	x
6.0	6.1	321.169	320.652	1.0200	0.0125
7.0	7.1	315.901	315.362	1.0204	0.0125
8.0	8.1	310.410	309.848	1.0205	0.0125
9.0	9.1	304.666	304.076	1.0209	0.0125
10.0	10.1	298.629	298.007	1.0213	0.0126
11.0	11.1	292.249	291.590	1.0216	0.0126
12.0	12.1	285.461	284.757	1.0221	0.0126
13.0	13.1	278.173	277.412	1.0230	0.0127
14.0	14.1	270.251	269.418	1.0238	1.0127
15.0	15.1	261.497	260.565	1.0252	0.0128
16.0	16.1	251.569	250.491	1.0272	0.0129
17.0	17.1	239.802	238.477	1.0302	0.0130
18.0	18.1	224.466	222.564	1.0358	0.0132

4.3.2 Modified Two-Point Load-Flow Calculation (MTPLC) Method

As presented before, E and x can be taken as two group values. The step-by-step procedure carried out in plot Q-V curve is as follows:

1) For a study node and the initial load P_1 and Q_1, calculate its voltage V_1.

2) Set $P_2 = P_1$, $Q_2 = Q_1 + 0.1$, then calculate V_2.

3) Solve equation (4.4), and take positive real one as the value of x_1.

4) Calculate E_1 by substituting x_1 into equation (4.3).

5) Use x_1, E_1 to plot the first section of Q-V curve.

6) Calculate x_2 and E_2 around the point when voltage drops to certain value (note: this value, for example, 0.75 p.u. for these three test systems, depends on the load condition and the network configuration. Different case may use different value which is chosen according to the practical situation.)

7) Use x_2, E_2 to plot the second section of Q-V curve.

After calculating two groups of E and x, a complete Q-V curve is plotted. This approach is called Modified TPLC (MTPLC) method.

If the step 2 is $Q_2 = Q_1$, $P_2 = P_1 + 0.1$, P-V curves can be plotted.

4.4 Test Results

To demonstrate the method for stability analysis described in this thesis, three study systems have been used. System A is EPRI-36 system, System B is WSCC system (3 generators, 9 buses), and System C is New-England 39-Bus Power System (10 generators, 39 buses). Details of these three systems may be found in Appendices.

Table 4.3 Comparison of the maximum error of Q

	A20-1.5	A20-.719	A21-1.0	A9-4.0	BC-1.0	BA-1.25	C4-10.0	C3-3.22
Err_1 (p.u.)	0.3635	0.3180	0.3249	0.5284	0.0076	0.0006	0.3752	0.1044
Err_1 (%)	9.56	7.23	8.33	9.44	0.21	0.02	1.99	0.47
Err_2 (p.u.)	0.1127	0.0854	0.0461	0.0984	0.0026	0.0005	0.1452	0.0389
Err_2 (%)	3.41	2.25	1.49	2.00	0.09	0.18	0.77	0.19

Note: In the above Table 4.3,

- "A20-1.5" represents System A, Bus20, P=1.5 p.u.;
- "BC-1" represents system B, bus STAN C, P = 1.0 p.u..
- The others are similar.

Table 4.4 Summary of the maximum voltage magnitude errors

	System A	System B	System C
Err_1 (%)	0.99	1.12	1.22
Err_2 (%)	0.33	0.51	1.04

Fig. 4.4 to Fig. 4.9 are the simulation results of these three test systems. Table 4.3 shows the maximum error of Q using TPLC and MTPLC methods. The error is the different between the results of proposed methods and that calculated by full load flow method. The comparisons of voltage magnitude are also executed in different node. Table 4.4 is the summary of the maximum errors by using these two methods. In these two tables, "Err_1" represents error using TPLC method while "Err_2" represents error using MTPLC method.

As observed in Fig. 4.4 to Fig. 4.9, the actual Q-V curves and the calculated Q-V curves are different in the bottom region when using TPLC, while the two curves coincide well when using MTPLC. Table 4.3 and Table 4.4 show that the errors using MTPLC is much reduced when compared with those using TPLC.

Other cases have also been studied, and the results are similar in pattern to Fig. 4.4 to Fig. 4.9 and Table 4.3 to Table 4.4.

4.5 Summary

A new voltage stability analysis approach with network equivalence has been shown to provide a fast method to plot Q-V and P-V curves at the study node where voltage stability is to be studied. From the study node, a complex system can be reduced to equivalent E, x and θ. Many calculations indicate that E and x of the system can be represented by two groups of values. Then the Q-V and P-V curves can be plotted by these two groups of E and x. The proposed method called Modified Two-Point Load-flow Calculation (MTPLC) can be used to quickly plot Q-V and P-V curves with satisfactory accuracy.

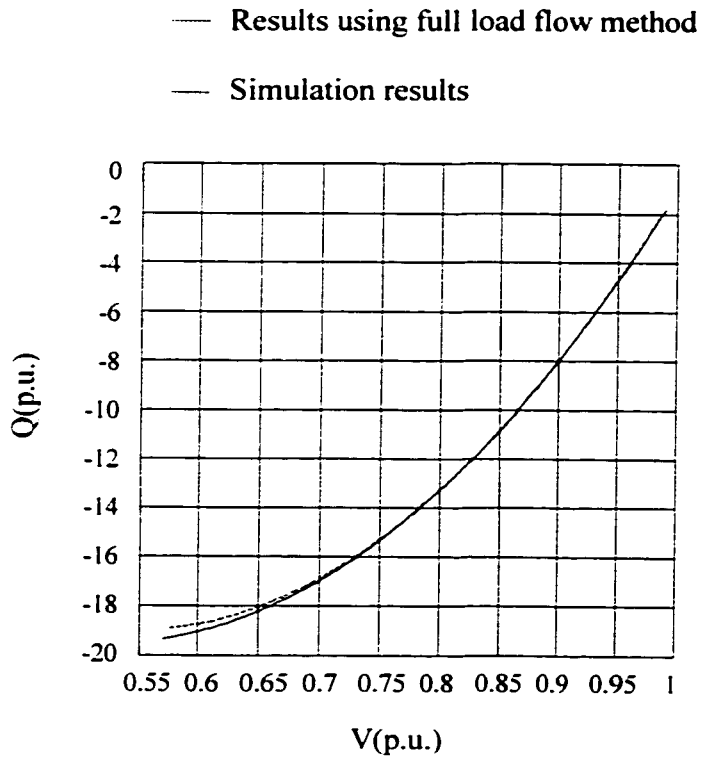

Fig. 4.4 *Q-V* curves of System A using TPLC (Bus 9, $P = 4.0$ p.u.)

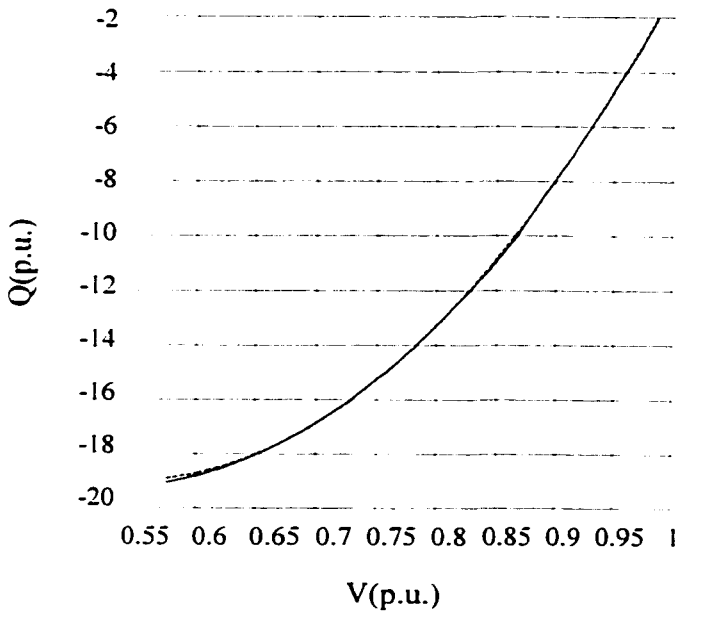

Fig. 4.5 *Q-V* curve of System A using MTPLC (Bus 9, $P = 4.0$ p.u.)

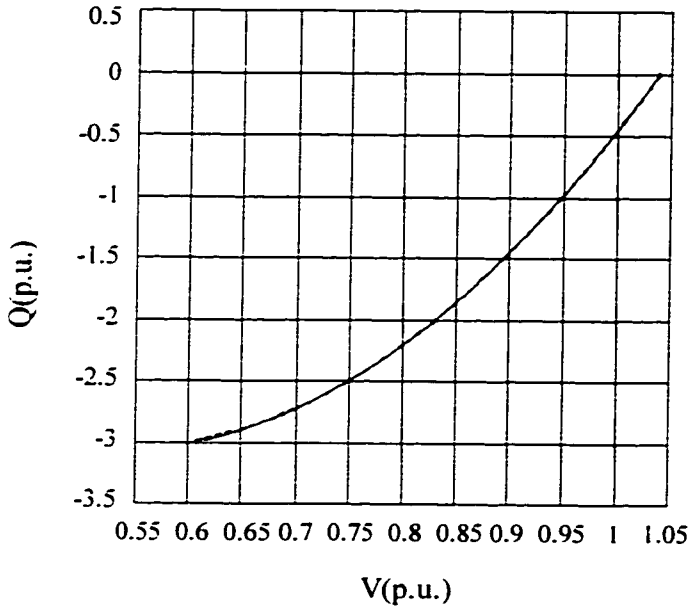

Fig. 4.6 *Q-V* curve of System B using TPLC (Bus STNA-230, P = 1.0 p.u.)

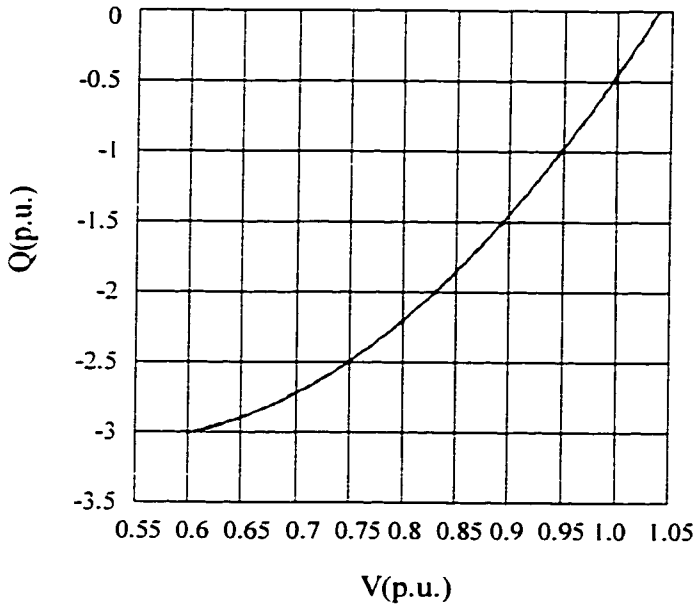

Fig. 4.7 *Q-V* curve of System B using MTPLC (Bus STNA-230, P = 1.0 p.u.)

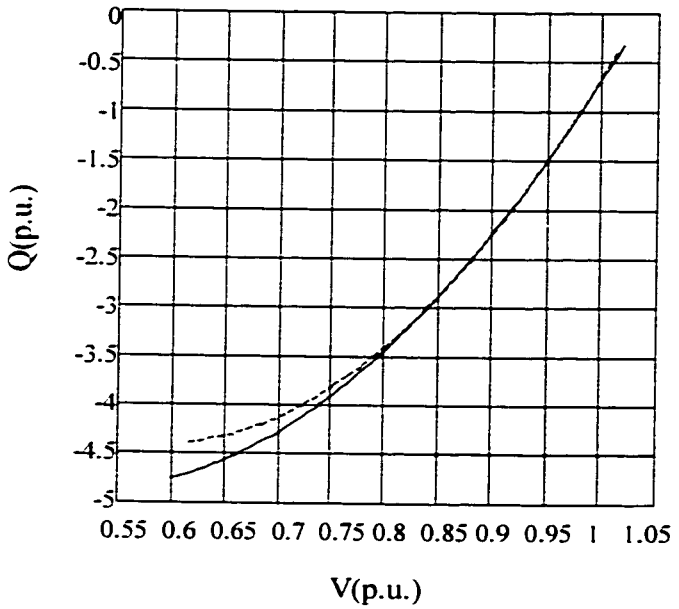

Fig. 4.8 *Q-V* curve of System C using TPLC (Bus 4, P = 10 p.u.)

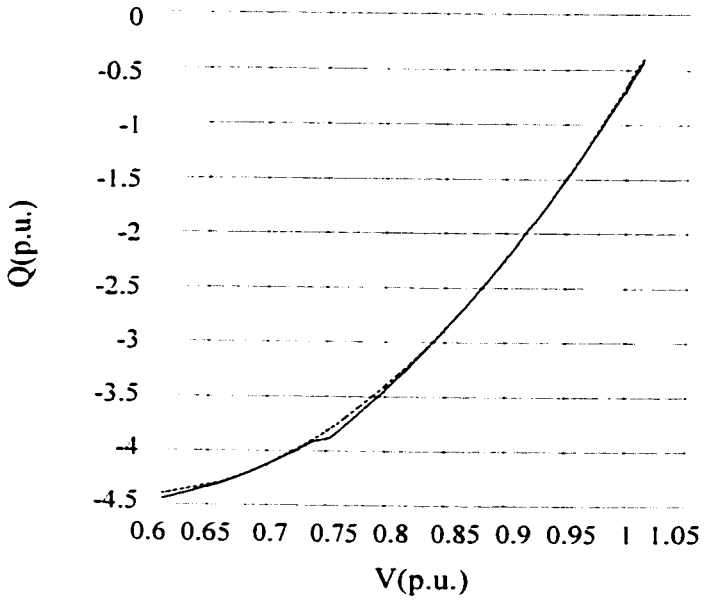

Fig. 4.9 *Q-V* curve of System C using MTPLC (Bus 4, P = 10 p.u.)

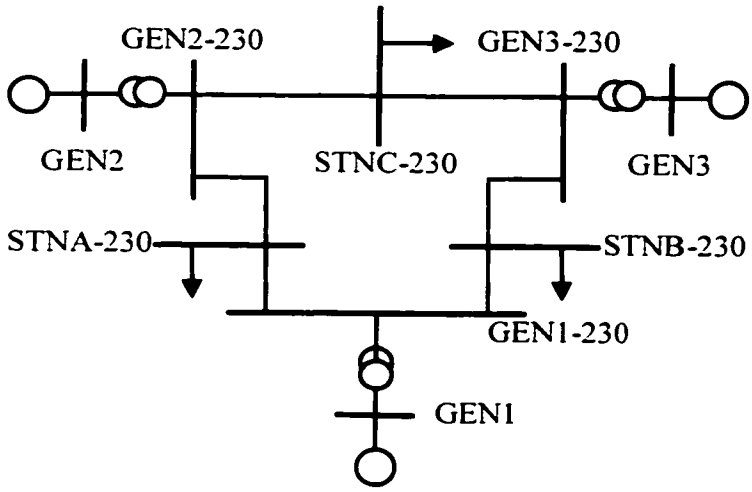

Fig. 4.10 WSCC 9-bus system

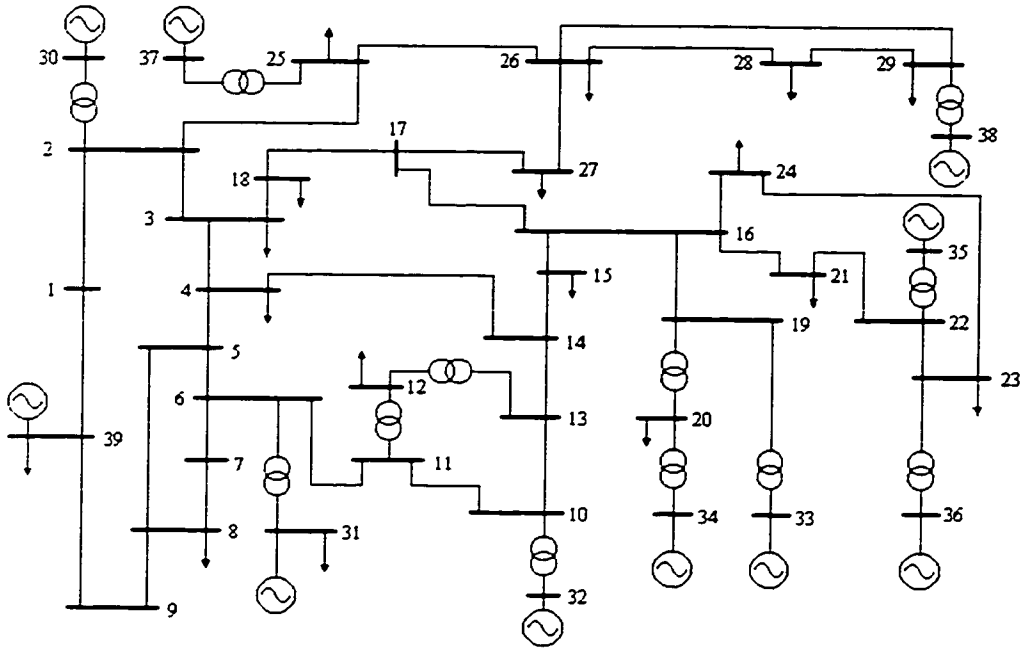

Fig. 4.11 New-England 39-bus system

Chapter 5

An Innovative Hybrid ANN External Equivalent Approach

5.1 Introduction

As mentioned before, modern power systems are large-scale systems in view of topology or system structure. In order to predict new system states caused by the possible disturbances and at the same time to assess the system security, it is necessary to model the remaining portions of the system. It is usually done by using equivalent models attached to the model of the controlled portion. Such approximate equivalents may be exchanged between co-operating control centers. Each control center may eventually modify certain parameters of the obtained equivalents taking into account the data telemetered via the tie lines.

There are various methods developed to address this problem [24, 42, 58, 92, 113]. The most popular equivalent approaches are Ward equivalent methods and radial equivalent independent (REI) method. The other methods are variations of these two basic methods.

The REI (redial equivalent independent) approach to external equivalent was invented by Dimo, and was brought to the attention of power engineers largely by Tinney and Powell [42, 92]. It has been applied to steady-state security analysis and different stability

problems. The main idea of the REI equivalent is to aggregate injections of a group of buses into one bus. The aggregated injection is distributed back to these buses through a radial network called the REI network. After the aggregation all buses with zero injection are eliminated by Gaussian elimination. The REI equivalent is derived as an equivalent that matched the solved load flow. For contingency evaluation, cases other than the base case are of interest. A mathematical analysis has shown [42] that very strict conditions have to be satisfied in order for the REI equivalent to match the incremental behaviour of the original unreduced load-flow model. The accuracy of the REI equivalent for contingency evaluation in practice depends on how the grouping is done. The equivalents are different when constructed for different operating conditions after boundary matching. Moreover, the REI network creates extra interconnections and the REI equivalent therefore tends to be denser [42]. Therefore, REI equivalent is not convenient for on-line application.

On the contrary, the Ward method consists of eliminating selected nodes of the network. The equivalent network of Ward-type equivalents is constructed using only the external network data and the external system operating-point data affects only the boundary injections.

Various Ward-type equivalents have been suggested and used for steady-state security analysis [10, 60, 94, 99]. The simplest Ward-type equivalent is obtained in the case when all load and generator nodes are eliminated from the reduced portion of the network. For steady-state security analysis, such equivalent usually does not provide sufficiently accurate results, especially for the reactive power response. In order to improve accuracy, certain additional reactive power support may be introduced. Such modified equivalent is called the

extended Ward equivalent. Many publications consider the extended Ward equivalent to be the most efficient method for implementation. The extended Ward equivalent includes two main steps: the construction of the equivalent network and the boundary matching.

Usually, the network configuration changes are according to schedule, while the load level is continuously changing throughout the day; so the boundary power injections would need to be updated from time to time. The extended Ward equivalent cannot simulate significant events in the external system and their impact on the internal system. It may cause some errors in on-line application. Therefore, much research work in recent years is on fast boundary matching and improving existing equivalent method for on-line applications [60-62].

For on-line solution, the application of the neural network-based approach appears to be the most promising. ANNs have been applied to voltage stability evaluation as they have been successfully applied to some power system problems where difficulties have been experienced with conventional techniques. Successful applications of ANN on power system include: voltage stability enhancement, reactive power planning, voltage security assessment, alarm processing, harmonics load identification, fault diagnosis, load forecasting, *etc*. How to use ANN on external equivalent area is seldom reported. The boundary power injection matching can be considered as a pattern recognition problem which is suitable for application of ANN. To reflect the topology changes of the internal system, when the information concerning external system is incomplete in on-line application, multi-layer neural networks is a good candidate for on-line identification of external system equivalent.

This chapter presents a hybrid approach to power system external system equivalent. The extended Ward equivalent is used to build boundary equivalent line modeling and ANN is used to match the boundary equivalent power injection on-line. Therefore, this new approach combines the advantages of the extended Ward equivalent and ANN.

5.2 Methodology

In Chapter 2, the applications of Ward equivalent have been reviewed. As it can be seen, under steady-state condition the effect of the external system on the internal system is reflected by the active and reactive power flow from the external system into the boundary buses. It is easy to calculate the equivalent injections at boundary buses by Ward equivalent method. When the loading conditions change or in contingencies, the equivalent power injections in Equations (2.6) and (2.7) will be updated using the real-time data. The equivalent power injection at boundary buses will reflect the power balance between the internal and the external system at different load levels or contingencies.

From circuit theory, the reactive power response from the external system can be equivalenced by an extended fictitious branch and a fictitious PV bus at every boundary bus as shown in Fig. 2.3. Before the contingency analysis is performed, the voltage magnitude in the fictitious PV bus extended from boundary bus is specified as V_i^0. In contingency analysis, the fictitious PV buses will respond with the supply or absorption of reactive power when the voltage magnitude of boundary buses is greater or less than that in the pre-contingency operation condition. The voltage magnitudes of these fictitious PV buses can

be obtained from the state estimation of the internal system. The reactive power response from the external system can then be simulated once the fictitious branches $\bar{B}_i$ are determined.

In order to monitor effectively the internal system and keep the external system model up to date and realistic $\bar{B}$ must be updated as the topology of the external system changes. Clearly, the value of $\bar{B}$ depends on the topology and parameters of the external system.

As stated in chapter 2, the extended Ward equivalent method is therefore not suitable for on-line modeling for significant configuration changes in the external system. Therefore, a hybrid ANN external equivalent approach is proposed to fulfil the requirements. Functionally, the method presented in this chapter is to design an equivalent model which represents those of the external system as seen by the study system. Then, the equivalent power injections at the boundary buses will reflect the power balance between the internal and the external system at different load levels or contingencies.

Two methods are developed in this Chapter.

5.2.1 Hybrid ANN External Equivalent: Method 1

For the large power system shown in Fig. 2.1, if the external system does not change a lot, the equivalent lines will remain unchanged. Then the power injection at the boundary buses depends mainly on the internal system which is reflected by the voltage magnitude and phase angles at the boundary buses.

It is assumed that there are m boundary buses. The output layer can be defined in $2m$ components which respond to the active and reactive power injection at the m boundary buses:

$$Y = [P_{B1}, Q_{B1}, P_{B2}, Q_{B2}, \cdots, P_{Bm}, Q_{Bm}] \tag{5.1}$$

The power injections at m boundary buses depend mainly on the voltage magnitudes (V) and phase angles (θ) of the internal and boundary buses. Therefore, there are $2m$ components in the input layer:

$$X = [V_{B1}, \theta_{B1}, V_{B2}, \theta_{B2}, \cdots, V_{Bm}, \theta_{Bm}] \tag{5.2}$$

The voltage magnitudes and phase angles of the boundary buses and the relatively boundary equivalent power injection have a dynamic relationship. To replace the external system boundary equivalent injection matching, the correct dynamic relationship between the injection power (P and Q) and bus voltage (V and θ) must be established. This will result in a two inputs, two outputs model. The relationship is defined as:

$$\{V_{Bi}, \theta_{Bi}\} \xrightarrow{A} \{P_{Bi}, Q_{Bi}\} \tag{5.3}$$

A represents the mapping relationship between (P, Q) and (V, θ).

Since ANN only depends on input/output samples to form its necessary parameters in pattern recognition, it is suitable for model identification with rapid response and robustness

after being properly trained. Hence, if V, θ are inputs and P, Q are outputs in ANN model, the training of ANN is mainly to identify A.

V and θ, which can be obtained from the real-time state estimation of the internal system, are considered as a pattern. The boundary equivalent power injections can be calculated by the extended Ward equivalent. The boundary equivalent power injections under various power systems operating conditions are recognized from trained ANN which stored some similar patterns. So the boundary equivalent power injections matching problem is then considered as a pattern recognition problem.

5.2.2 Hybrid ANN External Equivalent: Method 2

When the operation condition of the internal system changes, there will be changes in voltage magnitudes and phase angles in boundary buses.

$$\Delta V_i = V_i - V_i^0 \tag{5.4)}$$

$$\Delta \theta_i = \theta_i - \theta_i^0 \tag{5.5}$$

where V_i, θ_i and V_i^0, θ_i^0 are the voltage magnitudes and phase angles at boundary bus in post-contingency and pre-contingency operating conditions, respectively. Accordingly, the equivalent boundary power injection P_i^0, Q_i^0 will be updated to P_i and Q_i. Here we define $\Delta P_i = P_i - P_i^0$, $\Delta Q_i = Q_i - Q_i^0$.

Therefore, there is a dynamic relationship between ΔV, $\Delta\theta$ and ΔP, ΔQ. The implementation of the new approach can be expressed by the following mapping:

(change in operation condition)

$\Rightarrow$ (change in boundary equivalent power injection)

This mapping is carried out with a multi-layer feed-forward neural network trained by supervised learning. The input and output of the multi-layer neural network is described as follows.

It is assumed that there are m boundary buses, the output layer can be defined in $2m$ components which respond to the changes in active and reactive power injection at the m boundary buses:

$$Y = [\Delta P_{B1}, \Delta Q_{B1}, \Delta P_{B2}, \Delta Q_{B2}, \cdots, \Delta P_{Bm}, \Delta Q_{Bm}] \tag{5.6}$$

and there are $2m$ components in the input layer relatively:

$$X = [\Delta V_{B1}, \Delta \theta_{B1}, \Delta V_{B2}, \Delta \theta_{B2}, \cdots, \Delta V_{Bm}, \Delta \theta_{Bm}] \tag{5.7}$$

The step-by-step procedure carried out in this new approach are as follow:

1) Obtain the equivalent parameters of the external system under basic case.

2) Change the operation condition.

3) Use real-time state estimation to get the voltage magnitude and the phase angle at the boundary buses.

4) Calculate ΔV and $\Delta\theta$.

5) Obtain ΔP and ΔQ using trained ANN and calculated equivalent boundary power injections under new operation conditions.

In summary, with the hybrid ANN external equivalent, the flows into the boundary buses from the equivalent match exactly the tie-line flows. When the loading conditions change or in contingencies, the equivalent power injection will be updated using ANN.

5.3 Test Results

5.3.1 Test System

Simulation tests of the proposed method are conducted on two test systems: the New-England 39-bus system [84], which is a reduced version of New England utility, and a 59-bus system. The detailed data of the system can be found in Appendices.

The test systems are divided into four subsystems: internal, boundary, buffer and distant network. Buffer zone can be identified by performing sensitivity analysis, but here we use a more simple way. The tie lines between the boundary buses and the external

system are chosen to fall into buffer zone. The definition of the other lines is obtained by off-line analysis using full AC load flow program. If one line outage causes a 3% or greater change in the value of components of original fictitious branches $\tilde{B}$, the line should be included in buffer zone. The other lines are classified as distant network. The external network may be largely reduced using this rule. Sometimes a line is electrically far from the boundary buses but has significant impact on the internal system. However, this special case is not considered in this thesis.

Table 5.1 and Table 5.2 show the summary of the main topology characteristics of the test system. Table 5.3 to Table 5.6 are the results using Ward equivalent in the basic case. The Extended equivalent lines to fictitious PV buses are shown in Table 5.7 to Table 5.8. There are three boundary buses, 1, 4, 16, in these two test systems. Note that E1, E2, E3 are the corresponding fictitious PV buses extended from boundary bus 1, 4, 16.

Note: in the following Tables, "test system I" represents New-England 39-bus system, and "test system II" represents the 59-bus system.

Table 5.1 Characteristics of the test system I

	Full System	Internal network	Boundary	Buffer Zone	Distant Network
Buses	39	12	3	3	21
Lines	44	15	7	5	17
PV Buses	9	3	0	0	6

Table 5.2 Characteristics of the test system II

	Full System	Internal network	Boundary	Buffer Zone	Distant Network
Buses	59	14	3	9	33
Lines	70	18	7	10	35
PV Buses	15	4	0	1	10

Table 5.3 Power injection using Ward equivalent (test system I)

Boundary buses	P (p.u)	Q(p.u)
1	-0.2426	-0.2536
4	2.1260	0.9207
16	6.9602	0.1226

Table 5.4 Power injection using Ward equivalent (test system II)

Boundary buses	P (pu)	Q (pu)
1	0.5380	0.2323
4	1.2569	1.5703
16	2.1091	-0.8102

Table 5.5 Equivalent lines between boundary buses (test system I)

From	To	R	x
1	4	0.0209	0.5366

From	To	R	x
1	16	0.1343	6.7783
4	16	0.0024	0.0465

Table 5.6 Equivalent lines between boundary buses (test system II)

From	To	R	x
1	4	0.0285	0.6826
1	16	0.2077	3.4620
4	16	0.0020	0.0473

Table 5.7 Extended equivalent lines to fictitious PV buses (test system I)

From	To	R	x
1	E1	0	0.0252
4	E2	0	0.0214
16	E3	0	0.0171

Table 5.8 Extended equivalent lines to fictitious PV buses (test system II)

From	To	R	X
1	E1	0	0.03238
4	E2	0	0.02974
16	E3	0	0.02049

Equivalent lines are obtained by the extended Ward equivalent method. The parameters of the equivalent model are updated when the topology of the buffer system changes from the base case. The power injections are matched by ANN in order to respond to the variation of the external system.

5.3.2 Configuration of ANN and Data Description

The method 1 is applied in New-England 39-bus system and the 59-bus system. The method 2 is applied in the 59-bus system only.

The proposed multi-layer feed-forward neural network consists of three layers with one hidden layer. For three boundary buses, the output layer has six output neurons to matching the boundary power injections:

- Method 1: three boundary power (P and Q)
- Method 2: change in three boundary power (ΔP and ΔQ)

Since there are three boundary buses, the input layer has six input neurons:

- Method 1: voltage magnitudes (V) and phase angles (θ) of the boundary buses
- Method 2: change in voltage magnitudes (ΔV) and phase angles ($\Delta\theta$) of the boundary buses

The parameters of the multi-layer network are determined experimentally based on the complexity of the problems. Different sizes of hidden layer have been tried in order to achieve the best performance. Finally, 15 neurons in the hidden layer are found to be sufficient for this problem. The optimum values of learning rate η and momentum m are 0.9 and 0.15, respectively.

Usually, in the input layer, the number of neurons depends on the number of features of an input patter. In the output layer, each neuron corresponds to an equivalent active or reactive power injection / change in power injection of the boundary buses. The training data are generated to cover a wide variety of operation conditions, which including: (1) different loading conditions, (2) different generation/load patterns, and (3) different contingencies. Based on the test systems, the load level of the full system was changed uniformly by ±0.5%, ±1.0%, ±1.5%, ... and ±10%. This may not be the most ideal set of training patterns, but it should cover the two extremes of the intended load variations and some contingencies.

For test system I, 40 cases are then obtained by the offline load flow program; similarly, 80 cases are obtained by changing the load level of the external or the internal system only. Another 80 cases are obtained by changing the load in one or two node. 20 cases are for single line outages, and 10 cases are for double line outages. Another 70 cases are combined line outage (single line and double line outages) with load changing. Line outages include the case of tie line outage, line close to boundary and far from the

boundary, in external or/and internal system. There are in total 300 samples used to train the ANN. The network is trained on a Pentium II 300 computer in 2000 iterations.

For test system II, 40 cases are then obtained by the offline load flow program. Similarly, 80 cases are obtained by changing the load level of the external or the internal system only. Another 100 cases are obtained by changing the load in one or two node. 30 cases are for single line outages, and 15 cases are for double line outages. Another 85 cases are combined line outage (single line and double line outages) with load changing. In total 350 input pattern are generated to train the ANN. The network is trained in 3000 iterations.

5.3.3 Contingency Analysis

After the training is completed, the performance of the proposed neural network is evaluated by 50 testing patterns which are different from the training patterns. These testing patterns cover some typical operation conditions, such as:

- Load level change
- Single-line outages
- Double-line outages
- Line outages with load level changing

The boundary equivalent power injections are obtained immediately from the output of the trained ANN. The CPU time for training is long, however, done off-line. The time to get the inputs, i.e., voltage magnitudes and phase angles are those of state estimation of the internal system.

In most power systems, voltage magnitude is an indication of system voltage profiles. The active power and reactive power are also needed to represent the system voltage stability condition. In this respect, all responses of bus voltage magnitude and line active and reactive power flow in the internal system after contingency are calculated. All corresponding internal system bus voltage magnitudes and line active and reactive power flows are compared by using a full AC load flow program in the proposed equivalent model and unreduced network. Subscript *Eq* represents the results calculated by reduced network, and subscript *Org* denotes the results calculated by load flow program for the full-size interconnected network. The errors of voltage magnitude are defined as:

$$\Delta V\% = \frac{V_{Eq} - V_{Org}}{V_{Org}} * 100\% \tag{5.8}$$

Another error comparison is that of the line flows. Some line flows are very light, and the resulting errors will be very large if calculated using the comparison given by equation (5.8). In fact, this type of large error is insignificant for security assessment. The comparison is modified by normalizing the result based on the MVA rating of each transmission line. The percentage errors of line flows are defined as:

$$\Delta P\% = \frac{P_{Eq} - P_{Org}}{\text{Line}_{ij}^{\text{Rating}}} * 100\% \tag{5.9}$$

$$\Delta Q\% = \frac{Q_{Eq} - Q_{Org}}{\text{Line}_{ij}^{\text{Rating}}} * 100\% \tag{5.10}$$

The maximum error of each contingency case is defined as the largest error among the recording of errors corresponding to each line.

Fig. 5.1 shows the maximum voltage magnitude errors in the internal system of each case with conventional Ward equivalent. Fig. 5.2 and Fig 5.3 indicate the maximum voltage magnitude errors in the internal system of each case by using method 1 and method 2 for test system I, respectively. The maximum line flow errors in the internal system of each case by using the proposed methods for test system I are illustrated in Fig. 5.4 to Fig. 5.7, respectively. Table 5.9 shows the summary of largest maximum and RMS errors of these 50 testing patterns. The results of test system II using proposed method 2 are shown in Fig. 5.8 to Fig. 5.10 and Table 5.10.

As can be seen from Fig. 5.1 to Fig. 5.10 and Table 5.9 to Table 5.10, the results of the proposed methods are much better in accuracy than those of conventional Ward equivalent method and have high accuracy.

Table 5.9 Summary of errors for test system I

	Errors			
	Maximum		RMS	
ΔV %(Ward)	3.9775		0.2073	
Method	1	2	1	2
ΔV %(ANN)	0.0392	0.0418	0.00194	0.00193
ΔP %(ANN)	1.6231	1.4297	0.0903	0.0878
ΔQ %(ANN)	1.2654	1.5728	0.1042	0.1012

Table 5.10 Summary of errors for test system II

	Errors	
	Maximum	RMS
ΔV %	0.0322	0.00155
ΔP %	1.5138	0.1007
ΔQ %	1.3805	0.0963

Method I and Method II use the same concept but different patterns for training ANN. The performances of these two methods are similar. As can be seen from Table 5.9 to Table 5.10 and Fig. 2 to Fig. 10, the accuracy of these two methods is roughly the same.

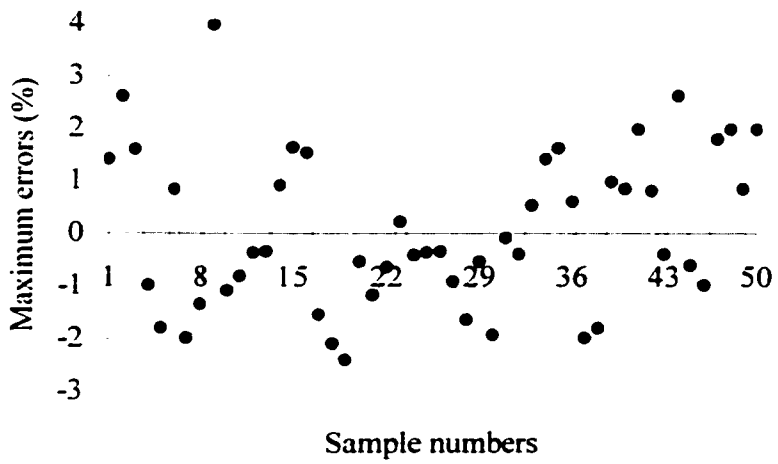

Fig. 5.1 Maximum voltage magnitude errors (conventional Ward equivalent)

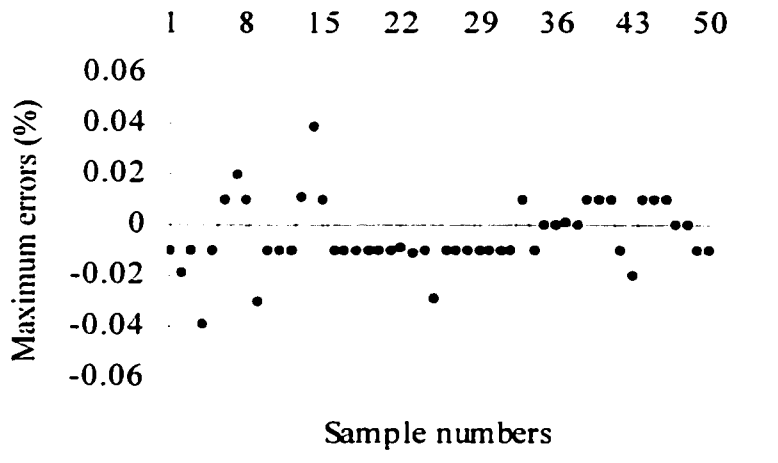

Fig. 5.2 Maximum voltage magnitude errors (system I, method 1)

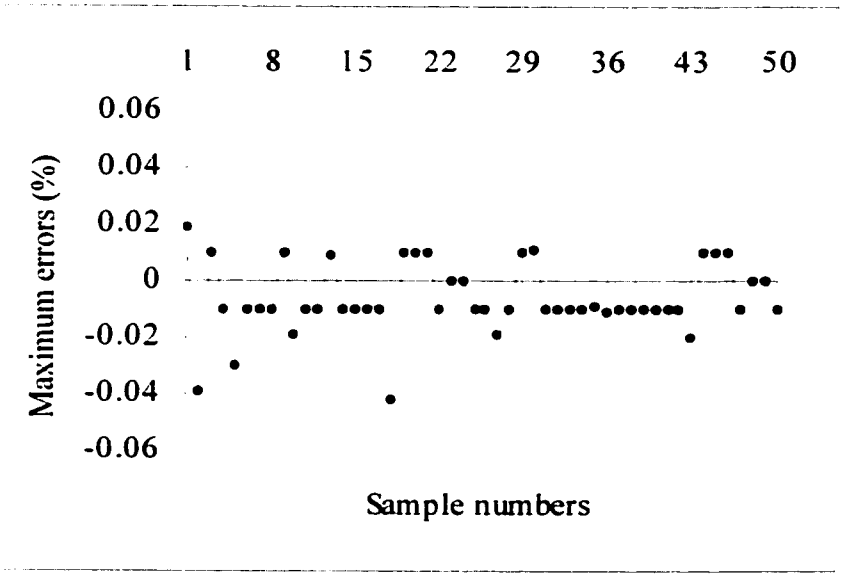

Fig. 5.3 Maximum voltage magnitude errors (system I, method 2)

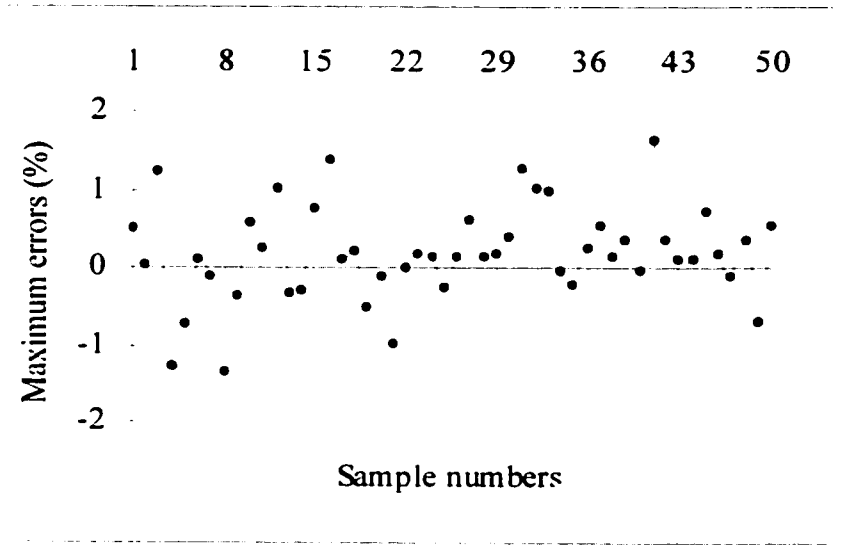

Fig. 5.4 Maximum active power errors (system I, method 1)

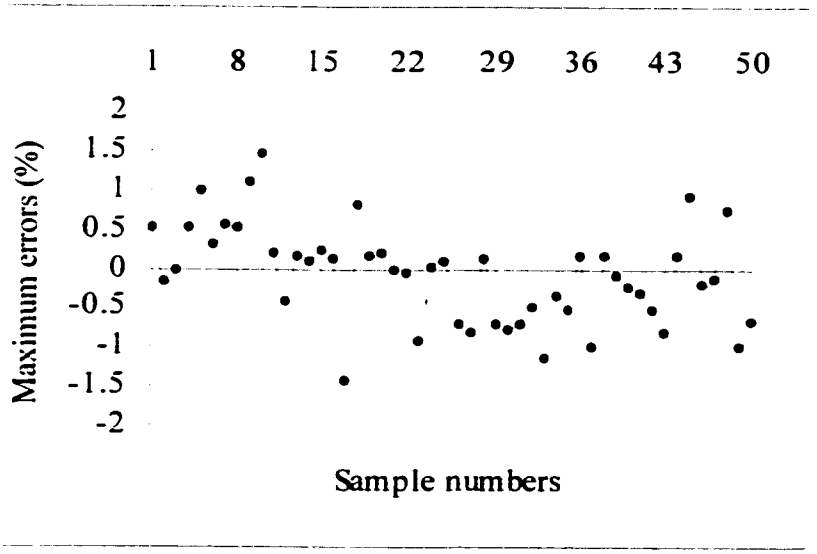

Fig. 5.5 Maximum active power errors (system I, method 2)

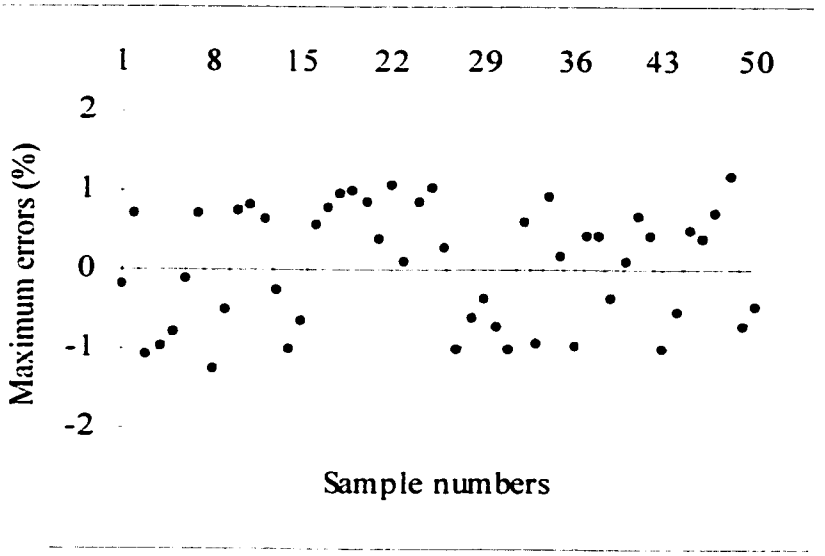

Fig. 5.6 Maximum reactive power errors (system I, method 1)

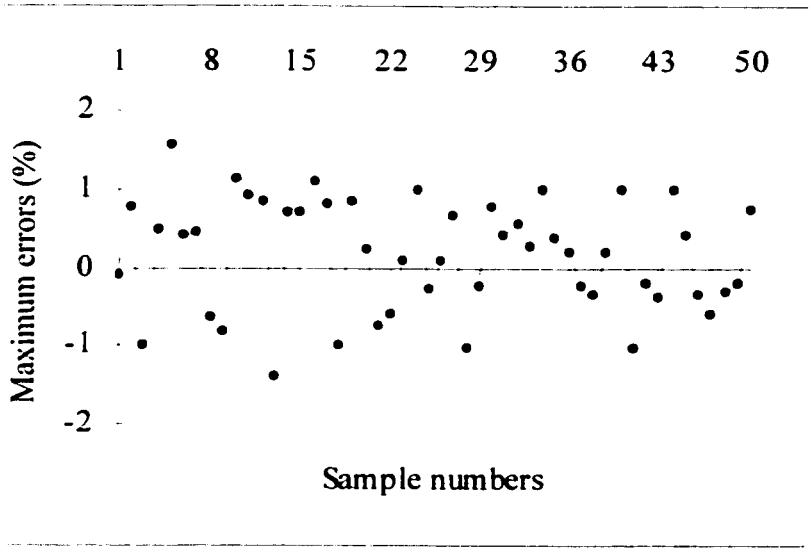

Fig. 5.7 Maximum reactive power errors (system I, method 2)

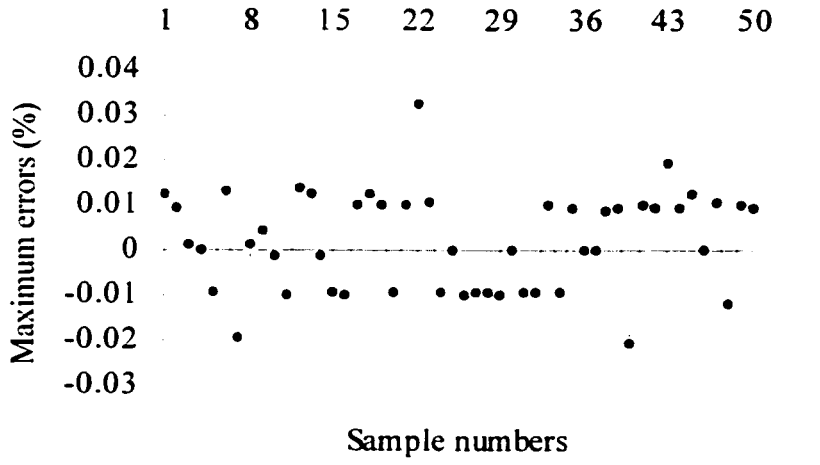

Fig. 5.8 Maximum voltage magnitude errors (system II, method 2)

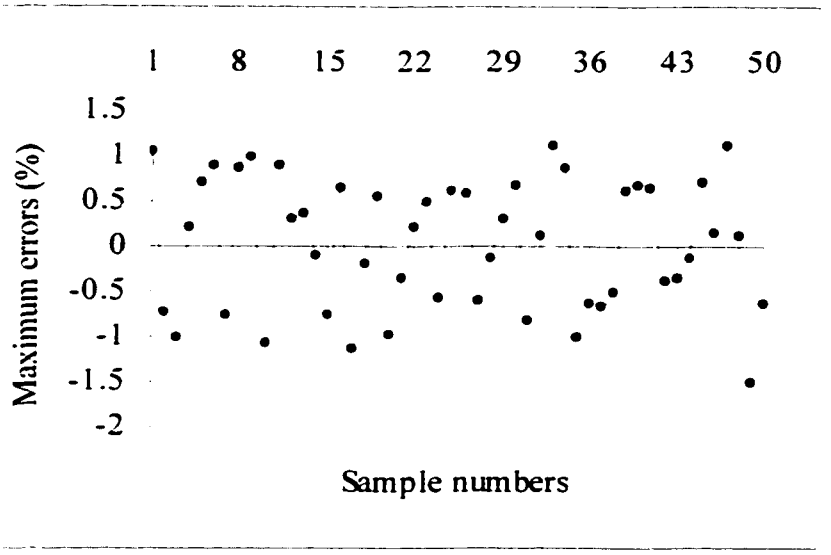

Fig. 5.9 Maximum active power errors (system II, method 2)

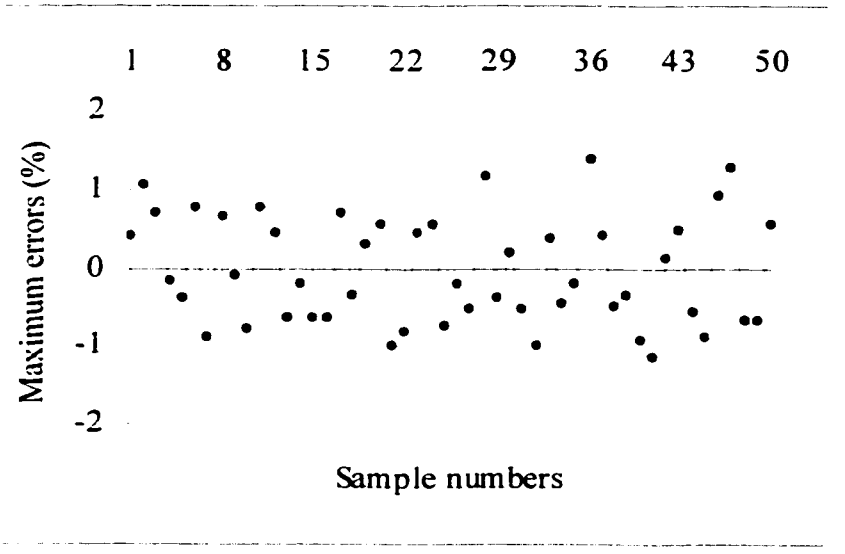

Fig. 5.10 Maximum reactive power errors (system II, method 2)

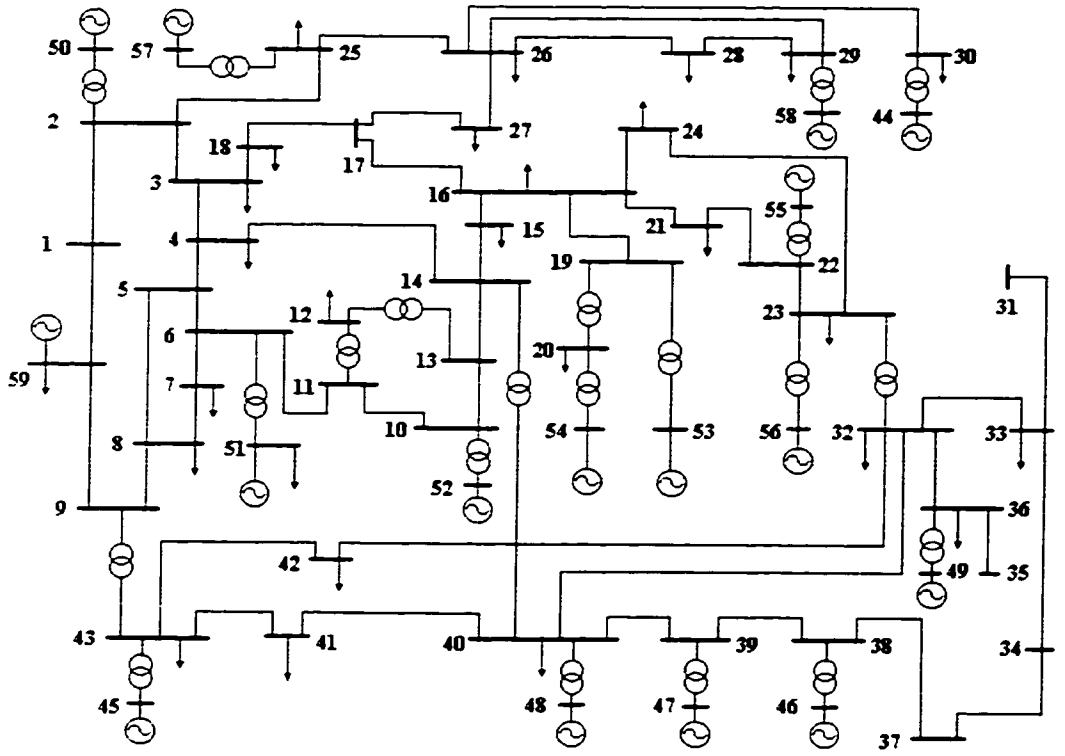

Fig. 5.11 59-bus test system

5.4 Summary

A novel hybrid ANN and extended Ward equivalent approach network reduction for on-line voltage security assessment is presented in this chapter. The new approach can update the equivalent parameters according to the line status in buffer zone and match the boundary equivalent power injections.

Test results show that the new equivalent approaches represent the system with good accuracy. It is of much promise to be used in fast on-line voltage security assessment scheme.

Chapter 6

Self-organizing Hierarchical Neural Network Based Voltage Stability Estimation

6.1 Introduction

As a result of severe voltage collapse incidents that have occurred, voltage stability has emerged to be one of the most challenging and important subjects in power system research. To obtain solution of voltage instability problem, both static and dynamic modeling have been used. Various voltage stability indicators have been proposed to evaluate the stability of the system [11, 82]. In the security assessment of a power system, it is important to predict line flows and bus voltages at different loading conditions of a power system [6, 19]. Several approaches such as the 1P-1Q iteration method [41], distribution factors [96], the bounding method and the concentric relaxation method have been proposed to estimate bus voltage in real time application. The pattern recognition method [23] is recently proposed to estimate bus voltage effectively.

There is a growing interest in the use of ANNs to solving power system problems. The objective of applying ANN to voltage stability analysis is to detect voltage instability of the system. If an ANN is trained to associate the stability level of power system with its operating condition, which is defined by the power system parameters and bus data, the

voltage instability of the system can be detected since a trained ANN is capable of giving fast voltage stability evaluation on-line.

Most of the published work in the area of voltage stability analysis is based on multi-layer feed-forward networks trained by back propagation (BP) for quantifying stability margins. However, in respect of voltage stability assessment of practical systems, a major difficulty of this type of neural networks is that it depends much on the number of training data because the network itself does not take into account the properties of input data. Thus there are voluminous input data related to the output and it would be very time-consuming to train a neural network with all the input data, and the number of connection weights and neurons would be extremely large. It is, thus, essential to reduce the number of inputs to a neural network. The developed approach reported here is used to address this issue.

Two hybrid neural networks which consists of a self-organizing map network and a multi-layer feed-forward network, called Self-organizing Hierarchical Neural Network (SHNN), are developed and used sequentially in this chapter. The input of the multi-layer feed-forward network comes from the self-organizing map network. The self-organizing map network is used for feature extraction of operating conditions in terms of voltage stability. The SHNN is trained by the samples of off-line simulation results. The first one indicates whether the system is stable or unstable, while the second one is used to predict the voltage magnitudes at all the *PQ* buses of power system at different loading conditions for the stable cases only. In this approach the voltage collapse proximity indicator is based on the line stability factors of individual lines.

6.2 Dynamic Load Models

In general dynamic load representation has received relatively little attention, with most of the industry still using static models [25]. This is partly because in many transient stability studies the inclusion of dynamic load models with moderately loaded systems has little impact upon stability [47], and partly because of the difficulty in developing and verifying dynamic models for an aggregate, time-varying load. For voltage stability problem, the use of dynamic load models has a significant impact on the assessment of system voltage stability.

Detailed load model studies have been performed, where quite extensive field measurements were included [30, 33, 73, 74]. In this Chapter, the characteristics of induction motors are studied. The dynamic phenomena of voltage collapse are analyzed by the method of dynamic simulation using induction motor models. The transient behavior of the system is influenced by the dynamic characteristics of the induction motor loads [3, 121].

In the conventional load flow calculation, it is assumed that active power and reactive power of every load node are fixed, but, in an actual power system, they vary with time. The static characteristics of load are usually classified into three categories: constant power, constant current and constant impedance loads. In practice, however, the characteristic of an actual load varies from one type to another as time lapses.

There are two types of dynamic load elements. Motors have the fast transient characteristics. On the other hand, controlled resistive loads have the slow transient characteristics. An induction motor model [87] is usually adapted to analyze the former and equivalent admittance model with first order delay can be adopted to analyze the latter [63]. Induction motors are usually adopted as dynamic load elements because of its simplicity and physically clear image.

6.2.1 Philosophy of the Simulation

The problem of voltage stability is closely related to the stability of dynamic load elements while the problem of traditional angle stability is associated mainly with generators. In this sense, the concept of voltage stability is in a position opposite to that of angle stability.

According to experiences, the effects of transient phenomena of generators are usually negligible in the analysis of voltage stability. In this thesis, only the transient phenomena of loads are considered and those of generators are ignored. This approach makes clear the transient phenomena of voltage collapse.

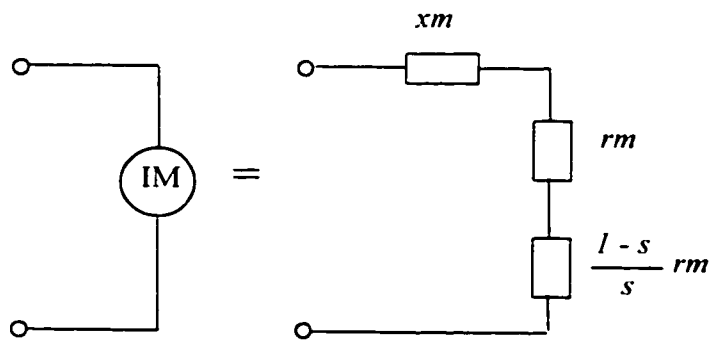

Fig. 6.1 Equivalent circuit of induction motor

In an actual power system, however, there are more complicated phenomena such as voltage collapse followed by accelerated out-of-step of generators. These phenomena concerning interconnected networks with multiple generators and loads must be analyzed taking into account dynamic characteristics of both generators and loads. At the first step of analyzing voltage collapse phenomena, a radial power system whose power source is represented by an infinite bus is adopted to make clear the basic characteristics of voltage collapse. The equivalent circuit of induction motor is shown in Fig. 6.1.

6.2.2 Fundamental Equations

Fundamental equations describing a power system are given below:

Load flow equations are represented as:

$$Pe_k + \{\sum_{j=1}^{N}(G_{kj}e_j - B_{kj}f_j)e_k + \sum_{j=1}^{N}(G_{kj}f_j + B_{kj}e_j)f_k\} = 0 \qquad (6.1)$$

$$Qe_k + \{\sum_{j=1}^{N}(G_{kj}e_j - B_{kj}f_j)f_k - \sum_{j=1}^{N}(G_{kj}f_j + B_{kj}e_j)e_k\} = 0 \qquad (6.2)$$

where

G_{kj}, B_{kj} : Conductance and susceptance between node k and j

e_k, f_k : Real and imaginary components of node voltage k

Pe_k, Qe_k : Active and reactive powers injected to node k

The induction motor is represented as:

$$Pe_k - \frac{rm_k / s_k}{(rm_k / s_k)^2 + xm_k^2}(e_k^2 + f_k^2) = 0 \tag{6.3}$$

$$Qe_k - \frac{rm_k / s_k}{(rm_k / s_k)^2 + xm_k^2}(e_k^2 + f_k^2) = 0 \tag{6.4}$$

where

rm_k , xm_k : Resistance and reactance of the equivalent circuit of induction motor k

s_k : Slip of induction motor k

In the steady-state, the electrical input power of the induction motor is equated to the mechanical load. This relationship is described as follows:

$$Pe_k(1 - s_k) - Pm_k = 0 \tag{6.5}$$

The dynamic equation of an induction motor can be derived from the equation of motion. This equation is described as a function of slip as follows:

$$\frac{ds_k}{dt} = \frac{1}{\Phi_k \omega_0^2}\left(\frac{Pm_k}{1 - s_k} - Pe_k\right) \tag{6.6}$$

where

Φ_k : Moment of inertia of induction motor k

ω_0: $\omega_0 = 2\pi f_0$, f_0 : frequency of the system

6.2.3 Procedure of Simulation

In the first step of dynamic simulation, the steady-state solution is calculated by means of Newton-Raphson method, where the load flow equations ((6.1) and (6.2)) and load characteristic equations ((6.3), (6.4), (6.5)) are numerically solved.

In the second step, a transient solution is calculated assuming that the voltage collapse is triggered by a kind of first disturbance such as a trip of a transmission line, step increase of mechanical load, disconnection of shunt capacitors. When the first disturbance occurs, the slip of the induction motor is kept invariant because of its inertial mass. So the equivalent impedance of the load is kept invariant before and after the first disturbance. Under this hypothesis, the initial state solution is obtained by load flow calculations.

As already assumed, it is supposed that the transient phenomena of generators and transmission lines are suppressed earlier than those of loads. This hypothesis usually holds in an actual bulk power system. Under this hypothesis, the step-by-step procedure carried out in the dynamic simulation are as follows:

1) Calculation of initial condition by Newton-Raphson mehod.

2) Calculation just after the first disturbance:

- Step increase of mechanichal load
- disconnection of a transmission line
- switching of shunt capacitor

3) Calculation of induction motor's slip at time t by solving the differential equation (6.6) using the Runge-Kutta method.

4) Calculation of system conditions at time t by Newton-Raphson method.

5) Increase the time, $t = t + \Delta t$ and repeat the procedure, *i.e.* go to step 3).

6.3 Voltage Collapse Proximity Indicator

The voltage collapse proximity indicator is based on the stability factors for individual lines [8-9]. The derivation of the factor is shown in the following.

6.3.1 Formulation of Voltage Collapse Proximity Indicator [8, 9]

Firstly, consider the power flow in Fig. 6.2.

Taking node i as the reference node and letting P_r be the real power entering node i+1 from node i, we obtain

$$P_r = P_i - R(P_i^2 + Q_i^2)/V_i^2 \tag{6.7}$$

Rearranging the above equation to its quadratic form.

$$RP_i^2 / V_i^2 - P_i + (P_r + RQ_i^2 / V_i^2) = 0 \tag{6.8}$$

Thus, for the real roots of P_i,

$$1 - 4(R / V_i^2)(P_r + RQ_i^2 / V_i^2) \geq 0 \tag{6.9}$$

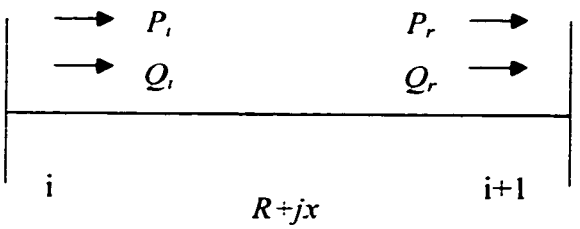

Fig. 6.2 Power flow from node i to node i+1

It should be noted that voltage collapse will occur if this condition is violated. By considering the reactive power flow in the same manner as real power flow, we can derive the reactive power flow condition as:

$$1 - 4(x / V_i^2)(Q_r + xP_i^2 / V_i^2) \geq 0 \tag{6.10}$$

By considering the power flow from node $i+1$ to node i, we can obtain the condition for real roots of P_r.

$$1 - 4(R / V_{i+1}^2)(-P_i + RQ_r^2 / V_{i+1}^2) \geq 0 \tag{6.11}$$

and for real roots of Q_r as.

$$1-4(x/V_{i+1}^2)(-Q_i+xP_r^2/V_{i+1}^2)\geq 0 \tag{6.12}$$

From the above conditions, we obtain four stability limits henceforth called the line stability factors designated as follows:

$$LPP=4(R/V_i^2)(P_r+RQ_i^2/V_i^2) \tag{6.13}$$

$$LQP=4(x/V_i^2)(Q_r+xP_i^2/V_i^2) \tag{6.14}$$

$$LPN=4(R/V_{i+1}^2)(-P_i+RQ_r^2/V_{i+1}^2) \tag{6.15}$$

$$LQN=4(x/V_{i+1}^2)(-Q_i+xP_r^2/V_{i+1}^2) \tag{6.16}$$

The above four line stability factors become indicators of voltage collapse by determining the voltage stability of the line. The voltage stability level of a line is indicated by the factor with the largest value closest to 1.0 (critical limit). It is shown that at the collapse point (i.e. the point of load flow divergence) the line stability factor reaches a critical value of 1.0.

6.3.2 Discussion of Voltage Collapse Proximity Indicator

These four line stability factors are based on the load flow calculation of individual lines, which have limitation when used as voltage collapse proximity indicator. For very simple system, or radial system it may give the right answer. However, the wrong result will

happen when solving the problem of complex system. The advantage of it is simple and easy to implement. It is used in this chapter only for generating the training samples.

There are many methods developed on the voltage collapse proximity indicator, which mainly include direct method [20-21], continuation method [108], optimization method [105], approximate method [22, 71, 76], and some other methods [7, 20, 25, 44, 46, 124]. In particular, the continuation load flow method remains well conditioned at and around the critical point. Consequently, divergence due to ill condition is not encountered at the critical point. As a result, single precision computations can be used to obtain power flow solutions at and near the critical point. It needs long time to get or approach the critical point, so it is useful for off-line study.

This Chapter highlights on using SHNN to minimize the time taken in the ANN learning process as well as the performance of ANN. The performance of SHNN is not dependent on the selection of indicator. If the voltage collapse indicator is replaced by the other alternative indicators, the training sample of SHNN will be changed. However, the finial results will be the same.

6.4 Neural Network Approach to Voltage Stability Analysis

6.4.1 Block Diagram of the Learning Model

A block diagram of the learning model for voltage stability analysis is presented in Fig. 6.3. Initially a large number of patterns are generated in the wide range of the load variation

(randomly) at each bus. Then feature self-organizing maps network are selected to reduce the dimensionality of the input as well as the size of the neural network (block-I). Clustered input data are normalized (block-II) and applied to the Multi-layer neural network for stability classification or along with a topology number to represent the *PQ* bus considered for voltage magnitude estimation (block-III). This learning model is called Self-organizing Hierarchical Neural Network (SHNN).

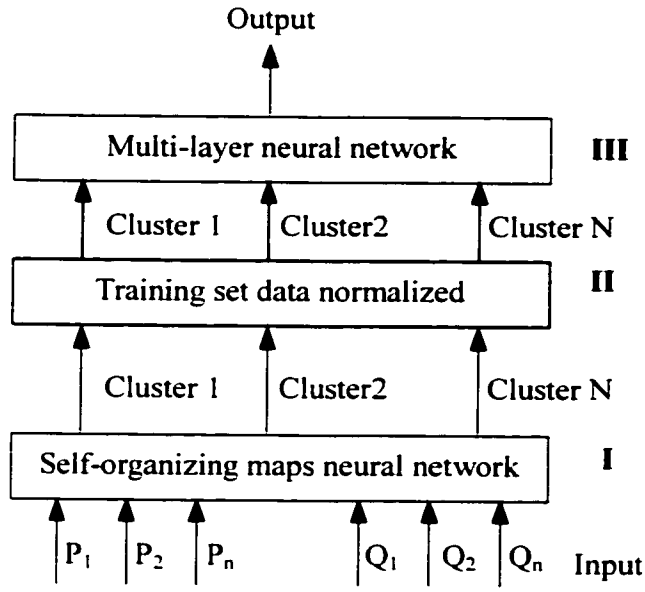

Fig. 6.3 Conceptual diagram of learning model for voltage stability analysis

The implementation of the SHNN can be expressed by the following two mappings:

Mapping I: (Operating conditions) $\Rightarrow$ (feature clusters)

Mapping II: (feature clusters) $\Rightarrow$ (voltage stability estimation)

The first mapping is carried out with a Kohonen neural network. Kohonen network is used for feature extraction of operating conditions in terms of voltage stability. Input patterns are clustered according to similarities discovered among the input features. Using the Kohonen network, different operating conditions can be efficiently clustered and mapped to the corresponding positions on the output neuron grid. The second mapping is carried out with a multi-layer feed-forward neural network trained by supervised learning. The input of the multi-layer neural network comes from the Kohonen network, *i.e.* the cluster information. The output of the multi-layer neural network gives the evaluation of voltage stability.

In block-I, a large number of patterns N are generated by perturbing the load on each bus randomly in a wide range of operating conditions and AC load flow is performed to obtain voltage stability for each case. The information is computed by observing the voltage at each bus for load disturbance at various buses in power system.

The ANN used in block-III is the 3-layer multi-layer neural network. The multi-layer neural network used here consists of one input layer, one hidden layer and one output layer. The input of the MLP is the output of the SOMs.

In summary, within the SHNN, the Kohonen network is used as a front end to a mapping network, *i.e.* the multi-layer neural network which maps the output of Kohonen networks in order to give voltage stability margin. In this way, robust mapping can be learned and hence the generalization capability of the multi-layer feed-forward network has been improved significantly.

6.4.2 Neural Network Approach to Voltage Stability Analysis

The proposed ANN technique for voltage stability analysis is carried out in two main steps with two SHNN models developed. The first model is used to classify the power system as to whether it is stable or unstable. The second model is used for the stable system to predict the voltage magnitudes at load buses. The net real (P) and reactive (Q) powers in all the PQ buses are chosen as the input sets for both SHNN. The first SHNN is trained to give an output of 0 or 1 for which 0 indicates that the system is stable and 1 indicates that the system is unstable. In this way, the network can be used to classify the stability state of the system for a given loading pattern. The output of the second SHNN model developed is the voltage magnitudes at PQ buss. The network is used to predict the voltage magnitudes at the all PQ buses when the system is found to be stable.

6.5 Result and Discussions

For the purpose of testing, the neural network approach for voltage stability analysis has been conducted on WSCC 9-bus test system and New-England 39-bus test system. The WSCC 9-bus system composes of 2 PV buses, 6 PQ buses, and 1 slack bus; where the New-England 39-bus system consists of 29 PQ buses, 9 PV buses and 1 slack bus. The data of both test systems are given in the Appendices.

The training sets generation is stated in the following section. In order to get better performance of MLP, only one output node is designed to estimate the bus voltage magnitude at all the PQ bus in the second SHNN model. So a topology number is required as input to represent the corresponding PQ bus. In WSCC 9-bus system, the topology

number is used in the form of a string of 3 bipolar digits (+1 -1) to represent the 6 *PQ* buses. For example, the first *PQ* bus is represented by a bipolar string (-1 -1 +1), and other *PQ* buses being represented as shown in Table 6.1. In New England 39-bus system, a string of 5 bipolar digits has been used to represent 29 *PQ* buses shown in Table 6.2.

Table 6.1 Bipolar string for PQ bus representation in WSCC 9-bus system

No.	PQ bus	Topology number		
1	GEN1-230	-1	-1	1
2	GEN2-230	-1	1	-1
3	GEN3-230	-1	1	1
4	STNA-230	1	-1	-1
5	STNB-230	1	-1	1
6	STNC-230	1	1	-1

Table 6.2 Bipolar string for PQ bus representation in New England 39-bus system

No.	PQ bus	Topology number				
1	1	-1	-1	-1	-1	1
2	2	-1	-1	-1	1	-1
3	3	-1	-1	-1	1	1
4	4	-1	-1	1	-1	-1
5	5	-1	-1	1	-1	1
6	6	-1	-1	1	1	-1

No.	PQ bus	Topology number				
7	7	-1	-1	1	1	1
8	8	-1	1	-1	-1	-1
9	9	-1	1	-1	-1	1
10	10	-1	1	-1	1	-1
11	11	-1	1	-1	1	1
12	12	-1	1	1	-1	-1
13	13	-1	1	1	-1	1
14	14	-1	1	1	1	-1
15	15	-1	1	1	1	1
16	16	1	-1	-1	-1	-1
17	17	1	-1	-1	-1	1
18	18	1	-1	-1	1	-1
19	19	1	-1	-1	1	1
20	20	1	-1	1	-1	-1
21	21	1	-1	1	-1	1
22	22	1	-1	1	1	-1
23	23	1	-1	1	1	1
24	24	1	1	-1	-1	-1
25	25	1	1	-1	-1	1
26	26	1	1	-1	1	-1
27	27	1	1	-1	1	1
28	28	1	1	1	-1	-1

No.	PQ bus	Topology number				
29	29	1	1	1	-1	1

6.5.1 Training Sets Generation

To generate the training set patterns, off-line simulations are carried out. In the simulation, a contingency state is created by increasing the constant power *P*-*Q* loads at the load bus. The line stability factors are then calculated to identify whether the system is stable or not.

The training set input patterns are obtained by varying the constant power *P*-*Q* loads at the load buss in the following manner:

1) Vary *P* only at individual load bus while the other loads are kept constant

2) Vary *Q* only at individual load bus while the other loads are kept constant

3) Vary *P* and *Q* evenly at all the load buses

4) Vary *P* and *Q* at individual load bus while the other loads are kept constant

The training sets have been generated by varying the constant power *P*-*Q* loads and carrying out the off-line simulations. The loads are varied randomly from zero loading to the maximum loading as stated before.

6.5.2 Selection of Network Parameters

Table 6.3 Summary of parameters of the SHNN

	WSCC 9 bus system	New England 39 bus system
Input neurons	12	58
Output neurons	1	1
Neurons in Kohonen layer	36 (6×6)	100 (10×10)
Hidden layer	1	1
Neurons in the hidden layer	5	10
Learning rate	0.9	0.85
Momentum	0.1	0.15
Threshold value of convergence	0.005	0.005

The parameters of the hybrid neural network, including Kohonen network and Multi-layer neural network, are determined experimentally based on the complexity of problems. In particular, the determination of the Kohonen network should depend on applications so that the Kohonen network is capable of forming sufficient clusters for the input vectors. Table 6.3 summarizes the design parameters of the hybrid neural network after a large number of experiments. Training of SHNN is accomplished on a Pentium II 300 computer.

6.5.3 Results of the First SHNN Model

The first SHNN developed for WSCC 9-bus system has 12 input neurons and one output neuron. A total number of 1200 patterns showing 200 load scenarios are generated.

Out of 1200 patterns, 900 patterns corresponding to 150 load scenarios are used to train the SHNN. Once the SHNN is trained, it is tested for remaining 300 test patterns (50 load scenarios).

Table 6.4 Training detail of the first SHNN model

System	ANN used	Structure	Training Iteration	Training time(cpu)
WSCC 9-bus system	MLP	12-25-1	50,000	25s
	SHNN	12-5-1	20,000	15s
New England 39-bus system	MLP	58-100-1	800,000	1200s
	SHNN	58-10-1	50,000	90s

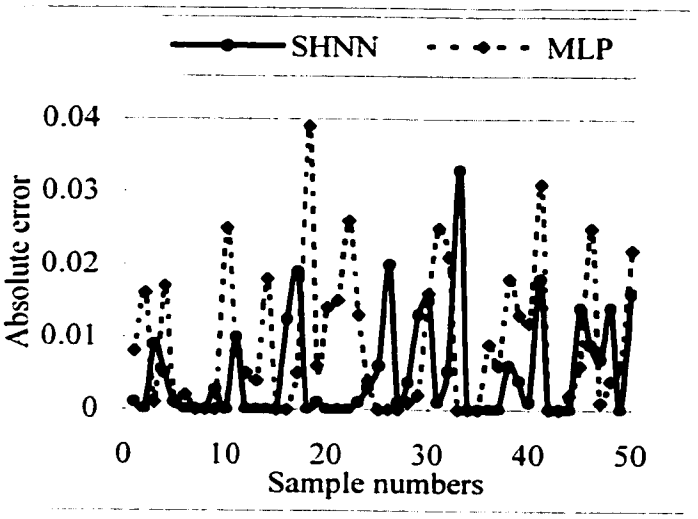

Fig. 6.4 Absolute error of stability indicator for WSCC 9-bus system

The first ANN is also developed for the New England 39-bus system which has 58 inputs and one output neuron. In this case, 2900 patterns corresponding to 100 load

scenarios are generated. 2175 patterns are used to train the SHNN and the remained 725 patterns are used to test the SHNN.

Table 6.5 Summary of stability indicator error

System	Method	Largest max. absolute error	RMS error
WSCC 9-bus system	MLP	0.039	0.00187
	SHNN	0.033	0.00124
New England 39-bus system	MLP	0.041	0.00320
	SHNN	0.032	0.00216

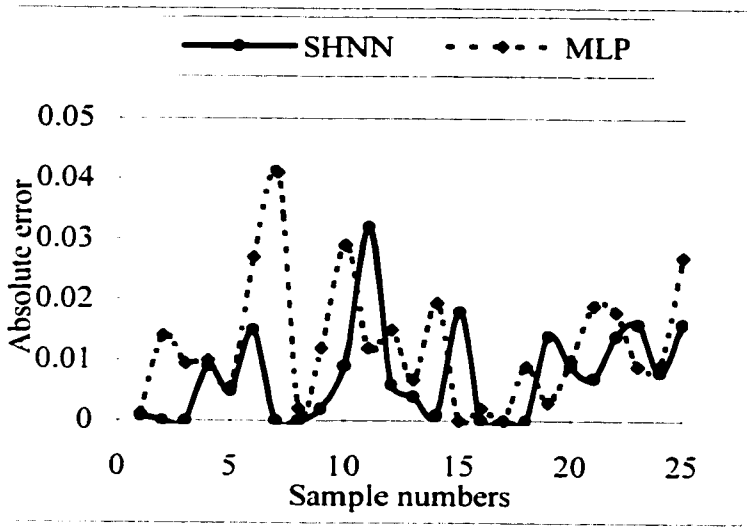

Fig. 6.5 Absolute error of stability indicator for New England 39-bus system

Training details using SHNN and multi-layer neural network (MLP) only are shown in Table 6.4. The test results are shown in Table 6.5, Fig. 6.4 and Fig. 6.5. From Table 6.4, it is observed that the MLP in SHNN required less training iterations to converge and less CPU time as compared to using the multi-layer neural network only. It is observed from Table 6.5 that for all the cases, the maximum absolute errors are 0.033 and 0.032, while the RMS

errors are 0.00124 and 0.00216 for WSCC and New England system, respectively. As can be observed from Fig. 6.4 and Fig. 6.5, the absolute errors for all test cases are less than 4%, and have better performance than those of multi-layer neural network. Hence, the first SHNN has been verified to provide accurate results.

6.5.4 Results of the Second SHNN Model

In order to train the second SHNN for WSCC system, 900 patterns showing 150 load scenarios are generated, among which 720 patterns corresponding to 120 load scenarios are used to train SHNN and the remaining 180 patterns (30 load scenarios). For New England 39 system, 2030 patterns (70 load scenarios) are generated in total. Out of these patterns, 1450 patterns (50 load scenarios) are generated for training and the remaining 580 patterns (20 load scenarios) are used to test the system. Training details are shown in Table 6.6. Table 6.7 and Table 6.8 show the maximum absolute error and RMS error of the voltage magnitude in all test cases. The error is the difference between the result calculated by approached method and that calculated by load flow program.

Table 6.6 Training detail of the second SHNN model

System	Structure	Training Iteration	Training time(cpu)
WSCC 9-bus system	12-25-1	25,000	15s
New England 39-bus system	58-10-1	50,000	90s

As can be seen from Table 6.7 and Table 6.8, the maximum absolute errors for all the test case are less than 0.0207 pu and 0.0515 pu respectively while the RMS errors are less than 0.0015 pu and 0.0093 pu for the two test systems.

Table 6.7 Summary of bus voltage estimation for WSCC system

S No	PQ Bus	Max. absolute error (pu)	RMS error (pu)
1	GEN1-230	0.0124	0.0012
2	GEN2-230	0.0103	0.0008
3	GEN3-230	0.0104	0.0007
4	STNA-230	0.0207	0.0015
5	STNB-230	0.0154	0.0014
6	STNC-230	0.0132	0.0009

Table 6.8 Summary of bus voltage estimation for New England 39-bus system

S No	PQ Bus	Max. absolute error (pu)	RMS error (pu)
1	1	0.0301	0.0015
2	2	0.0195	0.0009
3	3	0.0117	0.0005
4	4	0.0130	0.0013
5	5	0.0312	0.0020
6	6	0.0282	0.0026
7	7	0.0328	0.0032
8	8	0.0134	0.0036
9	9	0.0194	0.0039
10	10	0.0244	0.0042
11	11	0.0447	0.0044

S No	PQ Bus	Max. absolute error (pu)	RMS error (pu)
12	12	0.0135	0.0045
13	13	0.0515	0.0044
14	14	0.0351	0.0043
15	15	0.0439	0.0054
16	16	0.0462	0.0037
17	17	0.0432	0.0032
18	18	0.0366	0.0026
19	19	0.0318	0.0018
20	20	0.0102	0.0009
21	21	0.0090	0.0002
22	22	0.0104	0.0014
23	23	0.0322	0.0036
24	24	0.0139	0.0047
25	25	0.0262	0.0068
26	26	0.0189	0.0093
27	27	0.0122	0.0022
28	28	0.0162	0.0058
29	29	0.0214	0.0020

6.6 Summary

A hybrid neural network called Self-organizing Hierarchical Neural Network (SHNN) has been developed for voltage stability analysis. Two SHNN models are developed for two specific functions. One is to classify the stable or unstable system state and another is to predict the bus voltage magnitudes for the stable cases. To reduce the required training time and the accuracy of the ANN. a self-organizing hierarchical neural network is used. The developed SHNN models have been applied to a number of test systems. Results obtained show that the proposed approach is more effective and is better in accuracy than that of multi-layer neural network method.

Chapter 7

Conclusions

7.1 Summary

This thesis analyzes the issue of fast voltage stability analysis which is one of the main concerns of power system research. Two techniques, artificial neural networks (ANNs) and network reduction, are applied in order to get the fast solution of the problem. An overview of current trends in voltage stability analysis, as well as the external network reduction techniques, is presented in Chapter 1. Following the introductory background chapter, the extended Ward equivalent is discussed in Chapter 2 with discussion of other Ward-type equivalents. In Chapter 3, the theory of ANNs for voltage stability study is presented. Three different neural network models and their performances are also presented in Chapter 3. Chapter 4 develops a simple approach based on Q-V and P-V curves analysis. This approach uses the MTPLC method to build an equivalent model and can fast determine the slope of the Q-V and P-V curves for the further research of voltage stability. A more complex and accurate external network equivalent method is developed in Chapter 5. The theory is based on extended Ward equivalent and ANNs in an attempt to investigate the on-line boundary match of the external system. The contingency analysis using this method has been demonstrated. Chapter 6 applies ANNs in voltage stability. The ANN developed is called Self-organizing Hierarchical Neural Network (SHNN), which is a hybrid multi-layer

feed-forward and Kohonen neural network. A comparison between multi-layer neural network and SHNN is also discussed.

7.2 Main Contributions

In summary, the main contributions and findings of this thesis are as follows:

1. The voltage-collapse phenomenon is often explained by means of static techniques, and analyzed by means of Q-V and P-V. A new approach with network equivalence has been developed to provide a fast way to plot Q-V and P-V curves at the given node where voltage stability is to be studied. From the study node, a complex system is reduced to equivalent E, x and θ. Many calculations indicate that E and x of the system can be represented by two groups of values. Then after calculating load flow in two point, Q-V and P-V curves are quickly plotted out with satisfactory accuracy. The proposed method is called Modified Two-Point Load-flow Calculation (MTPLC) method.

2. External network equivalent is of vital importance in power system research. Ward equivalent is one of the most popular methods in external network equivalent. The extended Ward equivalent gives reasonable accuracy for both active and reactive power flows. Usually, the network configuration changes are according to schedule, while the load level is continuously changing throughout the day. In this context, the boundary power injections would need to be updated from time to time. The extended Ward equivalent cannot simulate significant events in the external system and their impact on the internal system.

3. ANN is shown to be suitable for external network equivalent as it is mainly an identification problem. A novel hybrid ANN and Ward equivalent approach network reduction for on-line voltage security assessment is developed. The new approach can update the equivalent parameters according to the line status in buffer zone and matching the boundary equivalent power injections. Test results show that the new equivalents approach represents with better accuracy than conventional Ward equivalent method. It is of much promise to be used in fast on-line voltage security assessment.

4. Most of the published work in the area of voltage stability analysis is based on multi-layer feed-forward networks. However, in respect of voltage stability assessment of practical systems, a major difficulty of this type of neural networks is that it depends much on the number of training data. To reduce the required training time and the accuracy of the ANN, a Self-organizing Hierarchical Neural Network (SHNN), which consists of a self-organizing map network and a multi-layer feed-forward network, is developed. The Kohonen Self-organizing network is used as a front end to a mapping network, *i.e.*, the multi-layer neural network which maps the output of Kohonen networks in order to give voltage stability margin. In this way, robust mapping can be achieved and thus the generalization capability of the multi-layer feed-forward network has been improved significantly.

5. Two SHNN models are developed with two specific functions for voltage stability assessment. One is to classify the stable or unstable system state and another is to predict the bus voltage magnitudes for the stable cases. The developed SHNN models

have been applied to a number of test systems. Results obtained show that the proposed approach is more effective and is better in accuracy than conventional ANN method.

7.3 Future Work

1. The simple way to plot Q-V and P-V curves developed in this thesis focuses on a single node and single load change. The concept of the multi-load-change is needed in further research.

2. Reactive power control and limits will play an important role in voltage stability. The limitation as well as the voltage characteristics of the controllable reactive source should also be considered.

3. The system used for hybrid external system equivalent is not complex enough. In order to show the effectiveness of this method, more complex large-scale interconnected system may be tested.

4. The characteristics of load model have impact influence on voltage stability. More detailed load model may be developed, and the load characteristics should be considered. The dynamic load models should be considered in the voltage stability analysis.

5. Reliable voltage collapse indicators should be developed and adopted.

6. ANN approach used for external equivalent and voltage stability analysis is shown to

be promising. Further systematic researches are required for external equivalent based voltage stability analysis for on-line application.

References

[1] A. A. El-Keib, X. Ma, "Application of artificial neural networks in voltage stability assessment", IEEE Trans. on Power Systems, Vol. 10, No. 4, November, 1995, pp. 1890-1895

[2] A. B. R. Kumar, A. Ipakchi, V. Brandwajn, M A El-Sharkawi and G. Cauley, "Neural networks for dynamic security assessment of large-scale power systems", Proc. of ANNPS'91, pp. 65-71, Seattle, WA, July, 1991

[3] A. Borghetti, R. Caldon, A. Mari, C. A. Nucci, "On dynamic load models for voltage stability studies", IEEE Trans. on Power Appar. Systems, Vol. 12, No. 1, February, 1997, pp. 293-303

[4] A. J. Germond, A. R. Podmore, "Development of dynamic equivalents for transient stability studies", Final Report on Epri Project EP763, System Control Inc., May 1977

[5] A. J. Germond, P. Podmore, "Dynamic aggregation of generating unit models", IEEE Trans. on Power Apparatus and Systems, Vol. PAS-97 1060-1069, July/Aug., 1978

[6] A. J. Wood and B. F. Wollenberg, Power Generation, Operation and Control, Wiley, New York, 1984

[7] A. M. Chebbo, M. R. Irving, and M. J. H. Sterling, "Voltage collapse proximity indicator: behavior and implications", IEE Proc. C, 1992, pp. 241-252

[8] A. Mohamed, New Techniques for Power Voltage Stability Studies. Ph. D Thesis, University of Malaya, 1994

[9] A. Mohamed, and G. B. Jasmon, "Neural network approach to dynamic voltage stability prediction", Electric Machine and Power Systems, 25 (5):509-523, 1997

[10] A. Monticelli, S. Deckmann, A. Garcia, B. Stott, "Real-time external equivalents for static security analysis", IEEE Transactions on Power Apparatus and Systems, PAS-98, (1979): 498-508

[11] A. Tiranuchit and R. J. Thomas, "Posturing strategy against voltage instability in electric power systems", IEEE Trans on Power Systems, Vol. 3, No. 1, Feb. 1988, pp. 87-93

[12] B. Gao, G. K. Morison, and P. Kundur, "Towards the development of a systematic approach for voltage stability assessment of large-scale power system", IEEE Trans. on Power System, Vol. 11, No. 3, Aug. 1996, pp. 1314-1324

[13] B. Gao, G. K. Morison, and P. Kundur, "Voltage stability evaluation using modal analysis", IEEE Trans. on Power Systems, 1992, 7 (4) pp. 1529-1542

[14] B. Jeyasurya. "Application of artificial neural networks to power system transient energy margin evaluation". Electric Power Systems Research. 26 (1993): 71-78

[15] B. Jeyasurya. "Artificial neural networks for power system steady-state voltage instability evaluation". Electric Power Systems Research. 1994. 29 (2). pp. 85-90

[16] B. M. Weedy. Electric Power Systems. Third Edition Revised. John Wiley & Sons. 1987 (earlier editions 1967. 1972. and 1979)

[17] B. Stott. "Review on load flow calculation methods". Proc. IEEE. Vol. 62 (July 1974). pp. 916-929

[18] B. Stott and O. Alsaç. "Fast decoupled load flow". IEEE Trans. on Power Appar. & Syst.. Vol. PAS-73 (May/June 1974). pp. 859-869

[19] B. Stott. O. Alsaç and A. J. Monticelli. "Security analysis and optimization". IEEE Proc. 75 (12). (1987) 1623-1644

[20] C. A. Canizares and F. L. Alvarado. "Point of collapse and continuation methods for large AC/DC systems". IEEE Trans. on Power Systems. 1993. 8 (1). pp. 1-8

[21] C. L. DeMarco and T. J. Overbye, "An energy based security measure for assessing vulnerability to voltage collapse", IEEE Trans. On Power Systems, Vol. 5, No. 2 May 1990, pp. 428-438

[22] C. Lemaitre, J. P. Paul, J. M. Tesseron, Y. Harmand, and Y. S. Zhao, "An indicator of the risk of voltage profile instability for real-time control applications", IEEE Trans. on Power Systems, Vol. 5, No. 1, Feb. 1990, pp. 154-161

[23] C. S. Chang, "Fast power system voltage prediction using knowledge based approach and on-line box data creation", IEE Proc. C, Vol 136-C, No. 2, March (1989): 87-99

[24] C. N. Lu, K. C. Liu, S. Vemuri, "An external network modeling approach for on-line security analysis", IEEE Transactions on Power Systems, 5 (2) (1990): 565-573

[25] CIGRE Task Force 38-02-10, Modeling of voltage collapse including dynamic phenomena, 1993

[26] CIGRE Working Group 38.01, "Planning Against Voltage Collapse", Electra, pp. 55-57, March 1987

[27] CIGRE Working Group 38.02, "Steady-state and dynamic equivalents state - of - art report", Electra, Vol. 134, pp. 93-117, 1990

[28] CIGRE Working Group 38.02. "Steady-state and dynamic equivalents", Electra. Vol. 135. pp. 103-111. 1990

[29] D. C. Park and M A El-Sharkawi. "Electric load forecasting using an artificial neural network". IEEE Trans. on Power Systems. 1991. 6 (2). pp. 442-449

[30] D. J. Hill. "Nonlinear dynamic load models with recovery for voltage stability studies". IEEE Trans. on Power Systems. Vol. 8. No. 1. February. 1993. pp. 166-176

[31] D. J. Sobajic and Y. H. Pao. W. Nio and K. L. Dolce. "Real-time security monitoring of electric power systems using parallel associative memories". IEEE Proc. of 1990 ISCAS. pp. 2929-2932. New Orleans. Louisiana. USA. May 1990

[32] D. J. Sobajic and Y. H. Pao. "Artificial neural-net based dynamic security assessment for electric power systems". IEEE Trans. on Power Systems. Vol. 4. No. 1. Feb. 1989. pp. 220-228

[33] D. Karlsson. D. J. Hill. "Modelling and identification of non-linear dynamic loads in power systems". IEEE Trans. on Power Systems. Vol. 9. No. 1. February. 1994. pp. 157-166

[34] D. Niebur. "Artificial neural networks for power system". Task Force 38-06-06 of study committee 38. Electra 159 (1995) 77-101

[35] D. Niebur, and A. J. Germond, "Power system static security assessment using the Kohonen neural network classifier", IEEE Trans. on Power Systems, vol. 7, no. 2, 1992, pp. 865-871

[36] D. Niebur, and A. J. Germond, "Unsupervised neural net classification of power system static security states", Electrical Power & Energy System, 1992, 12 (2/3), pp. 233-242

[37] D. Z. Fang, T. S. Chung, A. K. David, "Fast transient stability estimation using a novel dynamic equivalent reduction technique", IEEE Trans. on Power Systems, Vol. 9, No. 2, May 1994, pp. 995-1001

[38] E. Abu-Al-Feilat, M. Bettayeb, H. Al-Duwaish, M. Abido, A. Mantawy, "A neural network-based approach for on-line dynamic stability assessment using synchronizing and damping torque coefficients", Electric Power Systems Research 39 (1996) 103-110

[39] E. Bompard, E. Carpaneto, G. Chicco and R. Napoli, "A dynamic interpretation of the load-flow Jacobian singularity for voltage stability analysis", Electrical Power & Energy System, Vol. 18, No. 6, pp. 385-395, 1996

[40] EPRI Final Report EL-4610, Extended transient-midterm stability package: final report, Prepared by Ontario Hydro, November 1992

[41] F. Albuyeh, A. Bose and B. Heath, "Reactive power consideration in automatic contingency selection", IEEE Trans. Power Appar. Syst., PAS-101 (1) (1982) 107-112

[42] F. F. Wu and A. Monticelli, "Critical review of external network modelling for online security analysis", Electrical Power & Energy System, 1983, 5 (4) , pp. 222-235

[43] F. Gubina, B. Strmcnik, "A simple approach to voltage stability assessment in radial networks", IEEE Trans. on Power System, Vol. 12, No. 3, Aug. 1997, pp. 1121-1128

[44] F. Gubina, B. Strmcnik, "Voltage collapse location and proximity index determination using voltage phasors approach", IEEE Trans. on Power System, Vol. 10, No. 2, 1995

[45] F. Wang, X. T. Yang, "External system multi-level equivalent in power system static security analysis", Electrical Power System Automation, Vol. 12, No. 6, June 1988, pp. 20-27

[46] G. B. Jasmon, L. H. C. C. Lee, "Prediction of voltage collapse in power systems using a reduced system model", International Conference on Control'91, pp 32-36

[47] G. J. Berg, "Power-system load representation", Porc. IEE, Vol. 120, No. 3, March 1973, pp. 344-348

[48] G. K. Morison, B. Gao, and P. Kundur, "Voltage stability analysis using static and dynamic approaches", IEEE Trans. on Power Systems, Vol. 8, No. 3, Aug, 1993, pp. 1159-1171

[49] H. B. Wan and Y. H. Song, "Hybrid supervised and unsupervised neural network approach to voltage stability analysis", Electric Power Systems Research 47 (2) (1998) pp. 115-122

[50] H. C. Nallan, P. Rastgoufard, "Computational voltage stability assessment of large-scale power systems", Electric Power System Research 38 (1997) 177-181

[51] H. H. Yan, J. C. Chow, R. Fischl and R. X. Chen, "On the design of a practical neural network for on-line prediction of voltage drops and line flows", Proc. of Expert System Application in Power Systems, Melbourne, Australia, January 1993.

[52] H. Mori, Y. Tamaru, S. Tsuzuki, "An artificial neural network based technique for power system dynamic stability with the Kohonen model", 17th PICA'91, pp. 293-301

[53] IEEE Special Publication, 90TH0358-2-PWR, Voltage stability of power system: concept, analytical tools, and industry experience, 1990

[54] IEEE Special Publication, 93TH0620-5-PWR, Suggested techniques for voltage stability analysis, 1993

[55] J. Deuse and M. Stubbe, "Dynamic simulation of voltage collapse", paper 92 SM 396-2 PWRS, presented at IEEE/PES Summer Meeting, July 12-16, 1992

[56] J. H. Chow, J. R. Winkelman, M. A. Pai and P. W. Sauer, "Singular perturbation analysis of large-scale power systems", Electrical Power & Energy System, Vol. 12, No. 2, April 1990, pp. 117-126

[57] J. Machowski, A. Cichy, F. Gubina, P. Omahen, "External subsystem equivalent model for steady-state and dynamic security assessment", IEEE Trans. on Power Systems, Vol. 3, No. 4, November 1988, pp. 1456-1462

[58] K. I. Geisler, A. Bose, "State estimation based external network solution for on-line security analysis", IEEE Transactions on Power Apparatus and systems, PAS-102 (8) (1983): 2447-2454

[59] K. Kato, I. Dabbaghchi, J. K. Robinson, "Real-time data exchange for on-line security assessment", IEEE Trans. on Power System, Vol. 7, No. 3, August 1992, pp. 1322-1332

[60] K. L. Lo, L. J. Peng, J. F. Macqueen, A. O. Ekwue, D. T. Y. Cheng, "An extended Ward equivalent approach for power system security assessment", Electric Power System Research, 42 (1997), pp. 181-188

[61] K. L. Lo, L. J. Peng, J. F. Macqueen, A. O. Ekwue, N. H. Dandachi, "An extended ward equivalent of external system for on-line security analysis", APSCOM-93 Hong Kong (1993) 54-59

[62] K. L. Lo, L. J. Peng, J. F. Macqueen, A. O. Ekwue, D. T. Y. Cheng, "Hybrid approach using conterpropagation neural network for power-system network reduction", IEE Proc. - Gener. Transm. Distib., Vol. 144, No. 2, March 1997, 169-174

[63] K. M. Graf, "Dynamic simulation of voltage collapse Process in EHV Power Systems", EPRI EL-6183 Project 2473-21 Proc., pp. 6/45-6/54, Jan., 1989

[64] L. C. Wang, A. A. Girgis, "On-line Detection of power system small disturbance voltage instability", IEEE Trans. on Power Systems, Vol. 11, No. 3, August 1996, pp. 1304-1313

[65] L. Srivastava, S. N. Singh and J. Sharma, "Parallel self-organizing hierarchical neural network based fast voltage estimation", IEE Proc. Part-C, 145 (1) (1998) 98-104

[66] L. Wehenkel, M. Pavella, "Decision tree approach to power system security assessment", Electrical Power & Energy System, Vol. 15, No. 1, February 1993, pp. 13-36

[67] M A El-Sharkawi, "choice model of topology for external equivalent systems", IEE Trans. on PWRS, Vol. PAS-102, No. 12, December 1981, pp. 3761-68

[68] M A El-Sharkawi, D. Niebur, Security Assessment and Enhancement, IEEE Power Engineering Society, A Tutorial Course on Artificial Neural Networks with Applications to Power System, 1996, pp. 104-127

[69] M A El-Sharkawi, R. J. Marks, M. E. Aggoune, D. C. Park, M. J. Damborg and L. E. Atlas, "Dynamic security assessment of power systems using back error propagation artificial neural networks", Second Symposium on Expert System Application to Power Systems, Seattle, WA, July, 1991

[70] M. Djukanovic, B. Babic, D. J. Sobajic and Y. H. Pao, "Unsupervised/supervised learning concept for 24-hour load forecasting", IEE Proceedings - C, Vol. 140, No. 4, July 1993, pp. 311318-219

[71] M. H. Haque, "A fast method for determining the voltage stability limit of a power system", Electric Power System Research 32 (1995) 35-43

[72] M. Hanmandlu, G. Durga, Prasad and S. C. Tripathy, "Decoupled internal state estimation using external system equivalents", Electrical Power & Energy Systems, Vol. 9, No. 1, January 1987, pp. 23-28

[73] M. K. Pal, "Voltage stability conditions considering load characteristics", IEEE Trans. on Power Systems, Vol. 7, No. 1, February, 1992, pp. 243-249

[74] M. K. Pal, "Voltage stability: analysis needs, modelling requirement, and modelling adequacy", IEE Proceedings-C, Vol. 140, No. 4, July 1993, pp. 279-286

[75] M. M. A. Salama, A. Y. Chikhani, "A simplified network approach to the Var control problem for radial distribution systems", IEEE Trans. on Power Delivery, Vol. 8, No. 3, July 1993, pp. 1529-1535

[76] N. Flatabo, R. Ognedal, and T. Carlsen, "Voltage stability condition in a power transmission system calculated by sensitivity methods", IEEE Trans. on Power Systems, 1990, 5 (4), pp. 1286-1293

[77] N. Hadjsaid, J. Fandino, Q. T. Tran, J. C. Sabonnadiere, G. Nerin, "An adaptive correction for voltage security analysis using a local approach solution", IEEE Trans. on Power Systems, Vol. 9, No. 2, May 1994, pp. 660-667

[78] Neural computing - a technology handbook for professional II. Plus and neural works explorer, Neural Ware, Inc., 1993

[79] O. O. Obadina, G. J. Berg, "Identifying electrically weak and strong segments of power systems from a voltage stability viewpoint", IEE Proc. C, 137 (3) 1990, pp. 205-212

[80] P. A. Lof, G. Andersson, and D. J. Hill, "Voltage stability indices for stressed power systems", IEEE Trans. on Power Systems, 1993, 7 (1), pp. 326-335

[81] P. Bonanomi, R. Bertschi, "On-line identification of an equivalent reactance for stability applications", IEEE Trans. on Power Apparatus and System, Vol. PAS-100(2) 822~827, 1981

[82] P. Kessel, and H. Glavitsch, "Estimating the voltage stability of a power system", IEEE Trans. on Power Delivery, 1986, 3, pp. 346-354

[83] P. Kundur, Power System Stability and Control, EPRI series, McGraw-Hill, Inc., 1994

[84] Power System Analysis Software Package, Electric Power Research Institute, Beijing, 1993

[85] Q. Zhou, J. Davidson, and A. A. Fouad, "Application of artificial neural networks in power system security and vulnerability assessment", IEEE Trans. on Power Systems, Vol. 9, No. 1, Feb. 1994, pp. 525-532

[86] R. A. M. van Amerongon and H. P. van Meeteren, "A generalized Ward equivalents for static security analysis", IEEE Trans. Power Appar. & Syst. Vol PAS-101, Vol. 6, 1982, pp. 1519-1526

[87] R. J. Thomas, "Analytical methods for analysis, assessment and control of voltage instabilities", Panel Session on Voltage Instabilities, IEEE-PES Summer Meeting, San Francisco, July, 1987

[88] R. Lippmann, An Introduction to Computing with Neural Nets, IEEE ASSP Mag., (4) (1987) 4-22

[89] R. L. Watrous, "Learning algorithm for connectionist networks, applied gradient methods of nonlinear optimization", Proc. of IEEE 1st International Conference on Neural Networks, Vol. 2, pp. 619-628, June, 1987

[90] R. Podmore, "Identification of coherent generators for dynamic equivalents", IEEE Trans. on Power Apparatus and Systems, Vol. PAS-97 1344-1354, July/Aug., 1978

[91] R R Shoults and W J Jr Bierck, "Buffer system selection of a steady-state external equivalent model for real-time power flow using an automated sensitivity analysis procedure", IEEE Trans. on Power System, 3 (3) (1988) 1104-1111

[92] S. C. Savulescu. "Equivalents for security analysis of power systems". IEEE Trans. on Power Apparatus and Systems. PAS-100 (5) (1981): 2672-2681

[93] S. Deckmann. A. Pizzolante. A. Monticelli. B. Stott. O. Alsaç. "Numerical testing of power system load-flow equavalencing". IEEE Transactions on Power Apparatus and Systems. PAS-99 (6) (1980): 2292-2300

[94] S. Deckmann. A. Pizzolante. A. Monticelli. B. Stott. O. Alsaç. "Studies on power system load flow equivalencing". IEEE Transactions on Power Apparatus and Systems. PAS-99 (6) (1980): 2301-2310

[95] S. Ghosh and B. H. Chowdhury. "Design of an artificial neural network for fast line flow contingency ranking". Electrical Power & Energy Systems. Vol. 12. no. 5. 1996. pp.271-277

[96] S. N. Singh and S. C. Srivastava. "Improved voltage and reactive power distribution factor for outages studies". IEEE Trans. on Power Systems. PWRS-12 (3) (1997) 1085-1093

[97] S. T. Chen. D. C. Yu and A. R. Moghaddamjo. "Weather sensitive short-term load forecasting using an non-fully connected artificial neural network". IEEE Trans. on Power Systems. 1992. 7 (3). pp. 1098-1105

[98] S. Weerasooriya and M A El-Sharkawi, "Use of Karhunen-Loeve expansion in training neural networks for static security assessment", Proc. of ANNPS'91, pp. 59-64, Seattle, WA, July 1991

[99] S. Y. Hao, A. Papalexopoulos, "External network for optimal power flow application", IEEE Transactions on Power Systems, 10 (2) (1995): 825-837

[100] T. J. Overbye and C. L. DeMarco, "Improved techniques for power system voltage stability assessment using energy method", IEEE Trans. on Power Systems, 1991, 6 (4), pp. 1446-1452

[101] T. J. Overbye and C. L. DeMarco, "Voltage stability enhancement using energy based sensitivities", IEEE Trans. on Power Systems, 1991, 6 (3), pp. 1196-1202

[102] T. J. Overbye, I. Dobson, "Q-V curve interpretations of Energy measure for voltage security", IEEE 93 WM 184-2 PWRS, 1993, pp. 331-340

[103] T. Kohonen, Self-organization and associative memory, Springer, Berlin, 2nd edn., 1987

[104] T. S. Dillon, "Artificial neural network applications to power system and their relationship to symbolic methods", Electrical Power and Energy system, vol. 13, no. 2, 1991, pp. 66-72

[105] T. V. Cutsem, "A method to compute reactive power margins with respect to voltage collapse", IEEE Trans. on Power Systems, 1991, 6 (1) pp. 145-156

[106] T. V. Cutsem, C. Vournas, Voltage Stability of Electric Power System, Power Electronics and Power Systems series, Kluwer Academic Publishers, 1998

[107] U. M. Al-Saggaf, "Reduced-order models for dynamic control of a power plant with an improved transient and steady-state behavior", Electric Power Systems Research, 16 (1993), pp. 79-85

[108] V. Ajjarapu, and C. Christy, "The continuation power flow: a tool for steady state voltage stability analysis", IEEE Trans. on Power Systems, 1992, 7 (1), pp. 416-423

[109] V. Q. Do, M. M. Gavrilovic, "A synthesis method for one-port and multi-port equivalent networks for analysis of power system transients", IEEE Trans. on Power Systems, Vol. PWRD-1, No. 2, April 1986, pp. 103-113

[110] V. S. S. Vankayala, and N. D. Rao, "Artificial neural networks and their applications to power systems - a bibliographical survey", Electric Power Systems Research, 28 (1993), pp. 67-79

[111] W. J. Smolinski, "Equivalent circuit analysis of power system reactive power and voltage control problems", IEEE Trans. on Power Appar. Systems, Vol. PAS-100, No. 2, February, 1981, pp. 837-842

[112] W. J. Wilson, J. D. Aplevich, "Dynamic equivalent power system models", IEEE Trans. on Power Apparatus and System, Vol. PAS-102, No. 12, December 1983, pp.3753-3760

[113] W. L. Snyder, S. Vemuri, A. D. Paralexopoulos, M. L. Oatts, G. C. Contaxis, J. Singh, R. Smith, S. C. Savulescu, "External network modeling-recent practical experience", IEEE Transactions on Power Systems, 9 (1) (1994): 216-228

[114] W. W. Price, D. G. Klapper, N. W. Miller, S. Kurita, and H. Okubo, "A multiple faceted approach to power system voltage stability analysis", CIGRE, paper 38-205, 1992

[115] X. Y. Li, Y. H. Song, J. Y. Liu, Y. Fu and M. Zeng, "Post-fault voltage security assessment of complex power system based on ANN", Chinese Society for Electrical Engineering Proceedings of the CSEE, Vol. 16 No. 3, May 1996, pp. 147-150

[116] Y Fu, M Zeng, X. Y. Li, J. Y. Liu, G. D. Wang, "The effect of hidden layers on voltage security assessment", Electrical Engineering and Automation, Vol. 20, No. 11, November 1996, pp. 13-17

[117] Y. H. Song, H. B. Wan and A. T. Johns, "Kohonen neural network based approach to voltage weak buses/areas identification", IEE Proc. - Gener. Transm. Distriv., Vol. 144, No. 3, May 1997, pp. 340-344

[118] Y. H. Song, J. F. Macqueen, D. T. Y. Cheng, and A. Arnal, "On voltage stability in electric power system", Proc. IEEE International Conference on Power system technology, 1994, pp. 566-570

[119] Y. L. Chen, A. Bose, "Security analysis for voltage problems using a reduced model", IEEE Trans. on Power Systems, Vol. 3, August 1990, pp. 933-940

[120] Y. L. Chen, C. W. Chang, and C. C. Liu, "Efficient methods for identifying weak nodes in electrical power networks", IEE Proc. Gener. Transm. Distrib., 1995, 142 (3), pp. 317-322

[121] Y. Sekine, and H. Ohtsuki, "Cascaded voltage collapse", IEEE Trans. On Power Systems, 1990, vol. 5, no. 1, pp. 250-256

[122] Y. Tamura, "a scenario of voltage collapse in a power system with induction motor loads with a cascaded transition of bifurcations", Proceedings: Bulk Power System Voltage Phenomena II: Voltage Stability and Security, Deep Creek Lake, Maryland, pp. 143-146, 4-7 August 1991

[123] Y. Tamura, H. Mori, and S. Iwamoto, "Relationship between voltage instability and multiple load flow solutions in electric power systems", IEEE Trans., 1983, PAS-102, pp. 1115-1125

[124] Y. Y. Hong, and C. H. Gau, "Voltage stability indicator for identification of the weakest bus/area in power systems", IEE Proc. Gener. Transm. Distrib., 1994, 141 (4), pp. 305-309

[125] Y. Yu, M A El-Sharkawi, M. D .Wvong, "Estimation of unknown large power system dynamic", IEEE Trans. on Power Apparatus and System, Vol. PAS-98 (1) 279~289, 1979

[126] Y. Z. He, Z. Y. Wen, F. Y. Wang, Q. H. Zhou, *Power System Analysis*, Huazhong University of Science and Technology Press, 1988

Appendices

Appendix I System Data of New-England 39-Bus Test System

Table I.1 System data of New-England 39-bus test system

Bus	Bus	Voltage pu		Generation pu		Load pu		Induction motor data		
Name	Type	Magn.	Angle	Real	Reactive	real	reactive	rm	xm	slip s
1	PQ	1.	0.0	0.0	0.0	0.0	0.0	0.0	0.0	0.0
2	PQ	1.	0.0	0.0	0.0	0.0	0.0	0.0	0.0	0.0
3	PQ	1.	0.0	0.0	0.0	3.22	0.024	0.0167	0.05	0.005
4	PQ	1.	0.0	0.0	0.0	5	1.84	0.08	0.05	0.02
5	PQ	1.	0.0	0.0	0.0	0.0	0.0	0.0	0.0	0.0
6	PQ	1.	0.0	0.0	0.0	0.0	0.0	0.0	0.0	0.0
7	PQ	1.	0.0	0.0	0.0	2.338	0.84	0.0175	0.05	0.005
8	PQ	1.	0.0	0.0	0.0	5.22	1.76	0.04	0.08	0.02
9	PQ	1.	0.0	0.0	0.0	0.0	0.0	0.0	0.0	0.0
10	PQ	1.	0.0	0.0	0.0	0.0	0.0	0.0	0.0	0.0
11	PQ	1.	0.0	0.0	0.0	0.0	0.0	0.0	0.0	0.0
12	PQ	1.	0.0	0.0	0.0	.075	0.88	0.035	0.1	0.01
13	PQ	1.	0.0	0.0	0.0	0.0	0.0	0.0	0.0	0.0
14	PQ	1.	0.0	0.0	0.0	0.0	0.0	0.0	0.0	0.0
15	PQ	1.	0.0	0.0	0.0	3.2	1.53	0.165	0.05	0.02
16	PQ	1.	0.0	0.0	0.0	3.29	0.323	0.05	0.15	0.01
17	PQ	1.	0.0	0.0	0.0	0.0	0.0	0.0	0.0	0.0
18	PQ	1.	0.0	0.0	0.0	1.58	0.3	0.035	0.08	0.01
19	PQ	1.	0.0	0.0	0.0	0.0	0.0	0.0	0.0	0.0
20	PQ	1.	0.0	0.0	0.0	6.28	1.03	0.0	0.0	0.0
21	PQ	1.	0.0	0.0	0.0	2.74	1.15	0.02	0.08	0.04
22	PQ	1.	0.0	0.0	0.0	0.0	0.0	0.0	0.0	0.0

Bus Name	Bus Type	Voltage pu		Generation pu		Load pu		Induction motor data		
		Magn.	Angle	Real	Reactive	real	reactive	rm	xm	slip s
23	PQ	1.	0.0	0.0	0.0	2.475	0.046	0.03	0.10	0.02
24	PQ	1.	0.0	0.0	0.0	3.086	-0.922	0.01	0.05	0.003
25	PQ	1.	0.0	0.0	0.0	2.24	0.472	0.0175	0.05	0.004
26	PQ	1.	0.0	0.0	0.0	1.39	0.17	0.08	0.03	0.01
27	PQ	1.	0.0	0.0	0.0	2.81	0.755	0.0	0.0	0.0
28	PQ	1.	0.0	0.0	0.0	2.06	0.276	0.0265	0.05	0.005
29	PQ	1.	0.0	0.0	0.0	2.835	0.269	0.02	0.10	0.01
30	PV	1.0475	0.0	2.5	1.451	0.0	0.0	0.0	0.0	0.0
31	VD	0.982	0.0	5.63	2.055	.092	0.046	0.0	0.0	0.0
32	PV	0.9831	0.0	6.5	2.057	0.0	0.0	0.0	0.0	0.0
33	PV	0.9972	0.0	6.32	1.091	0.0	0.0	0.0	0.0	0.0
34	PV	1.0123	0.0	5.08	1.67	0.0	0.0	0.0	0.0	0.0
35	PV	1.0493	0.0	6.5	2.113	0.0	0.0	0.0	0.0	0.0
36	PV	1.0635	0.0	5.6	1.005	0.0	0.0	0.0	0.0	0.0
37	PV	1.0278	0.0	5.4	.007	0.0	0.0	0.0	0.0	0.0
38	PV	1.0265	0.0	8.3	.228	0.0	0.0	0.0	0.0	0.0
39	PV	1.03	0.0	10	.86	11.04	2.5	0.0	0.0	0.0

Table I.2 AC line data

Line	From	To	Resistance pu	Reactance pu
1	1	2	.0035	.0411
2	1	39	.001	.025
3	2	3	.0013	.0151
4	2	25	.007	.0086
5	3	4	.0013	.0213
6	3	18	.0011	.0133
7	4	5	.0008	.0128
8	4	14	.0008	.0129

Line	From	To	Resistance pu	Reactance pu
9	5	6	.0002	.0026
10	5	8	.0008	.0112
11	6	7	.0006	.0092
12	6	11	.0007	.0082
13	7	8	.0004	.0046
14	8	9	.0023	.0363
15	9	39	.001	.025
16	10	11	.0004	.0043
17	10	13	.0004	.0043
18	13	14	.0009	.0101
19	14	15	.0018	.0217
20	15	16	.0009	.0094
21	16	17	.0007	.0089
22	16	19	.0016	.0195
23	16	21	.0008	.0135
24	16	24	.0003	.0059
25	17	18	.0007	.0082
26	17	27	.0013	.0173
27	21	22	.0008	.014
28	22	23	.0006	.0096
29	23	24	.0022	.035
30	25	26	.0032	.0323
31	26	27	.0014	.0147
32	26	28	.0043	.0474
33	26	29	.0057	.0625
34	28	29	.0014	.0151

Table I.3 Transformer data

No.	From	To	R	x	T_k
35	11	12	.0016	0.0435	1.006
36	13	12	.0016	0.0435	1.006
37	31	6	.0007	0.025	1.07
38	32	10	0	0.02	1.07
39	33	19	0.0007	0.0142	1.07
40	34	20	0.0009	0.018	1.009
41	35	22	0	0.0143	1.025
42	36	23	0.0005	0.0272	1
43	37	25	0.0006	0.0232	1.025
44	30	2	0	0.0181	1.025
45	38	19	0.0008	0.0156	1.025
46	20	19	0.0007	0.0138	1.06

Appendix II System Data of WSCC 9-bus Test System

Table II.1 System data of WSCC 9-bus test system

Bus Name	Bus Type	Voltage pu		Generation pu		Load pu		Induction motor data		
		Magn.	Angle	real	reactive	Real	reactive	rm	xm	slip s
GEN1	VD	1.04	0.0	0.0	0.0	0.0	0.0	0.0	0.0	0.0
GEN2	PV	1.025	0.0	1.63	1.0	0.0	0.0	0.0	0.0	0.0
GEN3	PV	1.025	0.0	.05	1.0	0.0	0.0	0.0	0.0	0.0
GEN1-230	PQ	1.0	0.0	0.0	0.0	0.0	0.0	0.0	0.0	0.0
GEN2-230	PQ	1.0	0.0	0.0	0.0	0.0	0.0	0.0	0.0	0.0
GEN3-230	PQ	1.0	0.0	0.0	0.0	0.0	0.0	0.04	0.08	0.01
STNA-230	PQ	1.0	0.0	0.0	0.0	1.25	0.5	0.01	0.05	0.005
STNB-230	PQ	1.0	0.0	0.0	0.0	0.9	0.3	0.05	0.05	0.005
STNC-230	PQ	1.0	0.0	0.0	0.0	1.0	0.35	0.03	0.1	0.02

Table II.2 Network parameters

Line	From	To	Resistance pu.	Reactance pu.
1	GEN1-230	STNA-230	0.01	0.085
2	STNA-230	GEN2-230	0.032	0.161
3	GEN2-230	STNC-230	0.0085	0.072
4	STNC-230	GEN3-230	0.0119	0.1008
5	GEN3-230	STNB-230	0.039	0.17
6	STNB-230	GEN1-230	0.017	0.092
7	GEN1	GEN1-230	0.0	0.0576
8	GEN2	GEN2-230	0.0	0.0625
9	GEN3	GEN3-230	0.0	0.0586

Appendix III System Data of the 59-bus Test System

Table III.1 AC line data

No.	From	To	R	x	B/2
1	1	2	.0035	.0411	.3494
2	1	59	.001	.025	.375
3	2	3	.0013	.0151	.1286
4	2	25	.007	.0086	.073
5	3	4	.0013	.0213	.1107
6	3	18	.0011	.0133	.1069
7	4	5	.0008	.0128	.0671
8	4	14	.0008	.0129	.0691
9	5	6	.0002	.0026	.0217
10	5	8	.0008	.0112	.0738
11	6	7	.0006	.0092	.0565
12	6	11	.0007	.0082	.0695
13	7	8	.0004	.0046	.039

No.	From	To	R	x	B/2
14	8	9	.0023	.0363	.1902
15	9	59	.001	.025	.6
16	10	11	.0004	.0043	.03645
17	10	13	.0004	.0043	.03645
18	13	14	.0009	.0101	.08615
19	14	15	.0018	.0217	.183
20	15	16	.0009	.0094	.0855
21	16	17	.0007	.0089	.0671
22	16	19	.0016	.0195	.152
23	16	21	.0008	.0135	.1274
24	16	24	.0003	.0059	.034
25	17	18	.0007	.0082	.06595
26	17	27	.0013	.0173	.1608
27	21	22	.0008	.014	.1283
28	22	23	.0006	.0096	.0923
29	23	24	.0022	.035	.1805
30	25	26	.0032	.0323	.2565
31	26	27	.0014	.0147	.1198
32	26	28	.0043	.0474	.3901
33	26	29	.0057	.0625	.5145
34	26	30	.0537	.19	.1653
35	28	29	.014	.0151	.1245
36	31	33	0	.0001	0
37	32	33	0	.0001	0
38	32	36	.0033	.0333	0
39	32	40	.0578	.218	.1887
40	32	42	.0165	.0662	.2353
41	33	34	0	.0001	0
42	34	37	.0106	.074	0
43	35	36	0	.001	0

No.	From	To	R	x	B/2
44	37	38	0	.0001	0
45	38	39	0	.0001	0
46	39	40	.0196	.0854	.081
47	40	41	.0114	.037	0
48	41	43	.015	.0607	.2198
49	42	43	.0214	.0859	.3008

Table III.2 Transformer data

No.	From	To	R	x	T_k
50	11	12	.0016	.0435	1.006
51	13	12	.0016	.0435	1.006
52	50	19	.0007	.0138	1.06
53	32	23	0	.0328	1.025
54	40	14	0	.064	1.025
55	43	9	0	.0124	1.075
56	44	30	0	.0337	1.025
57	45	43	0	.0124	1.075
58	46	39	0	.0438	1.025
59	47	38	0	.0328	1.025
60	48	40	0	.064	1.025
61	49	36	0	.0375	1.075
62	50	2	0	.0181	1.025
63	51	6	0	.025	1.07
64	52	10	0	.02	1.07
65	53	19	.0007	.0142	1.07
66	54	20	.0009	.018	1.009
67	55	22	0	.0143	1.025
68	56	23	.0005	.0272	1.0
69	57	25	.0006	.0232	1.025

No.	From	To	R	x	T_k
70	58	29	.0008	.0156	1.025

Table III.3 Generator Data

No.	Bus Name	Pg	Qg	V0
1	44	-.01	1.25	1.0
2	45	3.1	.05	1.0
3	46	2.25	1.0	1.0
4	47	3.06	2.54	1.0
5	48	1.6	.7	1.0
6	49	4.3	3.34	1.0
7	50	2.5	1.451	1.0475
8	51	5.63	2.055	.982
9	52	6.5	2.057	.9831
10	53	6.32	1.091	.9972
11	54	5.08	1.67	1.0123
12	55	6.5	2.113	1.0493
13	56	5.6	1.005	1.0635
14	57	5.4	.007	1.0278
15	58	8.3	.228	1.0265
16	59	10.0	.86	1.03

Table III.4 Load Data

No.	Bus Name	Pl	Ql	V0
1	51	.092	.046	.982
2	59	9.04	2.5	1.03
3	3	3.22	.024	1.0
4	4	5.0	1.84	1.0
5	7	2.338	.84	1.0

No.	Bus Name	Pl	Ql	V0
6	8	5.22	1.76	1.0
7	12	0.075	.88	1.0
8	15	3.2	1.53	1.0
9	16	3.29	.323	1.0
10	18	1.58	.3	1.0
11	20	6.28	1.03	1.0
12	21	2.74	1.15	1.0
13	23	2.475	.846	1.0
14	24	3.086	-.922	1.0
15	25	2.24	.472	1.0
16	26	1.39	.17	1.0
17	27	2.81	.755	1.0
18	28	2.06	.276	1.0
19	29	2.835	.269	1.0
20	30	2.87	1.44	1.0
21	32	.2	.2	1.0
22	33	5.2	.1	1.0
23	36	4.3	2.2	1.0
24	40	.864	.662	1.0
25	42	.719	.474	1.0
26	41	.7	.5	1.0
27	43	2.265	1.69	1.0

Appendix IV System Data of EPRI 36-bus Test System

Table IV.1 AC line data

No.	From	To	R	x	B/2
10	9	22	.0559	.218	.1954
11	9	23	.0034	.0131	0
12	9	24	.0147	.104	0
14	11	25	0	.0001	0
16	12	26	0	.0001	0
17	12	27	0	.0001	0
19	13	28	0	.0001	0
21	14	19	.0034	.02	0
23	16	18	.0033	.0333	0
24	16	19	.0578	.218	.1887
25	16	20	.0165	.0662	.2353
26	16	21	.0374	.178	.164
27	16	29	0	.0001	0
28	19	21	.0114	.037	0
29	19	30	.0196	.0854	.081
30	20	22	.0214	.0859	.3008
31	21	22	.015	.0607	.2198
32	22	23	.0537	.19	.1653
33	23	24	.0106	.074	0
34	25	26	.0033	.0343	1.8797
35	27	28	.00245	.0255	1.395
36	16	16	0	-1	0
37	18	32	0	.001	0
38	25	25	0	.7318	0
39	26	26	0	.7318	0

No.	From	To	R	x	B/2
40	27	27	0	.7318	0
41	30	31	0	.0001	0
42	29	34	0	.0001	0
43	31	33	0	.0001	0

Table IV.2 Transformer data

No.	From	To	R	x	T_k
1	1	24	0	.015	1.075
2	2	9	0	.0217	1.075
3	3	2	0	.0124	1.075
4	4	19	0	.064	1.025
5	5	18	0	.0375	1.075
6	17	6	0	.0337	1
7	7	30	0	.0438	1.025
8	8	31	0	.0328	1.025
9	10	9	0	-.002	1
13	10	11	0	.018	1.025
0	10	51	0	.001	1
15	15	12	0	.018	1.025
18	17	13	0	.01	1.025
20	15	14	0	-.0032	1
0	15	52	0	.0001	1
22	17	16	0	.001	1.027

Table IV.3 Generator Data

Bus Name	Type	Pg	Qg	V0
1	VD	0	0	1.0
2	PQ	6	3.5	1.0
3	PV	3.1	0	1.0
4	PQ	1.6	.7	1.0
5	PQ	4.3	3.34	1.0
6	PV	-.01	0	1.0
7	PV	2.25	0	1.0
8	PV	3.06	0	1.0

Table IV.4 Load Data

Bus Name	Type	Pl	Ql	V0
9	PQ	3.76	2.21	1.0
16	PQ	5.0	2.3	1.0
18	PQ	4.3	2.2	1.0
19	PQ	.864	.662	1.0
20	PQ	.719	.474	1.0
21	PQ	.7	.5	1.0
22	PQ	2.265	1.69	1.0
23	PQ	2.87	1.44	1.0
29	PQ	5.2	.1	1.0